1-1-2011

The Association Between Traumatic Brain Injury and Alzheimer's Disease: Mouse Models and Potential Mechanisms

Hien Tran
Washington University in St. Louis

WASHINGTON UNIVERSITY IN ST. LOUIS

Division of Biology and Biomedical Sciences

Neurosciences

Dissertation Examination Committee:
David L Brody, Chair
Randall Bateman
Marc Diamond
David Holtzman
Jeffery Gidday
Paul Shaw

The Association between Traumatic Brain Injury and Alzheimer's Disease: Mouse Models and Potential Mechanisms

by

Hien Thuy Tran

A dissertation presented to the Graduate School of Arts and Sciences
of Washington University in partial fulfillment of the
requirements for the degree
of Doctor of Philosophy

December 2011

Saint Louis, Missouri

Abstract of the Dissertation

The Association between Traumatic Brain Injury and Alzheimer's Disease: Mouse Models and Potential Mechanisms

by

Hien Thuy Tran

Doctor of Philosophy in Biology and Biomedical Sciences (Neurosciences)

Washington University in St. Louis, 2011

Professor David L Brody

Alzheimer's disease (AD) is a neurodegenerative disorder characterized pathologically by progressive neuronal loss, extracellular plaques containing the amyloid-β (Aβ) peptides, and neurofibrillary tangles (NFTs) composed of hyperphosphorylated tau proteins. Aβ is thought to act upstream of tau, affecting its phosphorylation and therefore aggregation state. One of the major risk factors for AD is traumatic brain injury (TBI). Acute intra-axonal Aβ and diffuse extracellular plaques occur in approximately 30% of human subjects following severe TBI. Intra-axonal accumulations of total and phospho-tau and less frequently NFTs have also been found in these patients. Due to the lack of an appropriate small animal model, it is not completely understood if and how these acute accumulations contribute to subsequent AD development. Furthermore, mechanisms underlying Aβ and tau pathologies post TBI have not been thoroughly investigated, nor is it known if Aβ also acts upstream of tau in this context.

Here we report that controlled cortical impact TBI in 3xTg-AD mice resulted intra-axonal Aβ accumulations and increased phospho-tau immunoreactivity within hours and up to 7 days post TBI. Given these findings, we investigated the relationship between Aβ and tau pathologies following trauma in this model by systemic treatment of Compound E to inhibit γ-secrectase activity, a proteolytic process required for Aβ production. Compound E treatment successfully blocked post-traumatic Aβ accumulation in these injured mice. However, tau pathology was not affected. Furthermore, rapid intra-axonal amyloid-β accumulation was similarly observed post TBI in APP/PS1 mice, another transgenic Alzheimer's disease mouse model, and acute increases in total and phospho-tau immunoreactivity were also evident in single transgenic Tau_{P301L} mice subjected to TBI. These data provide further evidence for the causal effects of TBI on acceleration of acute

Alzheimer-related abnormalities and the independent relationship between amyloid-β and tau in the setting of brain trauma.

We next used the 3xTg-AD TBI model to investigate mechanisms responsible for increased tau phosphorylation post brain trauma. We found that TBI resulted in abnormal axonal accumulation of a number of kinases found to phosphorylate tau, including protein kinase A (PKA), extracellular signal-regulated kinase 1/2 (ERK1/2), cyclin-dependent kinase-5 (CDK5), glycogen synthase kinase-3 (GSK-3), and c-jun N-terminal kinase (JNK). Notably, JNK was markedly activated in injured axons and colocalized with phospho-tau. We therefore treated mice intracerebroventricularly immediately after TBI with a peptide inhibitor of JNK, D-JNKi1, which specifically blocks interaction of JNK and its substrates. We found that moderate reduction of JNK activity (40%) was sufficient to significantly reduce total and phospho-tau accumulations in axons of TBI mice. These data suggest targeting JNK pathway may be useful in reducing tau pathology and its adverse effects in the setting of brain trauma.

Finally, we investigated whether these acute pathologies negatively contribute to long-term neurodegenerative and behavioral deficits, act as a protective response, or play a neutral role following TBI. In addition, we sought to understand the role of mutant $PS1_{M146V}$ in TBI-induced neurodegeneration. Overall, we found that TBI resulted in chronic axonal Aβ pathology in the absence of plaques in injured 3xTg-AD mice. TBI also caused chronic tau pathology as evidenced by PHF1 tau staining in both injured 3xTg-AD and PS1 littermate controls. Furthermore, TBI caused progressive neurodegeneration and impairments in spatial learning of injured mice, regardless of genotypes. In summary, these data demonstrate a single episode of TBI can have long lasting effects on neuronal functions and contributes to cognitive deficits, which are independent of the acute post-traumatic Aβ and tau pathologies.

Acknowledgments

This thesis work would not have been possible without the following people.

First and foremost, I would like to thank my mentor, David Brody. He has been incredibly supportive in everything I have done. He has not only provided me guidance, but also allowed me the space to explore and mature into a true scientist. I find his enthusiasm for science truly inspiring. This was what kept me going when I was at the lowest point on my "confidence curve." I am forever grateful for everything that I've learned from him.

Second, I would like to thank all members of the Brody lab for being so instrumental and helpful throughout the years. I am especially in debt to Christine Mac Donald and TJ Esparza. Both Christine and TJ have taught me so much about different techniques that I used for my thesis work. Their thoughtful suggestions have helped me to better design my experiments, and to more effectively present my findings in oral and written formats. Besides science, we have established meaningful friendships that I believe will be long-lasting. I would also like to thank Laura Sanchez, a WashU undergraduate who has worked me with during the last one and a half year. Not only has she been a tremendous help to my thesis work, but she has also taught me how to be a good and effective mentor.

Third, I would like to thank my thesis committee for their valuable inputs and guidance. My thesis work has benefited greatly from all the discussions and suggestions from every committee member. I especially want to thank David Holtzman for being an incredible committee chair and collaborator. In addition to the great scientific and professional advices, he has generously offered many resources, without which my thesis work would not have been possible.

Fourth, I am grateful for the opportunity to work with Guojun Bu and Qiang Liu. I started out as a completely naïve rotation student in the Bu lab, for I have just switched from computational biophysics. Both Bu and Liu were so willing to teach me the very basic elements of 'wet lab', and were extremely patient while I slowly learned. The knowledge and techniques I have learned from the Bu lab have prepared me to face the challenges that my thesis work has brought. I will always remember their kindness, and hope to help mentor others in the same way they have mentored me.

Next, I would like to acknowledge my best friends from middle school, Nhi Duong, Quyen Phung, and Dan Thu Do, and friends that I made here in St. Louis, Abena Redwood, Pascal Guiton, Deborah Chen, and Tamira Butler. Their love and confidence in me, as well as the time we have spent together, are so meaningful to me.

I am truly thankful for my family. I feel extremely blessed to have the most loving and supportive parents in the world. They have worked and sacrificed much of their lives for my siblings and my wellbeing and happiness. They have let me find my own way in life, yet have always assured me a welcome home if life turns awry. I cannot have asked for more.

Finally, I want to thank my husband, Yue, who is my partner in both life and science. I am very much inspired by his inquisitive mind and kind heart. I am grateful for his understanding and love, and I very much look forward to the new chapter of our lives.

Hien Thuy Tran

Washington University in St. Louis

December 2011

Table of Contents

List of Tables

List of Figures

Chapter 1

Introduction to Traumatic Brain Injury and Alzheimer's disease

1.1 Traumatic Brain Injury

1.1.1 Introduction

Traumatic brain injury (TBI) is a major public health problem. Annual TBI costs are approximately 60 billion in direct medical costs and indirect costs such as lost of productivity. It accounts for a third of all injury-related deaths in the U.S alone. Those who survive from TBI often suffer from cognitive and behavioral dysfunctions (Coronado et al., 2011). As a result, it is not surprising that TBI is a major environmental risk factor for subsequent development of dementia of the Alzheimer's type (Mortimer et al., 1991; Plassman et al., 2000; Fleminger et al., 2003).

TBI, a form of acquired brain injury, occurs when physical forces cause damage to the brain and its functions. TBI can result from penetrating head injury or closed-head injury. Penetrating injury occurs when an object pierces through the skull and directly damages the brain matter. Closed-skull injury refers to damage to the brain without breaking of the skull. Common causes of TBI are motor vehicle accidents, falls, assaults, contact sports, and blast.

Brain damage following TBI is a result of both primary mechanical disruption of brain tissue and secondary injury mechanisms. These delayed/secondary injury

processes provide a therapeutic window for lessening the adverse effects of TBI. One such delayed process is traumatic axonal injury (TAI), which is also known as diffuse axonal injury. TAI refers to the widespread axonal damage observed in many brain structures following various injury severities in human and multiple animal models (Strich, 1956; Adams, 1982; Gennarelli et al., 1982; Adams et al., 1984; Grady et al., 1993; Blumbergs et al., 1994; Sherriff et al., 1994b; Blumbergs et al., 1995). TAI is believed to contribute to morbidity and cognitive dysfunctions following TBI. As such, much of TBI research has focused on mechanisms of TAI and ways to reduce TAI following injury.

1.1.2 Pathology

Traumatic Axonal Injury

TAI is a prominent feature of TBI (Strich, 1956; Adams, 1982; Gennarelli et al., 1982; Adams et al., 1984; Grady et al., 1993; Blumbergs et al., 1994; Sherriff et al., 1994b; Blumbergs et al., 1995). TAI causes axonal transport impairments, which lead to accumulations of vesicles and organelles transported along axons. These accumulations result in reactive axonal swellings or retraction bulbs, leading to disconnection and degeneration (Povlishock and Christman, 1995). TAI can be detected within minutes to hours following injury in both humans and animal models using various immunohistochemical approaches. For instance, silver stain (Strich, 1956; Oppenheimer, 1968; Strich, 1970; Gennarelli et al., 1982), amyloid precursor protein (APP) and neurofilament immunohistochemistry (Yaghmai and Povlishock, 1992; Gentleman et al., 1993; Grady et al., 1993; Christman et al., 1994; Sherriff et al., 1994a; Graham et al., 1995; Povlishock and Christman, 1995; Chen et al., 1999; Stone et al.,

2000, 2001; Marmarou et al., 2005) have all been used to document incidents of TAI. APP is transported along axons via the fast axonal transport machinery (Koo et al., 1990). APP rapidly accumulates in retraction bulbs or varicosities following injury (Sherriff et al., 1994b; Graham et al., 1995; Stone et al., 2000; Marmarou et al., 2005). Neurofilament, on the other hand, makes up the axonal cytoskeleton. Increased neurofilament immunoreactivity is believed to result from misalignment and collapse of these structural proteins following injury (Erb and Povlishock, 1988; Yaghmai and Povlishock, 1992; Pettus et al., 1994). APP and neurofilament have since served as robust signatures of axonal injury. TAI can persist months to years following injury, although to a lesser extent than what being observed in the acute phase. Importantly, degree of TAI correlates with morbidity in humans and animal models and contributes to cognitive deficits (Adams, 1982; Gennarelli et al., 1982).

Neuronal Cell Death and Atrophy

Similar to axonal injury, neuronal and glial death has been documented at focal as well as diffuse locations throughout the brain following TBI (Povlishock and Katz, 2005). Cell death at contusional, pericontusional, and distant sites triggered by TBI appears to involve both necrotic and apoptotic cascades (Raghupathi, 2004). Necrotic cell death is characterized by swollen neurons containing dilated mitochondria and pyknotic nuclei. Necrosis is associated with membrane failure and collapse of the cytoskeletal network. Meanwhile, apoptotic cell death is linked to double strand DNA breaks and nuclear condensation in the absence of membrane perturbation. Apoptosis has been hypothesized to be result from excitotoxicity, calcium dyshomeostasis, and deregulation of the apoptotic and anti-apoptotic pathways (Raghupathi, 2004). There is,

however, dissociation between cell death and morbidity/cognitive functions, as evidenced in humans and experimental TBI models (Strich, 1956; Lyeth et al., 1990; Laurer et al., 2001; DeFord et al., 2002). Furthermore, emerging evidence suggests that neuronal somata connected to injured axons often don't die but atrophy over time (Singleton et al., 2002; Lifshitz et al., 2007).

Inflammation

Activation of astrocytes and microglia in response to TBI is evident within hours and persists for months post injury (Oppenheimer, 1968; Gennarelli et al., 1982; Geddes et al., 1997; Oehmichen et al., 1999; Hausmann et al., 2000). Activated astrocytes exhibit hypertrophic somata, while reactive microglia have reduced ramifications and ameboid-like morphologies. At the light microscopic level, astrocytes can be detected by staining with antibodies against glial fibrillary acidic protein (GFAP) and vimentin, both of which are intermediate filament proteins specific to astrocytes in the CNS (Smith et al., 1995; Dunn-Meynell and Levin, 1997; Hausmann et al., 2000; Chen et al., 2003). Microglia can be detected by antibodies against different cell surface receptors such as CD11b and CD68 (Oppenheimer, 1968; Soares et al., 1995; Geddes et al., 1997; Oehmichen et al., 1999; Chen et al., 2003; Kelley et al., 2007; Harting et al., 2008), and by staining with Iba1 antibody, a calcium binding protein specific to microglia and macrophage (Sandhir et al., 2008; Shitaka et al., 2011). Both astrocytes and microglia are believed to have dual roles in the setting of TBI and various CNS injuries (Floyd and Lyeth, 2007; Loane and Byrnes, 2010). Depending on the time of activation, activated astrocytes and microglia can either contribute to secondary injury

or recovery following trauma. As such, this is an active area of research for TBI and various neurodegenerative diseases.

1.1.3 Animal Models

Several animal models have been developed to study the mechanisms of TBI. These range from non-human primates (Gennarelli et al., 1982; Maxwell et al., 1993), pigs (Smith et al., 1997; Raghupathi et al., 2004), sheep (Lewis et al., 1996; Van Den Heuvel et al., 2000; Grimmelt et al., 2011), cats (Povlishock and Becker, 1985; Christman et al., 1997), and small rodents such as rats and mice (Smith et al., 1991; Smith et al., 1995; Laurer et al., 2001; Longhi et al., 2005; Marmarou et al., 2005; Kelley et al., 2007; Lifshitz et al., 2007; Mac Donald et al., 2007a; Dikranian et al., 2008; Garman et al., 2011; Koliatsos et al., 2011; Shitaka et al., 2011). Several injury paradigms have also been tested to model different modes and aspects of injury severity spectrum. These include angular/rotational acceleration (Gennarelli et al., 1982; Smith et al., 1997), lateral fluid percussion (Smith et al., 1991; Hicks et al., 1993), weight drop (Foda and Marmarou, 1994), controlled cortical impact (Smith et al., 1995; Mac Donald et al., 2007a), repetitive closed-skull impacts (Laurer et al., 2001; Raghupathi et al., 2004; Shitaka et al., 2011), and blast (Garman et al., 2011; Koliatsos et al., 2011). Although experimental TBI using primates and pigs closely recapitulate post TBI pathobiology in humans, these models face multiple ethical issues, are costly and not feasible for mechanistic studies. Therefore, experimental TBI models using rodents have been extensively utilized. Thus far, these models have proved useful in studying secondary injury mechanisms following injury. Notably, regardless of species or injury paradigms employed, TAI has been found as a universal consequence.

1.2 Alzheimer's Disease

1.2.1 Introduction

Alzheimer's disease (AD) is the most common form of dementia in the elderly (Abbott, 2011). It is characterized by progressive cognitive, linguistic, and behavioral impairments and memory loss. Two core pathological hallmarks of AD are the extracellular plaques composed of the amyloid-beta (Aβ) peptides and the intracellular neurofibrillary tangles composed of the microtubule-associated protein tau. In addition to these two pathologies, progressive synaptic and neuronal loss and neuroinflammation are also prominent. Brain structures that are primarily damaged in AD are the limbic system and association cortices, which have important roles in memory and cognitive functions (Selkoe, 2001).

AD can be classified into familial and sporadic forms. Familial AD accounts for less than 5%, while the rest of all the AD cases are sporadic. Familial AD has an early age of onset, which ranges from 30 – 60 years of age. Sporadic AD typically starts in the 60s. Apart from the age-of-onset difference, familial and sporadic AD cases share almost identical clinical and histopathological characteristics (Selkoe, 2001).

Familial AD is inherited in an autosomal dominant fashion, and is caused by mutations in the APP (Chartier-Harlin et al., 1991; Crawford et al., 1991; Goate et al., 1991), presenilin 1 (PS1) and presenilin 2 (PS2) genes (Levy-Lahad et al., 1995; Rogaev et al., 1995; Sherrington et al., 1995). APP is the precursor protein from which Aβ is derived (Kang et al., 1987); PS1 and PS2 proteins form part of the γ-secretase machinery that cleaves APP to generate Aβ (De Strooper et al., 1998). Virtually all

mutations in APP, PS1 and PS2 result in increase Aβ production, in particular the Aβ isoform which has 42 amino acids (Citron et al., 1992; Citron et al., 1994; Haass et al., 1994; Lemere et al., 1996b; Mann et al., 1996; Scheuner et al., 1996; Citron et al., 1997). The only genetic factor proven to increase the risk of sporadic AD is the apolipoprotein E (ApoE) genotype (Saunders et al., 1993; Strittmatter et al., 1993): individuals inherited the ε4 allele of ApoE (ApoE4) have increased likelihood and decreased age-of-onset to AD development compared to individuals with ε3 (ApoE3) and ε2 alleles (ApoE2) (Corder et al., 1993). Presence of ApoE4 allele increases Aβ plaque load (Schmechel et al., 1993; Polvikoski et al., 1995; Tiraboschi et al., 2004), possibly by affecting Aβ clearance (Castellano et al., 2011). Together, these studies support the hypothesis that increases in Aβ generation and/or aggregation is central to AD pathogenesis.

1.2.2 Amyloid beta (Aβ)

Aβ peptide is the principal component of the extracellular plaques in AD (Masters et al., 1985). Sequential proteolytic cleavages of APP by β- and γ-secretases generate Aβ peptides that are typically 40 to 42 amino acids long. Once generated, Aβ can exist in monomeric state, or aggregate to form oligomers and fibrills. Aggregation of Aβ is concentration dependent, and occurs both intracellularly (Gouras et al., 2000; D'Andrea et al., 2001; Gyure et al., 2001; Mori et al., 2002a) and extracellularly (Muller-Hill and Beyreuther, 1989; Lemere et al., 1996a; Selkoe, 2004; Finder and Glockshuber, 2007). Mechanisms of toxicity of aggregated Aβ include: impaired axonal transport, impaired long-term potentiation, synaptic and spine loss, neuronal death, and ultimately leading to impairments in learning and memory (Chui et al., 1999; Wirths et al., 2001; Zhang et al., 2002; Oddo et al., 2003a; Casas et al., 2004; Shankar et al., 2007; Klyubin et

al., 2008; Shankar et al., 2008; Ittner et al., 2010; Vossel et al., 2010). Several lines of evidence support cerebral Aβ accumulation as an early and necessary step in AD pathogenesis. First, all patients with AD have abundance Aβ plaques (Dickson, 1997). Second, all mutations in familial AD invariably lead to increased Aβ production and aggregation (Selkoe, 2001). Third, Down's patients who are trisomic for the APP gene have progressive Aβ buildup, followed by neurofibrillary tangle formations, and manifested clinical AD symptoms at an early age (Mann and Esiri, 1989; Iwatsubo et al., 1995; Lemere et al., 1996a). As a consequence, most AD research and recent therapeutics have focused on reducing Aβ production and aggregation, or enhancing Aβ clearance (Carter et al., 2010; Blennow, 2011; Morgan, 2011).

1.2.3 Tau

The microtubule-associated protein tau is a major component of the neurofibrillary tangles (NFTs) found in AD, Pick's disease, progressive supranuclear palsy, and frontal temporal dementias (FTDs), collectively known tauopathies. Tau is hyperphosphorylated and aggregates into straight or paired helical filaments in these diseases (Ballatore et al., 2007).

Tau's physiological function is to stabilize microtubule (Drechsel et al., 1992). Due to alternative splicing of a single tau gene, there are 6 major isoforms of tau expressed in the adult brain. These isoforms differ in the numbers of tubulin-binding repeats (either 3 or 4 repeats, and thus are known as 3R or 4R tau isoforms) and the absence or presence of one or two 29-amino acids inserts in the N-terminal domain of the protein (Goedert et al., 1989b; Goedert et al., 1989a). Expressions of these isoforms are tightly regulated, such that in the adult brain, 3R and 4R tau expression is

maintained at a one to one ratio. Deviation from this ratio can result in familial FTDs (Hong et al., 1998).

Tau binding to microtubule is regulated by serine/threonine phosphorylation. Upregulation of activities of a number of kinases, such as cyclin-dependent kinase 5, glycogen synthase 3-β or downregulation of protein phosphatases have been proposed mechanisms underlying abnormal tau phosphorylation (Gong et al., 1993; Mazanetz and Fischer, 2007). Hyperphosphorylated tau has reduced microtubule binding capability, resulting in destabilized microtubules (Drechsel et al., 1992; Bramblett et al., 1993; Alonso et al., 1994; Merrick et al., 1997). This in turn compromises structural and functional integrity of the cytoskeleton, leading to axonal degeneration (Roy et al., 2005). This is the basis of the hypothesis of how loss-of-function tau can promote neurodegeneration in tauopathies. Hyperphosphorylated tau can also gain toxic function such as sequestration of normal tau and other microtubule-associated proteins, further exacerbating the consequences of tau loss-of-function (Alonso et al., 1996; Alonso et al., 1997; Guo and Lee, 2011).

On the one hand, many studies suggest tau as a mediator of Aβ toxicity. For instance, tau knockout hippocampal neurons in culture were protected from degeneration induced by fibrillar Aβ (Rapoport et al., 2002). Further, axonal transport deficits induced by oligomeric Aβ were ameliorated by deletion of tau (Vossel et al., 2010). In mouse models overexpressing human APP, tau deletion reduced behavioral deficits, excitoxicity and Aβ-induced cell death (Roberson et al., 2007; Ittner et al., 2010). On the other hand, there is direct evidence to support the hypothesis that tau malfunction is sufficient to induce neurodegeneration in the absence of other

pathogenic insults. For instance, many mutations in the tau gene have been found to be causative of FTD with parkinsonism linked to chromosome-17 (FTDP-17) (Goedert and Jakes, 2005). Consequently, targeting tau either by reducing its phosphorylation state or aggregation may prove useful in the setting of AD and related dementias. This has gotten more attention in recent years (Brunden et al., 2009; Ballatore et al., 2010; Brunden et al., 2010a).

1.3 Link between TBI and AD

Several lines of evidence link TBI and subsequent development of AD. First, many epidemiological studies demonstrate that a history of head trauma substantially increases the risk of dementia of the AD type (Mortimer et al., 1991; Plassman et al., 2000; Fleminger et al., 2003). Second, both intracellular and extracellular accumulations of Aβ have been documented in approximately 30% of cases with severe TBI, but less frequently following mild, concussive TBI (Roberts et al., 1990; Roberts et al., 1991; Tokuda et al., 1991; Smith et al., 2003c; Ikonomovic et al., 2004; Uryu et al., 2007; Johnson et al., 2011). Notably, Aβ accumulations could occur within hours to days following injury in young individuals who do not have a preexisting history of neurodegeneration. Third, NFTs containing hyperphosphorylated tau are prominent pathological features in the brain of boxers and athletes with a lifelong history of concussions, resulting in a condition known as dementia pugilistica or chronic traumatic encephalopathy (Roberts et al., 1990; Schmidt et al., 2001; McKee et al., 2009). Severe TBI has also been reported to cause acute accumulations of total and phosphorylated tau in injured axons (Ikonomovic et al., 2004; Uryu et al., 2007), and NFTs years

following injury (Johnson et al., 2011). Fourth, individuals with TBI who are ApoE4 carriers are at greater risk of AD (Mayeux et al., 1995; Katzman et al., 1996). Further, ApoE4 genotype is associated with poorer outcome following TBI (Sorbi et al., 1995; Teasdale et al., 1997; Friedman et al., 1999; Lichtman et al., 2000; Diaz-Arrastia et al., 2003; Teasdale et al., 2005; Zhou et al., 2008), possibly by acting via exacerbation of Aβ and tau accumulation (Verghese et al., 2011). Together, these findings support the hypothesis that TBI is causally linked to AD.

This hypothesis was supported by findings in rotational head injury using pigs: within days following injury, diffuse Aβ plaques, axonal Aβ and tau accumulation, as well as NFTs were documented (Smith et al., 1999b). However, it is difficult to perform mechanistic studies using pigs. Therefore, a number of groups have attempted to model these pathologies by subjecting small rodents to various experimental TBI paradigms. For instance, experimental TBI in the rats have been reported to cause intra-axonal Aβ accumulations within hours post injury (Stone et al., 2002); this pathology could persist up to a year (Iwata et al., 2002). While Smith et al. reported that controlled cortical impact TBI (CCI) in transgenic mice overexpressing mutant APP (PDAPP) resulted in an increase in tissue Aβ levels at 2 hours post injury (Smith et al., 1998), our lab observed the contrary (Schwetye et al., 2010). Further, Nakagawa et al. observed regression of Aβ plaques in PDAPP mice months following CCI (Nakagawa et al., 1999; Nakagawa et al., 2000). Meanwhile, Hartman et al. reported that CCI accelerated Aβ plaque formation in PDAPP and ApoE4 double transgenic mice (Hartman et al., 2002). Uryu et al. demonstrated that multiple closed-skull impacts accelerated Aβ plaque load at 16 weeks post injury in Tg2576 mice, another transgenic APP line (Uryu et al., 2002).

However, using a similar repetitive impact model, Yoshiyama et al. observed accelerated NFTs formation in only 1 of 12 injured tau transgenic mice (Yoshiyama et al., 2005). These models have not only reported mixed findings on TBI and AD interaction, but also have fallen short of reproducing both the Aβ and tau pathological features observed in humans. Furthermore, they did not allow assessment of the interaction between human Aβ and tau in the setting of brain trauma. Consequently, prior to this work, the field as a whole was in need of an appropriate small animal TBI model to investigate the pathomechanisms linking TBI and AD.

1.4 Summary

To summarize, TBI and AD are important public health issues. There exists an unequivocal link between them. However, mechanisms linking TBI and AD remain incompletely understood in part because of the lack of an appropriate small animal model. Therefore, the goals of my thesis were to 1) develop a mouse TBI model that more closely resembled post-traumatic pathologies in human, 2) use the model to understand the interaction between Aβ and tau in the setting of trauma, 3) determine the mechanisms underlying tau pathology following injury, and 4) investigate the long-term behavioral and neurodegenerative consequences of the acute Aβ and tau pathologies observed post injury.

Chapter 2

Experimental Designs and Methods

2.1 Animals

We utilized 5-7 month old homozygous 3xTg-AD mice (Oddo et al., 2003b) of both sexes on B6/SJV129 background in all experiments. 3xTg-AD mice were generated by microinjection of the APP_{swe} and Tau_{P301L} transgene constructs, both under the control of the mouse Thy1.2 promoter, into single-cell embryos of mutant homozygous $PS1_{M146V}$ knockin mice (Guo et al., 1999). These 3xTg-AD mice breed as readily as a "single" transgenic line because the APP_{swe} and Tau_{P301L} transgene cassettes cosegregated, and the M146V mutation was "knocked in" to the endogenous mouse PS1 locus. 3xTg-AD mice used in most experiments were derived from founders received from the LaFerla lab in 2007, unless otherwise noted. Aβ and tau pathologies have been stable since that time, with no evidence of drift.

We also used 2 month old heterozygous APP_{swe}/PSEN1ΔE9 (APP/PS1) transgenic mice (line 85, Stock number 004462, The Jackson Laboratory). APP/PS1 mice overexpress human APP swedish gene and human *PSEN1* with an exon 9 deletion (Jankowsky et al., 2004).

We also used 6 month old heterozygous TauP301L mice. Tau_{P301L} mice overexpress human tau gene with P301L mutation (Gotz et al., 2001) under the Thy1 promoter.

For behavioral assessment in the Morris water maze, we crossed 3xTg-AD mice to homozygous $PS1_{M146V}$ mice, the line from which the original 3xTg-AD line was derived from. These $PS1_{M146V}$ mice were received from the Mattson lab in 2009 (Guo et al., 1999). Since differences in genetic background strains may influence behavioral performance (Owen et al., 1997; Holmes et al., 2002), we generated homozygous 3xTg-AD mice and $PS1_{M146V}$ littermates and used them for behavioral assessment. The following breeding scheme was employed. First, homozygous 3xTg-AD mice were crossed to homozygous $PS1_{M146V}$ to generate offspring that were heterozygous in human APP_{swe} and Tau_{P301L} genes and homozygous in $PS1_{M146V}$ ($APP^{+/-}Tau^{+/-}PS1^{+/+}$). Non-sibling $APP^{+/-}Tau^{+/-}PS1^{+/+}$ mice were then crossed to generate mice which had the following genotypes with expected Mendelian ratios: $APP^{+/+}Tau^{+/+}PS1^{+/+}$ (denoted 3xTg), $APP^{+/-}Tau^{+/-}PS1^{+/+}$, and $APP^{-/-}Tau^{-/-}PS1^{+/+}$ (denoted PS1). $APP^{+/-}Tau^{+/-}PS1^{+/+}$ heterozygous mice were not used in any of the experiments.

Mice were housed in standard cages in 12 h light, 12 h dark cycle and given food and water *ad. lib.* Mice of both sexes were randomly assigned to experimental groups. All experiments were approved by the animal studies committee at Washington University in St Louis.

2.3 Genotyping

Genotyping of 3xTg-AD, Tau_{P301L}, and APP/PS1 mice were done as previously described (Gotz et al., 2001; Oddo et al., 2003b; Jankowsky et al., 2004).

A real-time PCR comparative CT method was developed to discriminate between 3xTg homozygous and heterozygous mice generated in our lab. Using

sequence derived from the transgene cassette, primers for APP, Tau and endogenous β-actin were generated using Primer Express 3.0 software (Applied Biosystems (ABI), Carlsbad, California): β-actin-sense (AGTGTGACGTTGACATCCGTA), β-actin-antisense (GCCAGAGCAGTAATCTCCTTCT), APP-sense (AAACCGGGCAGCATCGA), APP-antisense (GGAACTCTTGGCACCTAGAGGAT), Tau-sense (GGTGGGTGGCGGTGACT), Tau-antisense (TAGCTTTCCCCACCACAGAATC).

For genotyping, 1–2 mm sections of tail biopsy were processed using the DNeasy Blood & Tissue Kit (Qiagen, Valencia, CA) to isolate genomic DNA. PCR analysis was performed using an Applied Biosystems 7500 Fast Real-Time PCR system with Syber Green PCR Master Mix (ABI). The delta-CT between the β-actin gene and APP or Tau was measured against known homozygote and heterozygote animals and found to be stable and able to clearly distinguish unknown genotypes. Genotyping of $PS1_{M146V}$ transgene expression was done as previously described (Guo et al., 1999).

2.4 Controlled Cortical Impact Experimental TBI

The experimental TBI methods used in this study were performed as described previously (Brody et al., 2007; Mac Donald et al., 2007b). Briefly, mice were anesthetized with isoflurane (5% induction, 2% maintenance) and placed on a stereotaxic frame. After midline skin incision, a 5 mm left lateral craniotomy was made using a motorized drill. Controlled cortical impact was produced with an electromagnetic impact device using a 3 mm diameter metal tip. The impact was

centered at 2.7 mm lateral to midline and 3.0 mm anterior to lambda. Injury severities of 1.0 mm, 1.5 mm, and 2.0 mm below the dura were chosen to model mild, mild-moderate, and moderate injuries, respectively. After injury, the impact site was covered with a plastic skull cap, skin was sutured, and mice were allowed to recover on a heated pad. Mice were kept at 37 ˚C via a rectal temperature probe and feedback temperature controller throughout the duration of the surgery (Cell MicroControls). Temperature control is important because hypothermia alone has been reported to cause tau accumulation and hyperphosphorylation (Planel et al., 2004). Sham mice underwent the same surgical procedure including anesthesia and craniotomy but were not injured.

2.5 Antibodies

Antibodies used are listed in Table 2.1.To avoid using anti-mouse secondary antibodies on injured tissues, most monoclonal antibodies were conjugated to biotin or directly labeled. 3D6 and HJ3.4 was biotinylated with NHS-LC-biotin from Pierce. Conjugation of 3D6 to Alexa Fluor® 596 was done via commercially available kit (A20185, Invitrogen Corp).

Table 2.1 List of antibodies used in all experiments

Protein	Antibody	Epitope	Host/Application Dilution	Source/Cat #
Aβ	3D6	aa1-5 requiring free N terminus.	Mouse/IHC, ELISA 1 μg/ml	Eli Lilly and Co
	m266	aa13-28	Mouse/ELISA 10 μg/ml	Eli Lilly and Co
	2G3	aa35-40	Mouse/ELISA 20 μg/ml	Eli Lilly and Co
	21F12	aa33-42	Mouse/ELISA 20 μg/ml	Eli Lilly and Co
	HJ3.4	aa1-13	Mouse/IHC 0.75 μg/ml	Dr. David Holtzman
	panAβ	aa15-30	Rabbit/IHC 0.8 μg/ml	Invitrogen (44-136)
	Aβ40	aa34-40	Rabbit/IHC 0.5 μg/ml	Invitrogen (44-348A)
	Aβ42	aa36-42	Rabbit/IHC 5 μg/ml	Chemicon (AB5078P)
	82E1	requires free N-terminus	Mouse/IP 10 μg	IBL-America 10323
APP	APP	full-length, C-terminal	Rabbit/IHC, WB 0.5 μg/ml	Invitrogen (51-2700)
	6E10	Aβ/APP	Mouse/IP (10 μg)/WB (1 μg/ml)	Covance SIG-39300
Tau	HT7	panTau	Mouse/IHC 0.2 μg/ml	Pierce (MN1000)
	pAb Tau	panTau	Sheep/IHC 1 μg/ml	Pierce (PN1000)
	Tau46	panTau	Mouse/WB 1:1000	Cell Signaling (4109)
	AT8	pS199, pS202, pT205	Mouse/WB 1:1000	Pierce (MN1020)
	AT100	pS212, pT214	Mouse/WB 1:1000	Pierce (MN1060)
	AT180	pT231	Mouse/WB 1:1000	Autogen Bioclear (90218)
	S199	pS199	Rabbit/IHC 1:2000	Invitrogen (44734G)
	T205	pT205	Rabbit/IHC 1:1000	Invitrogen (44738G)
	T231	pT231	Rabbit/IHC 1:1000	Invitrogen (44746G)
	S396	pS396	Rabbit/IHC 1:1000	Invitrogen (44751G)

	S422	pS422	Rabbit/IHC 1:1000	Invitrogen (44764G)
	PHF1	pS396/pS404	Mouse/IHC 1:500	Dr. Peter Davies
Neurofilament	NF-L	NF-L 68kD	Mouse/IHC 0.5 μg/ml	Sigma (N5139)
Tubulin	Tubulin	α-tubulin	Mouse/WB 1 μg/ml	Sigma (T5168)
PKA	PKA	α and β catalytic subunits	Goat/WB 0.4 μg/ml	Santa Cruz Biotechnology (sc-30668)
	p-PKA	pT198 of α and β catalytic subunits	Rabbit/WB, IHC 0.4 μg/ml	Santa Cruz Biotechnology (sc-32968)
ERK1/2	p44/42 MAPK	full length, C-terminus	Rabbit/WB 1:500	Cell Signaling (4695)
	p-p44/42 MAPK	pT202 and pY204	Rabbit/WB, IHC 1:500	Cell Signaling (4370)
GSK3β	GSK3β	full length	Rabbit/WB 1:1000	Cell Signaling (9315)
	p-GSK3β	pS9	Rabbit/WB, IHC 1:500	Cell Signaling (#9323)
	p-GSK3	pY279 of α and pY216 of β subunits	Rabbit/IHC 1:500	Invitrogen (44604G)
JNK	JNK	full length	Rabbit/WB 1:1000	Cell Signaling (9258)
	p-JNK	pT183 and pY185	Rabbit/WB, IHC 1:500	Cell Signaling (4668)
CDK5	CDK5	full length	Rabbit/WB, IHC 1:500	Cell Signaling (2506)
p35/25	p35/25	full length, C-terminus	Rabbit/WB 1:1000	Cell Signaling (2680)
c-jun	p-c-jun	pS63	Rabbit/IHC 1:500	Cell Signaling (2361)

IHC: immunohistochemistry; ELISA: enzyme-linked immuno absorbant assay; IP: immunoprecipitation; WB: western blot; p: phosphorylated.

2.6 Histology

2.6.1 Immunohistochemistry

Animals were sacrificed via deep isofluorane anesthesia, followed by transcardiac perfusion using ice-cold phosphate buffered saline (PBS) and 0.3 % heparin. Brains were removed and fixed in 4% paraformaldehyde for 24 h. Brains were subsequently cryoprotected and equilibrated in PBS solution containing 30% sucrose for 2 days. A sliding microtome was used to generate coronal 50 μm sections. All immunohistochemical studies were done on free-floating sections. All sections were washed with tris-buffered saline (TBS) between applications of antibody solutions. Antigen retrieval with 70% formic acid (3-5 minutes) was performed for Aβ and phospho-tau staining. Non-specific binding was blocked by incubation in TBS containing 0.25% Triton X (TBS-X) and 3% nonfat dry milk (monoclonal anti-Aβ antibodies) or 3% serum (monoclonal anti-tau and polyclonal antibodies) or 5% BSA (phospho-tau antibodies). Primary antibody was diluted in 1% nonfat dry milk, 1% serum or 1% BSA in TBS-X. **Table 2.1** listed of all antibodies used. Bound antibodies were detected with biotinylated secondary antibodies, except for 3D6 and HJ3.4, which were directly biotinylated. Horse-radish peroxidase method (ABC Elite kit, PK6100, Vector Laboratories) and DAB were utilized for visualization of bound antibodies.

To reduce background staining on injured tissues when staining with monoclonal NF-L and PHF1 antibodies, an additional blocking step for 1 hour with unconjugated anti-mouse monovalent Fab fragments (Jackson ImmunoResearch, 315-007-003, 130 μg/ml) was performed following blocking with serum.

Following color development with DAB, sections were mounted on glass slides, dried for at least 1 h, and then differentiated through a series of 50%, 70%, 90%, 100%, and 100% ethanol; 1 minute each. Slides were cleared in Xylene 2 times, for 4 minutes each. Slides were cover slipped in Cytoseal 60 resinous medium (Thermo Scientific, 8310), and allowed to dry overnight before quantification or photomicroscopy.

2.6.2 Double Immunofluorescence

In double labeling studies, primary antibodies were sequentially applied, followed by Alexa Fluor® conjugated secondary antibodies except for 3D6, which was conjugated to Alexa Fluor® 596.

For double labeling of phospho-tau and activated JNK (phospho-JNK, p-JNK), sections were first incubated with rabbit anti-pS199, followed by goat anti-rabbit secondary antibody conjugated to Alexa Fluor® 488 (Invitrogen, A11008, 2 μg/ml). Sections were blocked again for 30 minutes with 3% normal rabbit serum to saturate open binding sites on the first secondary antibody with IgG. Sections were then incubated for 1 hour in excess of unconjugated goat anti-rabbit monovalent Fab fragments (Jackson ImmunoResearch, 111-007-003, 130 μg/ml). This was done to cover the rabbit IgG so that the second secondary antibody would not bind to it. Rabbit anti-p-JNK was subsequently applied, followed by goat anti-rabbit conjugated to Alexa Fluor® 594 (Invitrogen, A11012, 2 μg/ml). Sections were washed with TBS 3 times for 5 minutes each between steps. Sections were mounted and cover slipped using VectaShield mounting medium (Vector Laboratories, H-1000). Images were obtained using LSM 5 Pascal software (Zeiss Physiology Software) coupled to an LSM Pascal Vario 2RGB confocal system (Zeiss).

2.6.3 Cresyl Violet Staining

Cresyl violet staining was used for delineation of cytoarchitecture. Sections were mounted on glass slides. After drying, slides were incubated for 2 min in 0.25 % cresyl violet solution (pH 3.5), rinsed in distill water, and differentiated in series of 50%, 70%, 95%, 100% and 100% ethanol; 1 minute each. Slides were cleared in Xylene 2 times, for 4 minutes each. Slides were cover slipped in Cytoseal 60 resinous medium (Thermo Scientific, 8310), and allowed to dry overnight before quantification or or photomicroscopy.

2.6.3 X-34 Staining

For detection of fibrillar structures, X-34 staining was performed. Mounted sections were first permeabilized with 0.25% Triton-X phosphate buffered saline (PBS) for 30 minutes. Slides were then incubated in 10 μM X-34 staining solution containing 40% ethanol, 60% PBS, and 0.02 N sodium hydroxide. After rinsing 3 times in 40% ethanol and 60% PBS buffer, for 5 minutes each, slides were cover slipped with VectaShield mounting medium (Vector Laboratories, H-1000).

2.7 Biochemical Assessments

2.7.1 Preparation of Tissues Homogenates for Aβ Detection by Human-Specific ELISAs

Separate groups of sham and TBI (2.0 mm) mice were sacrificed at 24 h post surgery; hippocampi ipsilateral and contralateral to impact site (including fimbria and surrounding white matter tracts) were dounce homogenized in 1:10 w/v of TBS.

Supernatants were kept and pellets were subsequently sonicated in a 1:5 w/v solution of 100 mM sodium carbonate, pH 11, containing 50 mM sodium chloride (Carbonate lysates). Finally, remaining pellets were homogenized in 1:5 w/v 5M Guanidine-hydrochloride, rotated at room temperature for 3-4 h (Guan lysates). All buffers used for homogenization contained protease and phosphatase inhibitor cocktails (Roche). Supernatants and pellets from all tissue suspensions were obtained by spinning at 13,300 g for 20 minutes at 4˚C. Protein concentrations were determined via BCA method (Pierce Biotech, Inc.). TBS, Carbonate, and Guanidine lysates prepared above were tested for Aβ contents using a human specific Aβ ELISA, as described (Cirrito et al., 2003; Kang et al., 2007). Capture antibodies were m266 for the total $A\beta_{1-x}$ ELISA, 2G3 for the $A\beta_{1-40}$ ELISA, and 21F12 for the $A\beta_{1-42}$ ELISA. Detection antibody was 3D6-biotin. These antibodies were gifts from Eli Lilly and Co.

2.7.2 Preparation of Tissue Homogenates for APP Western Blots

Bilateral cerebellar tissue was homogenized in modified RIPA buffer containing protease inhibitor cocktails (Roche), as described (Cirrito et al., 2003). Protein concentrations were determined via BCA method (Pierce Biotech, Inc.). Equal amounts of samples were electrophoresed on 4-12% Bis-Tris NuPAGE gels using MES buffer (Invitrogen Corp) and transferred to 0.2 μm pore nitrocellulose membrane. After transfer, membranes were blocked in 3% non-fat dry milk in 50 mM Tris, pH 7.6 buffer containing 150 mM NaCl and 0.1% Tween 20 (TBS-T) for 1 h at room temperature. After washing in TBS-T three times, 5 minutes each, membranes were incubated with polyclonal APP antibody (0.25 μg/ml) in blocking buffer overnight at 4 ˚C. Bound

antibodies were detected with HRP-conjugated donkey-α-rabbit IgG (GE Healthcare, at 1:10,000) and the ECL Advance Western Blotting detection kit (GE Healthcare). Blots were stripped and reprobed with anti-α-tubulin (1 μg/ml) for loading control. Images were taken on film and scanned.

2.7.3 Preparation of Tissue Homogenates for Tau Western Blotting and ELISAs

Separate groups of and injured (2.0 mm) 3xTg-AD mice were sacrificed at 24 h by rapid decapitation. Bilateral hippocampi were dissected, immediately frozen, and stored at -80°C. Frozen hippocampi were homogenized in modified RIPA buffer containing protease and phosphatase inhibitor cocktails (Roche), as described (Cirrito et al., 2003). Homogenates were centrifuged at 13,000 rpm for 20 minutes at 4 °C. After pre-clearing samples with protein G sepharose beads to remove endogenous mouse IgG, protein concentrations were determined using the BCA method (Pierce). Equal amounts of samples were electrophoresed on 10% BisTris NUPAGE gels (Invitrogen Corp). After transfer, 0.2 μm pore nitrocellulose membranes were blocked with 5% non-fat dry milk TBS-T for 1 h, and probed with AT8 (1:1000), AT100 (1:1000), or AT180 (1:1000) in 5% BSA TBS-T overnight at 4°C. Sheep-α-mouse HRP (GE Healthcare, 1:12,000) and ECL Advance Western Blotting kit (GE Healthcare) were used to detect bound antibodies. Blots were stripped and reprobed for total tau using Tau46 antibody (1:1000). Blots were scanned and densitometry was performed via Image J (NIH). Total and phospho-S199 tau ELISAs were performed per manufacturer's instructions (Invitrogen Corp).

2.7.4 Western Blotting of Tau Kinases

The RIPA homogenates from ipsilateral hippocampi prepared for tau western blots and ELISAs were used to assess total and activated levels of several tau kinases. Equal amounts of each sample (6 μg) were electrophoresed on 10% BisTris NUPAGE gels using MOPS buffer (Invitrogen). Gels were transferred to 0.2 μm nitrocellulose membranes, which were then blocked with tris buffered saline containing 0.1% Tween-20 (TBS-T) and 5% non-fat dry milk for 1 h at room temperature. Membranes were incubated overnight in TBS-T buffer containing 5% BSA and the appropriate primary antibodies. Corresponding anti-rabbit-HRP (GE Healthcare, 1:10,000) or anti-goat-HRP (Invitrogen, 1:10,000) and ECL Advance Western Blotting kit (GE Healthcare) were used for detection. Blots were washed 4 times for 5 minutes each with TBS-T between blocking and applications of antibodies. Blots were scanned, and densitometry was performed via Image J (NIH).

2.7.5 Immunoprecipitation and Western Blot to demonstrate specificity of HJ3.4 antibody toward Aβ, not APP

To verify the specificity of HJ3.4 for Aβ over amyloid precursor protein (APP), an immunodepletion assay was performed on brain homogenate from a 9 month old 3xTg-AD mouse. Whole brain was removed after transcardial perfusion with PBS containing 0.3% heparin and immediately dounce homogenized in RIPA buffer (150 mM NaCl, 50 mM Tris-HCl, 1% Triton X-100, 0.10% SDS, 0.5% deoxycholic acid, 2.5 mM EDTA, pH 8.0) containing protease inhibitor cocktail (Roche) at a 10:1 ratio (RIPA volume/tissue weight) using 25 strokes followed by brief sonication. The

resulting homogenate was centrifuged for 20 minutes at 17,000xg at 4°C to remove insoluble protein. Total protein was determined using a standard BCA protein assay. Individual aliquots containing 100 μg of homogenate were immunodepleted using 10 μg of each antibody (HJ3.4, 82E1, 6E10). After overnight incubation, complexes were captured using 150 μg Protein-G Dynabeads® (#100.03D, Invitrogen). The resulting immunodepleted supernatants were assayed by Western blot, as described below, to determine affinity in solution for APP.

Samples for Western blot analysis were combined with standard Laemmli buffer and heated to 85°C to denature for 5 minutes. Protein samples were size separated on NuPAGE® 12% Bis-Tris gels (Invitrogen) in 2-(N-morpholino)ethanesulfonic acid (MES) SDS running buffer at 150 Volts. SeeBlue® Plus-2 prestained standard (Invitrogen) was used to visualize and estimate the progression and size of the sample migration. Gels were then transferred to 0.2 μm nitrocellulose using Towbin buffer (25 mM Tris, 192 mM glycine, pH 8.6) containing 20% methanol at 150 mA for 1 hour. For Aβ western blotting, membranes were incubated at 95°C for 1 minute in PBS to allow for improved antigen binding and then cooled in room temperature PBS prior to blocking. Membranes were blocked in 2% non-fat dry milk (NFDM) PBS for 1 hour. Between all remaining steps, membranes were washed 3x for 10 minutes each with PBS-T (0.05% Tween 20). For detection of APP, the mouse monoclonal 6E10 was used at 1 μg/mL in 2% NFDM PBS overnight at 4°C. Bound primary antibodies were detected using a sheep anti-mouse-HRP (#NA931V, GE Healthcare) at 50 ng/mL in 2% NFDM PBS and then developed with ECL Advance Reagent (GE Healthcare) followed by exposure to film emulsion.

2.7.6 Protein Phosphatase Activity Assays

Serine/threonine phosphatase activity assay kits (V2460) were purchased from Promega Corp. Assays were performed on a 96-well plate format, per manufacturer's instructions. Briefly, to remove phosphatase inhibitors and endogenous phosphates from RIPA hippocampal lysates, samples were desalted using the Zeba micro spin desalting columns (Pierce, 89877). Each sample was run in duplicate reactions; each contained 2 μl of lysates, 10 μl of appropriate 5x phosphatase reaction buffer, 5 μl of 1 mM phosphopeptide, and 33 μl of deionized H_2O. Protein phosphatase 2A (PP2A) reaction buffer contained 250 mM imidazole, 1mM EGTA, 0.1% β-mercaptoethanol, and 0.5 mg/ml acetylated BSA (Promega, R3961). In addition to the reagents listed for PP2A reaction buffer, PP2B (calcineurin) reaction buffer also included 50 mM $MgCl_2$, 5 mM $NiCl_2$, 250 μg/ml calmodulin (Calbiochem, 208690). Plates were incubated at 30 ˚C for 30 minutes for phosphatase reactions to take place. Reactions were stopped by addition of 50 μl of Molybdate Dye/Additive mixture to each well. Plates were subsequently incubated at room temperature for 30 minutes to allow the Molybdate Dye to bind to free phosphates released from the reaction. Plates were read using a plate reader with 630 nm filter. Optical densities of the samples were determined based on the optical densities of free phosphate standards. Specific activities for PP2A and PP2B were expressed as pmol phosphates per minute per μg of total protein.

2.8 Drug Treatment

2.8.1 γ-secretase Inhibition with Compound E to Block Aβ Production

To prevent post-traumatic intra-axonal Aβ accumulation, mice were treated with intraperitoneal (i.p.) injections of vehicle or Compound E, a small molecule inhibitor of γ-secretase (10 mg/kg; Axxora) (Seiffert et al., 2000; Olson et al., 2001; Grimwood et al., 2005; Yang et al., 2008; Yan et al., 2009). One group of mice received Compound E (CmpE) or 0.8% DMSO vehicle starting at 1 h before injury, then again at 5 h, 11 h, and 17 h post injury. These mice were sacrificed 24 h after injury. Another group of mice received 4 CmpE or vehicle injections in the first 24 hours as noted above followed by injections twice daily until 7 days post injury. 10 mg/kg of Compound E was used because this dose has been shown to inhibit cortical γ-secretase activity in guinea pigs by 71 ± 4%, measured ex vivo (Grimwood et al., 2005). Furthermore, the frequent dosing regimen was employed due to the short half-life of Compound E: ~5-6 hours (Yan et al., 2009). Lastly, this relatively high dose was also chosen because of the presence of the presenilin1 ($PS1_{M146L}$) mutation in 3xTg-AD mice, as PS1 mutations have been shown to have diminished response to γ-secretase inhibition (Czirr et al., 2007). Mice tolerated these dosing regimens well without additional weight-loss, lethargy or unexpected mortality.

2.8.2 Inhibition of c-jun N-terminal Kinase (JNK) by peptide inhibitor, D-JNKi1

D-JNKi1 peptide (BML-EI355) and D-TAT control peptide (BML-EI384) were purchased from Enzo Life Sciences International, Inc. D-JNKi1 peptide is a specific inhibitor of JNK, which blocks the interaction between JNK (JNK-1, -2, -3) and its substrates (Bonny et al., 2001; Barr et al., 2002; Borsello et al., 2003b; Borsello et al., 2003a). D-JNKi1 is cell permeable and has longer half life than its L-stereoisomer. D-JNKi1 contains a 20-amino acid sequence of the JNK binding domain of the JNK-interaction protein JIP1 covalently linked to the 10-amino acid HIV-TAT sequence. D-TAT control peptide contains only the 10-amino acid HIV-TAT sequence. Prior to craniotomy and TBI induction, a 1 mm burr hole was drilled on the right hemisphere, at -0.5 mm posterior to bregma and 1.0 mm lateral to midline. Mice were randomly assigned to receive either D-JNKi1 or D-TAT (solublized in 0.1% DMSO PBS, 5 μg in 5 μl) immediately post injury at 0.3 μl/min rate. A 33 gauge needle attached to a Hamilton syringe and KDS310 nano pump system (KDS Scientific Inc) was lowered -2.2 mm below the dura through the burr hole to deliver peptide solutions (5 μl in total volume) into the right lateral ventricle. Mice recovered well after the combined injury and intracerebralventricular (i.c.v.) injection procedure. They lost approximately 10% of their original body weight, which was similar to mice that underwent only TBI procedure.

2.9 Quantitative Analyses of Histological Data

2.9.1 Stereology

Stereological methods were available via StereoInvestigator version 8.2 software. All assessments were made by investigators who were blinded to injury status, time sacrificed post injury, and treatment regimens of experimental animals. The optical fractionator method was employed for quantification of total numbers of markers of interest per cubic mm of tissue. Details on this stereological method have been described (Mac Donald et al., 2007b). Briefly, for quantification of HJ3.4, $A\beta_{40}$-positive axonal varicosities in ipsilateral fimbria and tau-positive somata in ipsilateral amygdala, a 200 μm x 200 μm sampling grid and a 75 μm x 75 μm counting frame were used. For quantification of total tau, APP and panAβ-positive puncta in ipsilateral fimbria, a 300 μm x 300 μm grid and a 40 μm x 40 μm counting frame were employed. For pS199-, and PHF1-positive puncta in the fimbria, a 200 μm x 200 μm grid and a 50 μm x 50 μm counting frame was used. Dissector height of 15 μm and guard zones of 2.5 μm were employed for all measurements. Four sections per mouse, each separated by 300 μm, were used for these estimations. These sections spanned approximately bregma -1.06 to -1.96 mm (Franklin and Paxinos, 1997). The spherical probe (aka 'space balls') method was used for quantification of the total length of tau immunoreactive processes in the dorsal contralateral CA1 region (Mouton et al., 2002). A sampling grid of 250 μm x 250 μm and a hemispherical probe with 17 μm radius were employed. Three sections per mouse from approximately bregma -1.46 to -2.06 mm were used for this quantification.

Stereological quantifications of D-JNKi1 and D-TAT treated mice were according to the aforementioned methods, except that each brain sections were separated by 400 μm.

2.9.2 Densitometry

Densitometric analysis of kinase IHC was performed on the ipsilateral fimbria/fornix of 4 sections per mouse; each section separated by 400 μm. Phospho-c-jun IHC quantification was performed on the ipsilateral thalamus using 5 sections per mouse. These sections spanned approximately bregma -0.8 mm to -2.6 mm. Slides were scanned using a Nanozoomer HT system (Hamamatsu Photonics) to obtain digitized images. Images were converted to 8-bit, thresholded, and percentage areas occupied by each kinase and p-c-jun stains were quantified using the Image J software (National Institutes of Health).

2.9.3 Estimations of Hippocampus and Fimbria Volume

Estimations were done on cresyl violet stained sections. Seven to eight sections per mouse, spanned approximately from bregma -0.94 mm to -3.1 mm were used for hippocampal volume estimation, while five to six sections were used for fimbria. Each section is separated by 300 μm. Images were digitally captured using the Nanozoomer HT system (Hamamatsu Photonics). Images were loaded into the ImageJ software (National Institute of Health). Areas of the hippocampus and fimbria were estimated based on the drawn contours around these regions via the polygon tools in ImageJ. Hippocampus and fimbria volume were calculated by multiplying total area to spacing between sections (300 μm), based on the Cavalieri principle.

2.10 Morris Water Maze

3xTg and PS1 littermates were randomly assigned to TBI or sham groups and tested on the Morris water maze at either 1 month or 6 months following TBI or sham surgeries. Investigator was blinded to genotypes and injury status of the mice. Detailed descriptions of the test were as previously described (Brody et al., 2007). Briefly, the circular pool was 109 cm in diameter; the platform was 11 cm in diameter. The water was opacified using non-toxic white paint. Each mouse was given 60 seconds to swim to find a visible platform above the water surface, marked with a pole. Training was repeated 4 times per day for 3 days. Then, mice were trained to locate a hidden platform which was submerged 0.5 cm below the water surface. Training took 4 days, 4 trials per day, and 60 seconds per trial. On the 5^{th} day, the platform was removed and a single probe trial lasting 30 seconds was performed; time spent swimming in the target quadrant where the platform was located was recorded.

2.11 Statistical Methods

All histological data were analyzed using Prism 5.0 (GraphPad Sofware, Inc). Shapiro Wilk tests were used to assess normal distribution of data. Mann Whitney U-tests were used to compare levels of Aβ and phospho-tau in hippocampal lysates of injured and sham 3xTg-AD mice, since the distribution of data was not normal. For pairwise comparisons of quantitative immunochemical data (e.g. injured vs. sham, drug vs. vehicle), one-sided Student's t-tests were used in these cases because unidirectional hypotheses were pre-specified. For changes of either Aβ or tau pathology as function of time or injury severities, one-way ANOVAs with Newman-Keuls post tests were

used because there were no prespecified hypotheses about the direction of change. For pairwise comparisons of Aβ immunohistochemical data between injured 3xTg-AD and APP/PS1 mice, and of tau immunohistochemical data between 3xTg-AD and Tau_{P301L} mice, student's t-tests were employed. Kruskal-Wallis with Dunn's post hoc tests were used for pairwise comparison of hippocampal and fimbria volumes between groups. Values are expressed as means ± SEM. Statistical significance was set at $p < 0.05$.

For pairwise comparisons of levels of tau kinases via western blot and immunohistochemistry and phosphatase activity between TBI and sham mice, two-tailed student's t-tests were used; p values of < 0.05 were considered significant. For comparisons of staining areas covered by activated kinases in the fimbria/fornix, a one-way ANOVA with Neuman-Keuls post-test was used. Values are expressed as means ± SEM.

For pairwise comparisons of quantitative histological data of D-JNKi1 experiments (e.g. D-JNKi vs. D-TAT), one-sided Student's t-test were used because unidirectional hypotheses were prespecified. There was a trend toward reduced tau pathology when we first analyzed results from 5 D-JNKi1 and 4 D-TAT treated mice. Therefore, additional 4 mice were added to each group, and data were re-analyzed. As such, statistical significance for these analyses was set to $p < 0.025$ due to the optional stopping design of the experiment. Values are expressed as means ± SEM.

Behavioral data were analyzed using Statistica 6.0 (Stat-Soft). Repeated measures ANOVA was used to compare visible and hidden platform performance on the Morris water maze task. Statistical significance was set to be < 0.05. Values are means ± SEM, unless otherwise noted.

Chapter 3

Characterization of the Acute Aβ and Tau Pathologies post TBI in Young 3xTg-AD Mice

3.1 Introduction

Traumatic brain injury (TBI) is a strong environmental risk factor for subsequent development of a number of neurodegenerative diseases, including Alzheimer's disease (AD). Pathological hallmarks of AD are extracellular deposition of amyloid-β (Aβ) plaques and intracellular accumulation of neurofibrillary tangle (NFT) containing hyperphosphorylated tau protein. Accumulations of Aβ and tau proteins are also thought to be among secondary insults that cause undesirable cognitive outcomes following TBI. Specifically, intra-axonal Aβ accumulation has been observed within hours to days following TBI in brains of young individuals who do not have preexisting neurodegeneration (Clinton et al., 1991; Roberts et al., 1991; Uryu et al., 2002; Smith et al., 2003b; Smith et al., 2003d; Chen et al., 2009). In addition, co-accumulations of APP, BACE1 (β-secretase), PS1, caspase-3, and Aβ have been observed in injured axons of human TBI patients (Smith et al., 2003c; Chen et al., 2009). These data provide basis for TBI, particularly traumatic axonal injury as the underlying mechanism for post-traumatic increase in Aβ production and aggregation. Moreover, accumulation of total and phospho-tau in injured axons have sometimes been observed in individuals

subjected to single severe TBI (Ikonomovic et al., 2004; Uryu et al., 2007). Meanwhile, exacerbation of NFT-containing tau has been extensively observed in individuals subjected to repetitive, concussive TBI (Corsellis and Brierley, 1959; Corsellis, 1989; Roberts et al., 1990; Geddes et al., 1999); this pathology positively correlates with cognitive impairments and brain atrophy. Thus, TBI can also play a causal role in acceleration of tau pathology. Although these post-traumatic Aβ and tau accumulations have been recapitulated in experimental TBI in pigs (Smith et al., 1999b), it is difficult to perform mechanistic studies using this model organism. Subsequently, attempts have been made to subject transgenic mice producing either human Aβ or tau to experimental TBI. For instance, acute increase in total Aβ in tissue homogenates has been observed in an APP transgenic line which has undergone controlled cortical impact TBI (Smith et al., 1998). Repetitive TBI has been shown to accelerate plaque pathology in another APP transgenic line at 16 weeks following injury (Uryu et al., 2002), while the same injury paradigm in a tau transgenic line only resulted in tau exacerbation in 1 of 12 animals (Yoshiyama et al., 2005). None of these models reliably reproduced both Aβ and tau features observed in humans, nor did they allow assessment of the interaction between human Aβ and tau (Johnson et al., 2010).

It is therefore crucial to develop a new experimental TBI mouse model to better understand pathophysiological mechanisms underlying the association of TBI to AD pathologies. Toward this end, we performed CCI TBI on young 3xTg-AD mice, a transgenic line that expresses both human forms of Aβ and tau. We characterized the acute spatial and temporal changes of Aβ and tau following injury in this section.

3.2 Characterization of the Acute Aβ Pathology following TBI in Young 3xTg-AD Mice

3.2.1 Axonal Aβ Pathology at 24 h post Injury in 3xTg-AD Mice

Acute intra-axonal Aβ accumulation is a prevalent feature of human traumatic axonal injury (Smith et al., 2003c; Uryu et al., 2007; Chen et al., 2009). Because of the age-related intra-axonal Aβ accumulation in 3xTg AD mice, we hypothesized that these animals would be useful in the assessment of TBI-related axonal Aβ pathology. More specifically, we hypothesized that experimental TBI would accelerate intra-axonal Aβ pathology in young 3xTg-AD mice. To test this hypothesis, we subjected these mice to controlled cortical impact TBI, as detailed (Brody et al., 2007). Mice were subjected to moderately severe injury: 2.0 mm below the dura. This resulted in significant hippocampal damage and behavioral deficits but low mortality, as described (Brody et al., 2007). Mice were sacrificed at 24 h following TBI; their brains were then processed and examined immunohistochemically for Aβ pathology. Negative controls included age-matched, sham 3xTg-AD mice (which underwent the same anesthesia and surgical procedures but were not injured), injured wild-type B6/SJL mice (2.0 mm), and omission of primary antibodies. The positive controls for Aβ staining were brain slices from 20 month old PDAPP mice (Games et al., 1995).

We found Aβ accumulations in pericontusional white matter of injured, young 3xTg-AD mice. The ipsilateral fimbria/fornix appeared to have the most prominent Aβ

accumulation (**Figure 3.1A**). These Aβ accumulations had spheroidal and 'beads-on-a-string' morphologies, consistent with the morphology of injured axons (**Figure 3.1D, G, J, M, P**).The specificity of this Aβ staining was confirmed with five Aβ specific antibodies: pan-Aβ against $A\beta_{15-30}$ (**Figure 3.1D**), monoclonal 3D6 against $A\beta_{1-5}$ (**Figure 3.1G**), monoclonal HJ3.4 against $A\beta_{1-13}$ (**Figure 3.1J**) polyclonal C-terminal antibody against $A\beta_{35-40}$ (**Figure 3.1M**), and polyclonal C-terminal antibody against $A\beta_{35-42}$ (**Figure 3.1P**). No Aβ staining was observed when primary antibodies were omitted (**Figure 3.1S**). No such axonal Aβ pathology was observed in sham (non-injured), age-matched 3xTg-AD mice (**Figure 3.1B, E, H, K, N, Q**), nor in injured wildtype mice (**Figure 3.1C, F, I, L, O, R**). Aβ was also observed in pericontusional hippocampal commissure, corpus callosum, and external capsule of injured 3xTg-AD mice, though to a lesser extent than the fimbria/fornix (**Figure 3.2**).

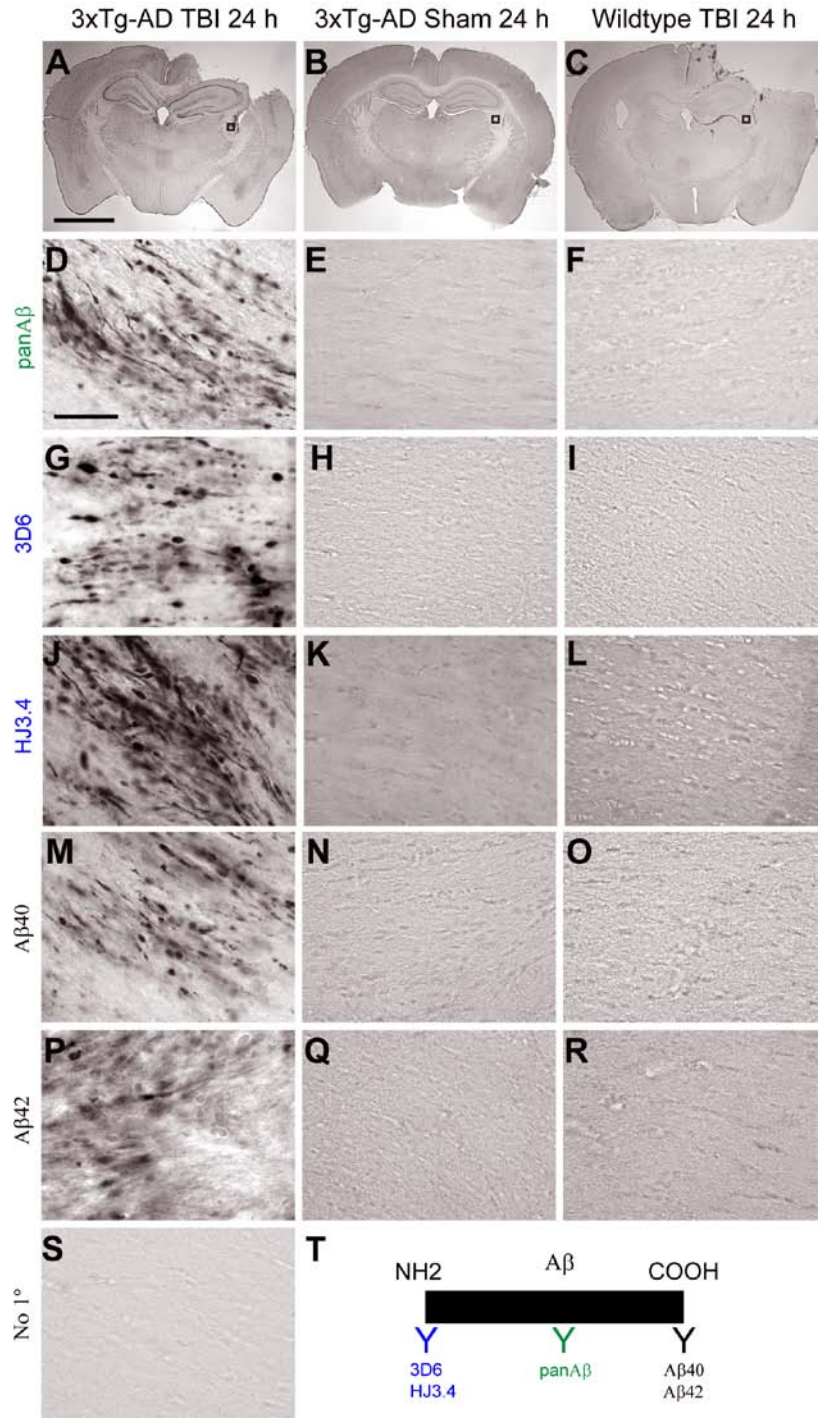

Figure 3.1 Controlled cortical impact TBI caused Aβ accumulation in ipsilateral fimbria/fornix of young 3xTg-AD mice.

A-C. Aβ immunohistochemistry from an injured 3xTg-AD mouse, a sham 3xTg-AD mouse, and an injured wildtype mouse, respectively. Scale bar: 2 mm. **D-R.** Higher magnification of the

ipsilateral fimbria/fornix (boxes in **A-C**). Scale bar: 50 μm. Presence of intra-axonal Aβ in the ipsilateral fimbria/fornix of a moderately injured 3xTg-AD mouse was confirmed using panAβ, a polyclonal antibody against amino acids 15-30 of Aβ (**D-F**), 3D6, a monoclonal N-terminus antibody against amino acids 1-5 of Aβ (**G-I**), HJ3.4, a monoclonal N-terminus antibody against amino acids 1-13 of Aβ (**J-L**), $Aβ_{40}$, a polyclonal C-terminus antibody against amino acids 35-40 of Aβ (**M-O**), and $Aβ_{42}$, a polyclonal C-terminus antibody against amino acids 35-42 of Aβ (**P-R**). No Aβ immunoreactivity was observed in sham 3xTg-AD mice and injured wildtype mice. **S.** No Aβ immunoreactivity was observed in injured 3xTg-AD mice when primary antibody was omitted. **T.** Schematic of anti-Aβ antibodies used.

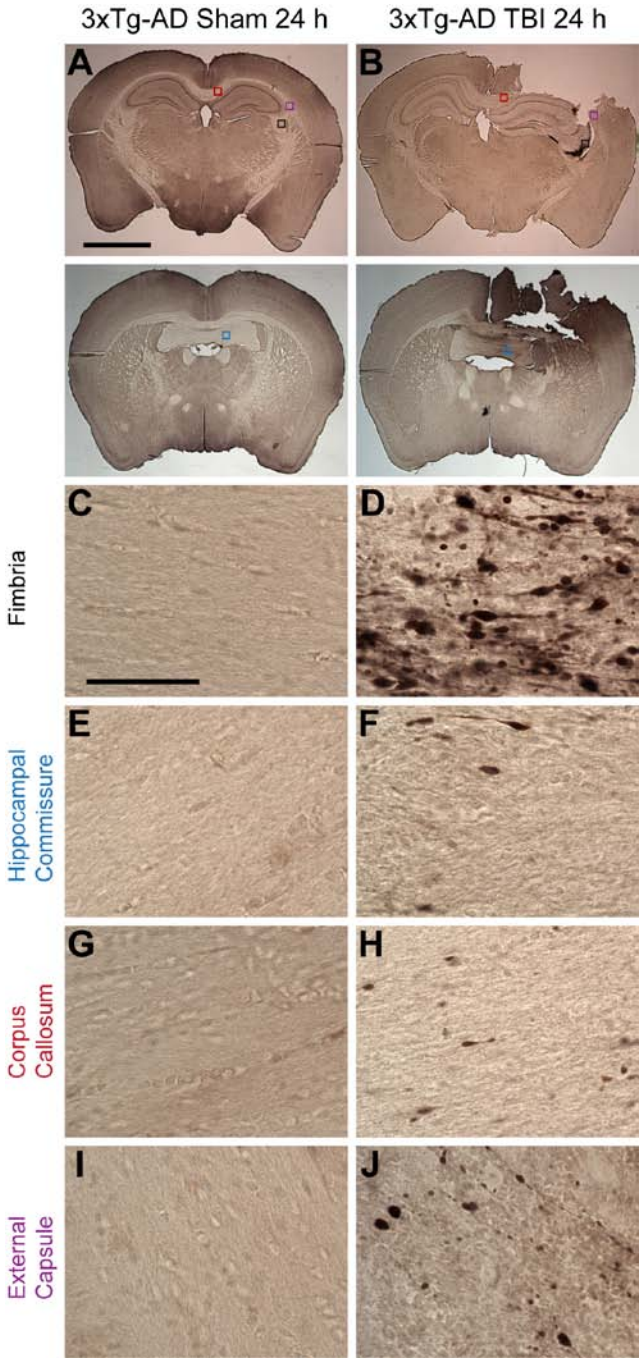

Figure 3.2 Controlled cortical impact TBI caused intra-axonal Aβ accumulation in pericontusional white matter tracts of young 3xTg-AD mice.

A-B. Aβ staining with panAβ antibody (against $Aβ_{15-30}$) in an uninjured (sham) and an injured (TBI) 3xTg-AD mouse. Scale bar: 2 mm. **C-J**. Higher magnification of intra-axonal Aβ accumulation in the ipsilateral fimbria (**C-D**, black box in **A-B**), ipsilateral hippocampal

commissure (**E-F**, blue box in **A-B**), ipsilateral corpus callosum (**G-H**, red box in **A-B**) and ipsilateral external capsule (**I-J**, purple box in **A-B**). Scale bar in C: 50 μm. Most prominent Aβ staining was observed in the ipsilateral fimbria/fornix of injured mice. Aβ staining has beads-on-a-string and varicose morphologies, consistent with morphologies of injured axons.

To further confirm the immunohistochemical findings, human specific $A\beta_{1-x}$, $A\beta_{1-40}$, and $A\beta_{1-42}$ ELISAs were employed to assess Aβ levels in hippocampal lysates of these moderately injured and sham 3xTg-AD mice. Both ipsilateral and contralateral hippocampi were assessed. These tissues were subjected to serial homogenization in TBS, Carbonate, and 5M Guanidine. This serial homogenization method produces extracts enriched in soluble Aβ from the extracellular compartment, soluble Aβ from intracellular compartments and residual insoluble Aβ, respectively. While there were similar levels of total Aβ ($A\beta_{1-x}$) in TBS and carbonate lysates in both ipsilateral and contralateral hippocampi (**Figure 3.3A-B**), a significant increase in insoluble total Aβ was detected in 5M Guanidine ipsilateral hippocampal lysates of injured as compared to sham 3xTg-AD (Mann Whitney U-test, $p = 0.0047$, **Figure 3.3C**). There was a non-significant trend toward increased Guanidine total Aβ levels in the contralateral hippocampi of injured mice compared to sham (**Figure 3.3C**). Furthermore, we found a significant increase in $A\beta_{1-40}$ and a trend toward increased $A\beta_{1-42}$ in the ipsilateral hippocampal lysates of injured 3xTg-AD mice (**Figure 3.3D-E**). Overall, these data are concordant with the immunohistochemical evidence of intracellular Aβ accumulation following TBI in these mice.

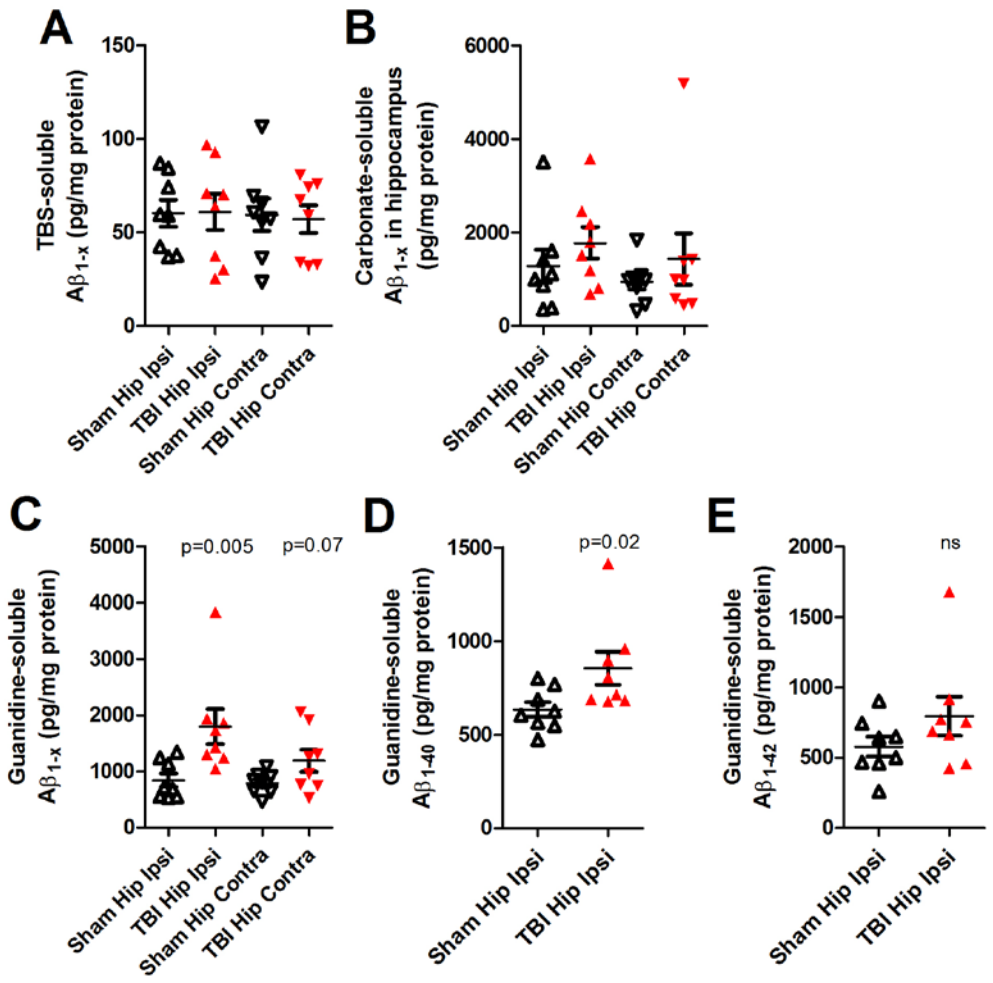

Figure 3.3 Controlled cortical impact TBI resulted in increased levels of relatively insoluble Aβ in 3xTg-AD mice.

Ipsilateral and contralateral hippocampal tissues of injured (2.0 mm) and sham 3xTg-AD mice were sequentially homogenized in TBS, carbonate, and guanidine buffers. TBS and carbonate lysates contain mostly soluble Aβ species; guanidine lysates are composed of relatively insoluble Aβ species. **A.** Total Aβ levels in TBS lysates of ipsilateral and contralateral hippocampi of sham and injured mice. **B.** Total Aβ levels in Carbonate lysates of ipsilateral and contralateral hippocampi of sham and injured mice. **C.** Total Aβ levels in guanidine lysates ipsilateral and contralateral hippocampi of sham and injured mice. Significantly more total Aβ levels were observed ipsilateral hippocampi, but not contralateral hippocampi of injured than sham mice (*** $p = 0.0047$, Mann Whitney U-test). **D.** $A\beta_{1\text{-}40}$. **E.** $A\beta_{1\text{-}42}$ levels in guanidine lysates of

ipsilateral hippocampi of sham and injured mice. Significantly more $A\beta_{1-40}$ and a trend toward increase in $A\beta_{1-42}$ were observed in ipsilateral guanidine hippocampal lysates of injured compared to sham mice (* $p = 0.013$, ns: not significant, Mann Whitney U-test). N = 7-8 mice per group. Bars represent mean ± SEM.

To summarize, intra-axonal Aβ accumulation appeared consistently in 3xTg-AD mice following experimental TBI. This intra-axonal Aβ appeared to be in a relatively insoluble form.

3.2.2 Axonal Aβ Pathology from 1 h to 24 h post TBI in 3xTg-AD Mice

Since Aβ accumulation has been detected as early as 2 h post TBI in humans (Ikonomovic et al., 2004), we tested the hypothesis that TBI causes very early axonal Aβ accumulation in 3xTg-AD mice by sacrificing independent groups of mice at 1, 6, 9, 12, and 24 h post injury. We analyzed Aβ axonal pathology with HJ3.4 antibody against $A\beta_{1-13}$ in these studies. To demonstrate that HJ3.4 recognizes only Aβ, but not APP, we performed an immunoprecipitation, followed by a Western blot analysis. Identical aliquots (100 μg) from brain lysates of a 9 month-old 3xTg-AD mouse was immunoprecipitated with monoclonal HJ3.4, 82E1, 6E10 antibodies, or no primary antibody control. Monoclonal 82E1 has been previously shown to be specific for Aβ (Osawa et al., 2008; Winton et al., 2011), while monoclonal 6E10 antibody can recognize both Aβ and APP (Winton et al., 2011). The resultant immunodepleted supernatants were subjected to Western blotting with 6E10 antibody. Our data demonstrated that HJ3.4 antibody, similar to 82E1 antibody, does not recognize APP (**Figure 3.4 A**). We found Aβ in injured axons at all time points following injury

(**Figure 3.4 C-G**). Morphologies of Aβ-positive axonal varicosities evolved from small swellings observed at 1 and 6 hours after injury (**Figure 3.4 C-D**) to larger spheroids, bulbs, and beaded varicose fibers at the later times (9, 12, and 24 h post TBI, **Figure 3.4 E-G**). Stereological quantification revealed moderate numbers of injured axons with Aβ accumulation in some but not all mice at the earliest time points examined (1 h and 6 h after injury, **Figure 3.4 H**). However, substantially greater numbers of Aβ-immunoreactive axonal varicosities were present at later time points, and all mice sacrificed between 9 and 24 hours had this pathology (9, 12, and 24 h, **Figure 3.4 H**). The increase in Aβ-positive axonal varicosities between 6 and 9 hours after TBI was statistically significant, as was the increase between 12 and 24 hours (**Figure 3.4 H,** $p < 0.05$).

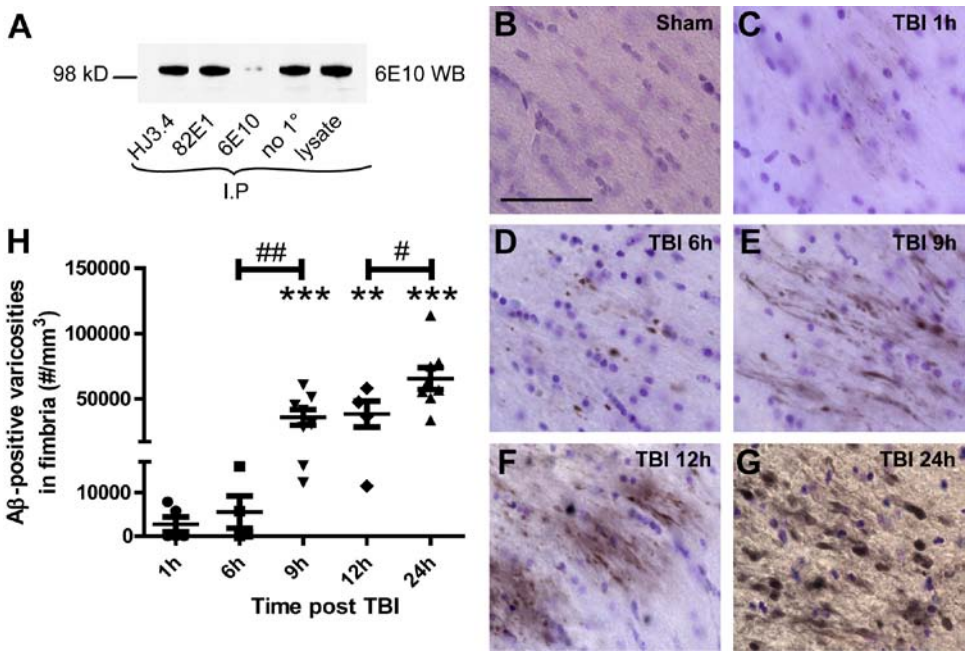

Figure 3.4 Intra-axonal Aβ accumulation monotonically increased from 1 to 24 hours post injury in 3xTg-AD mice.

A. Immunoprecipitation (I.P) and Western blot (WB) showed that HJ3.4 antibody, similar to 82E1 antibody, did not recognize APP, while, 6E10 antibody recognized APP; work done by TJ

Esparza. **B.**.Aβ staining with biotinylated HJ3.4 antibody (against $A\beta_{1-13}$) in the ipsilateral fimbria/fornix of a sham 3xTg-AD mouse. Sections were counterstained with cresyl violet. Scale bar: 50 μm.**C-G.** Aβ staining in the ipsilateral fimbria/fornix of an injured 3xTg-AD mouse at 1 h (**C**), 6 h (**D**), 9 h (**E**), 12 h (**F**) and 24 h (**G**) after TBI. **H.** Stereological quantification of total numbers of Aβ-positive axonal varicosities as a function of time after injury in 3xTg-AD mice. N = 4-8 mice per group per time point. Bars represent mean ± SEM. One-way ANOVA with Newman-Keuls post tests, # $p < 0.05$, ## $p < 0.01$: significant increase from injured mice from previous time point. ** $p < 0.01$, *** $p < 0.0001$: significant increase from sham mice at same time point.

In summary, controlled cortical impact TBI consistently accelerated Aβ axonal accumulation in young 3xTg-AD mice. Aβ accumulation appeared as early as 1 h post TBI, and continued to rise through 24 h.

3.2.3 Aβ Pathology as a Function of Injury Severity

Previous studies have found that more severe TBI results in more APP accumulation in damaged axons (Blumbergs et al., 1994; Bramlett et al., 1997). Since Aβ is derived from proteolytic cleavage of APP and accumulates in axons of 3xTg-AD mice following TBI, we hypothesized there would be a correlation between axonal injury severity and extent of Aβ accumulation in these mice. To test this hypothesis, we performed additional mild (1.0 mm impact below dura) and mild-moderate (1.5 mm impact below dura) injuries on 3xTg-AD mice. We compared Aβ and APP-labeled axonal pathologies among the mild, mild-moderate, and moderate (2.0 mm) TBI groups using immunohistochemistry and stereological quantification.

We found that both APP and Aβ accumulations in pericontusional white matter were dependent on injury severity in young 3xTg-AD mice. Specifically, few injured axons stained for APP were found in the ipsilateral fimbria/fornix of mildly injured

3xTg-AD mice (1.0 mm, **Figure 3.5 B, F**). Many more APP-stained axonal varicosities were observed in the same region in the other injured groups (1.5 mm and 2.0 mm, **Figure 3.5 C, D, G, H**), but none in the sham injured ones (**Figure 3.5 A, E**). Furthermore, we found a parallel relationship between the extent of the axonal injury and the amount of intra-axonal Aβ in the fimbria/fornix (**Figure 3.5 I-L**). Markedly fewer APP- and Aβ- stained varicosities were observed in other injured white matter regions such as the ipsilateral pericontusional hippocampal commissure, ipsilateral external capsule, and ipsilateral corpus callosum. In these other regions, the extent of both APP and Aβ staining was similarly dependent on injury severity (**Figure 3.6**).

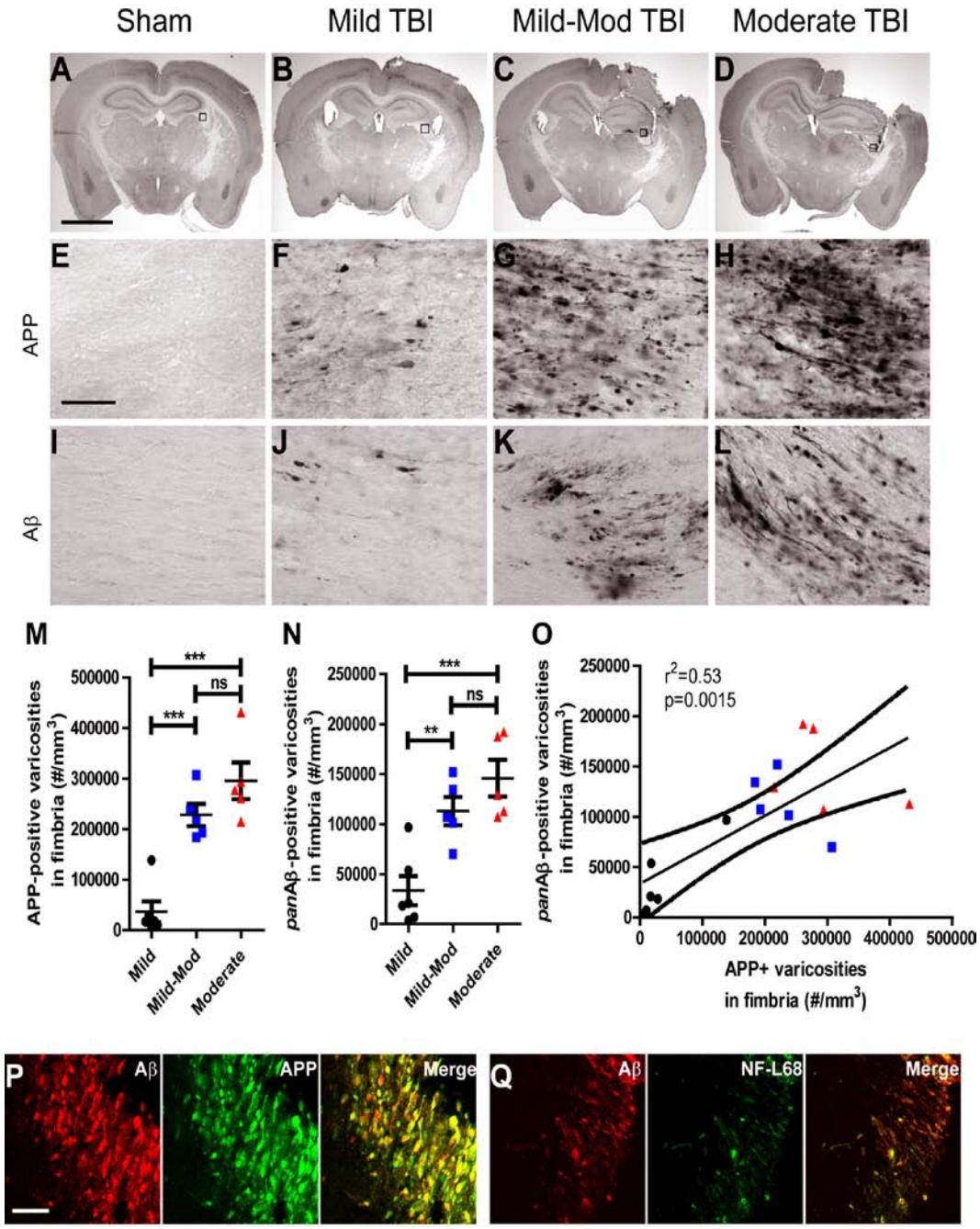

Figure 3.5 Aβ accumulation varied with injury severity and colocalized with markers of axonal injury in 3xTg-AD mice.

A-D. APP immunohistochemistry (IHC) of sham, mildly (1.0 mm), mild-moderately (1.5 mm), and moderately (2.0 mm) injured, young 3xTg-AD mice. Scale bar: 2 mm. **E-H.** Higher magnification of axonal injury detected by APP IHC in the ipsilateral fimbria (boxes in **A-D**).

Scale bar: 50 μm. **I-J.** Intra-axonal Aβ IHC in the ipsilateral fimbria using pan-Aβ antibody against $A\beta_{15\text{-}30}$. **M.** Stereological quantification of numbers of APP-stained varicosities per cubic mm of the ipsilateral fimbria as a function of injury severity. **N.** Stereological quantification of numbers of Aβ-stained varicosities per cubic mm of the ipsilateral fimbria as a function of injury severity. Bars represent mean ± SEM. One-way ANOVA with Newman-Keuls post-hoc test, ** $p < 0.01$, *** $p < 0.005$, ns: not significant. **O.** Pearson's correlation of numbers of Aβ- and APP-stained varicosities in injured fimbria, $r^2 = 0.53$, $p = 0.0015$. N = 5-6 mice per injury severity. **P.** Colocalization of Aβ with APP in injured fimbria of a 3xTg-AD mouse. Scale bar: 50 μm. **Q.** Colocalization of Aβ with neurofilament light chain 68kD (NF-L68), another marker of axonal injury, in injured fimbria of a 3xTg-AD mouse. Aβ was detected with monoclonal 3D6 antibody conjugated to Alexa Fluor® 594 (red). This antibody requires a free amino terminus of Aβ for binding and does not cross react with APP. APP and NF-L68 were visualized with secondary antibody conjugated to Alexa Fluor® 488 (green).

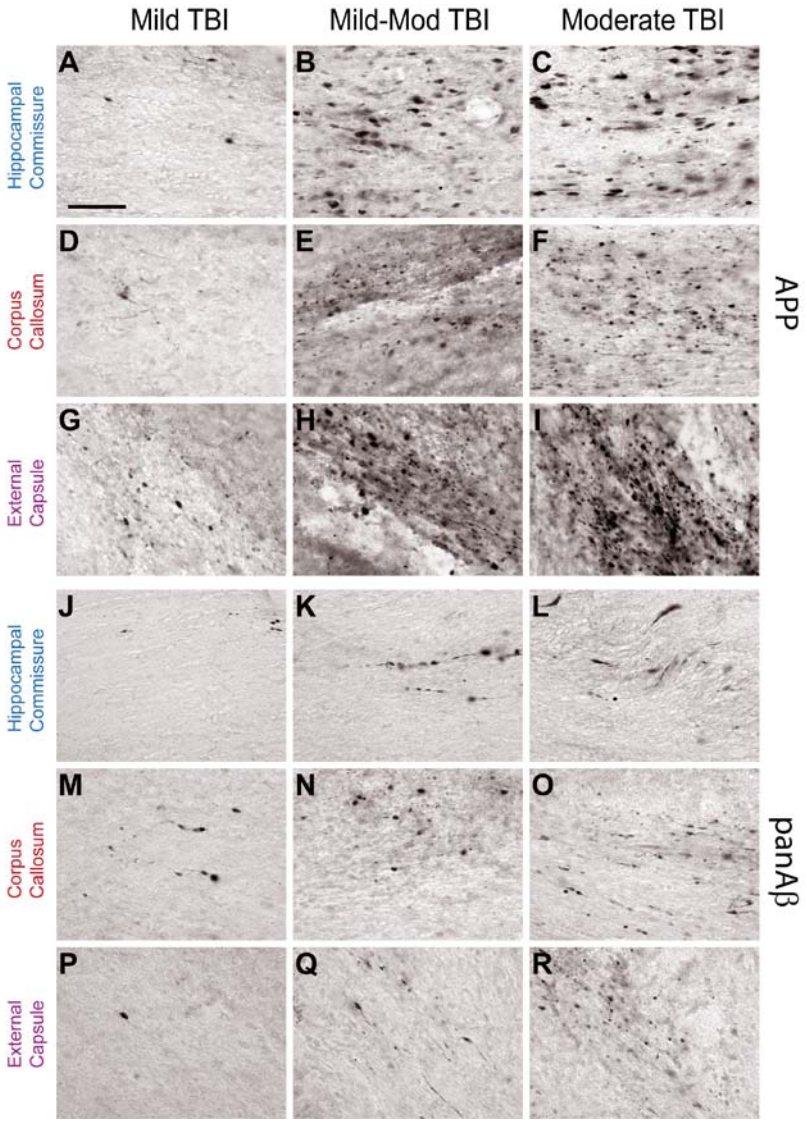

Figure 3.6 APP and Aβ accumulations in other white matter regions of injured 3xTg-AD mice varied with injury severity.

Aβ staining was performed with polyclonal panAβ antibody. **A-I.** APP staining of injured axons in hippocampal commissure **(A-C)**, corpus callosum **(D-F)**, and external capsule **(G-I)** of mice subjected to mild, mild-moderate, and moderate TBI, respectively. Scale bar: 50 μm. **J-R.** Aβ staining of injured axons in the hippocampal commissure **(J-L)**, corpus callosum **(M-N)**, and external capsule **(P-R)** of 3xTg-AD mice subjected to mild, mild-moderate, and moderate TBI.

To quantitatively characterize the observed relationship between injury severities and the extent of APP and Aβ accumulations in injured axons of the fimbria/fornix, we employed the optical fractionator stereological method. We found significantly more APP-stained varicosities in the mild-moderate and moderate TBI groups compared to the mild TBI group (**Figure 3.5 M,** One-way ANOVA, $p < 0.0001$).There was a trend toward increasing number of APP-stained varicosities in the moderate TBI group (2.0 mm) as compared to the mild-moderate TBI group (1.5 mm), but this was not statistically significant (**Figure 3.5 M**). A similar relationship between injury severities and numbers of Aβ-stained varicosities was observed: the more severe the injury, the more intra-axonal Aβ accumulation (**Figure 3.5 N,** One-way ANOVA, $p = 0.0005$). There was a statistically significant positive correlation between the numbers of APP- and Aβ-stained varicosities (**Figure 3.5 O,** Pearson $r^2 = 0.53$, $p = 0.0015$).

To determine definitively whether these accumulations of Aβ were found within injured axons, we performed double immunofluorescence labeling of Aβ and APP and separate double immunofluorescence with the 68kD neurofilament light chain subunit, NF-L68. APP and NF-L68 are well-established axonal markers and accumulations of both proteins are robust signatures of axonal injury (Gennarelli et al., 1982; Yaghmai and Povlishock, 1992; Gentleman et al., 1993; Grady et al., 1993; Christman et al., 1994; Sherriff et al., 1994a; Graham et al., 1995; Povlishock and Christman, 1995; Chen et al., 1999; Smith et al., 1999b; Stone et al., 2000, 2001; Marmarou et al., 2005). They have been shown to extensively colocalize with Aβ in injured axons from human TBI patients (Smith et al., 2003c; Uryu et al., 2007; Chen et al., 2009). We found that essentially all Aβ-immunoreactive axonal varicosities in injured 3xTg-AD mice were also

positive for APP and NF-L68 on confocal microscopy (**Figure 3.5 P-Q**). Aβ labeling was performed using the monoclonal anti-Aβ antibody 3D6 directly conjugated to Alexa Fluor® 594; 3D6 does not cross react with APP as it requires a free amino-terminus to bind (Johnson-Wood et al., 1997). No such colocalization was observed in sham 3xTg-AD mice (data not shown), nor when one of the primary antibodies was omitted (data not shown).

Thus, controlled cortical impact TBI in 3xTg-AD mice reproduced one of the hallmark features of human post-TBI neurodegenerative pathology: intra-axonal Aβ accumulation at sites of traumatic axonal injury. Moreover, Aβ colocalized with markers of axonal injury, and correlated with severity of axonal injury.

3.3 Characterization of the Acute Tau Pathology post TBI in 3xTg-AD Mice

3.3.1 Tau Pathology at 24 h post TBI in 3xTg-AD Mice

We next investigated the effects of TBI on tau accumulation and phosphorylation in the same injured and sham 3xTg-AD mice. We first performed immunohistochemistry using polyclonal tau antibody (pAb Tau) and monoclonal HT7 which recognize both normal and hyperphosphorylated human tau. Negative controls included injured wild-type mice and omission of primary antibodies. Brain slices from 12 month old 3xTg-AD mice served as a positive control.

In the pericontusional fimbria/fornix, abnormal punctate tau immunoreactivity was observed following moderate TBI in 3xTg-AD mice (**Figure 3.7 A, D**). There was minimal tau staining in the same region of sham injured mice (**Figure 3.7 B, E**), and

none in moderately injured wildtype mice (**Figure 3.7 C, F**). Interestingly, there were two additional regions in which there were marked increase in tau immunoreactivity in injured as compared to sham 3xTg-AD mice. These were the ipsilateral amygdala and contralateral CA1 regions (**Figure 3.7 A-B, G-H, J-K**). Tau immunoreactivity in the amygdala had a perinuclear cytoplasmic distribution, while that in the contralateral CA1 took the appearance of elongated neurites. These regions are distant from the site of injury but are anatomically connected to the ipsilateral hippocampus via the ipsilateral fimbria/fornix tract (Witter and Amaral, 2004). Similar patterns of tau staining were observed in injured and sham 3xTg-AD mice when monoclonal HT7 against total tau was used (**Figure 3.7 M-N, P-Q, S-T**). No total tau immunoreactivity was observed in injured wildtype mice (**Figure 3.7 C, F, I, L, O, R, U**). Total tau immunoreactivity in the ipsilateral hippocampus was not significantly affected by TBI in these mice (data not shown).

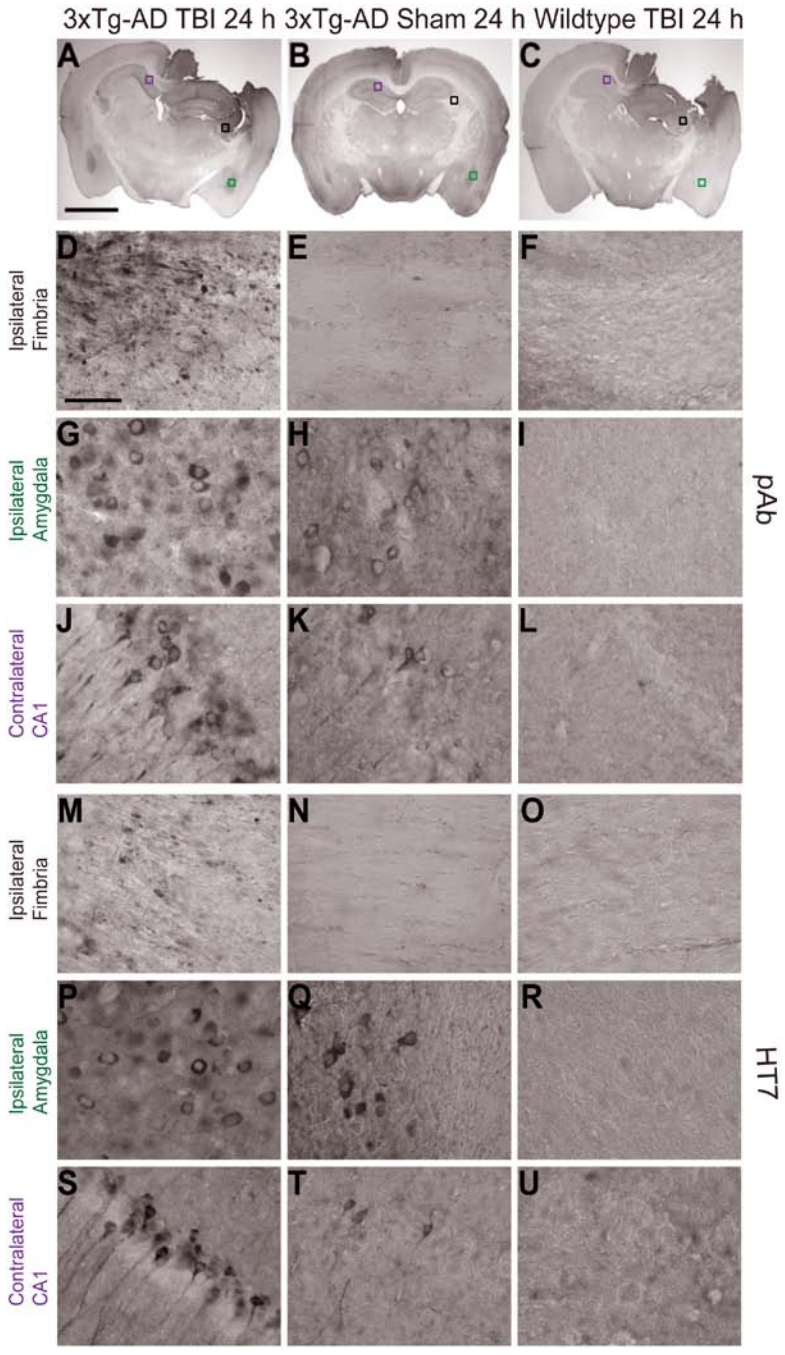

Figure 3.7 TBI accelerated tau pathology in young 3xTg-AD mice.

Total tau (independent of phosphorylation state) was detected with polyclonal total tau antibody (pAb Tau) and HT7 monoclonal antibody. **A-C.** pAb tau staining in injured 3xTg-AD mice, sham 3xTg-AD mice and injured wildtype mice, respectively. **D-F.** Higher magnification of the ipsilateral fimbria (black boxes in **A-C**). **G-I.** Higher magnification of the ipsilateral amygdala

(green boxes in **A-C**). **J-L.** Higher magnification of the contralateral CA1 (purple boxes in **A-C**). **M-U.** Total tau staining using HT7 antibody. More tau-positive puncta were observed in ipsilateral fimbria of injured 3xTg-AD mice compared to sham 3xTg-AD mice. More tau-positive somata were present in ipsilateral amygdala of injured compared to sham 3xTg-AD mice. More tau-positive processes were also observed in the contralateral CA1 of injured compared to sham 3xTg-AD mice. No tau immunoreactivity was observed in injured wildtype mice.

To test whether TBI increased the extent of tau phosphorylation in 3xTg-AD mice, we performed additional immunohistochemical studies using polyclonal antibodies against phosphorylated tau in sham and moderately injured mice. Injured mice exhibited more phospho-tau staining than sham mice for all the phospho-tau antibodies used. Specifically, phospho-S199 tau was observed in ipsilateral hippocampal CA1 and fimbria of moderately injured mice (**Figure 3.8 A, C**). Immunoreactivity for phospho-T205 was prominent in ipsilateral fimbria only (**Figure 3.8 E**). Tau also appeared to be heavily phosphorylated at T231, S396, and S422 in fimbria of 3xTg-AD mice following TBI (**Figure 3.8 G, I, K**). No phospho-tau immunoreactivity was observed in sham 3xTg-AD mice at 6 months of age (**Figure 3.8 B, D, F, H, J, L**).

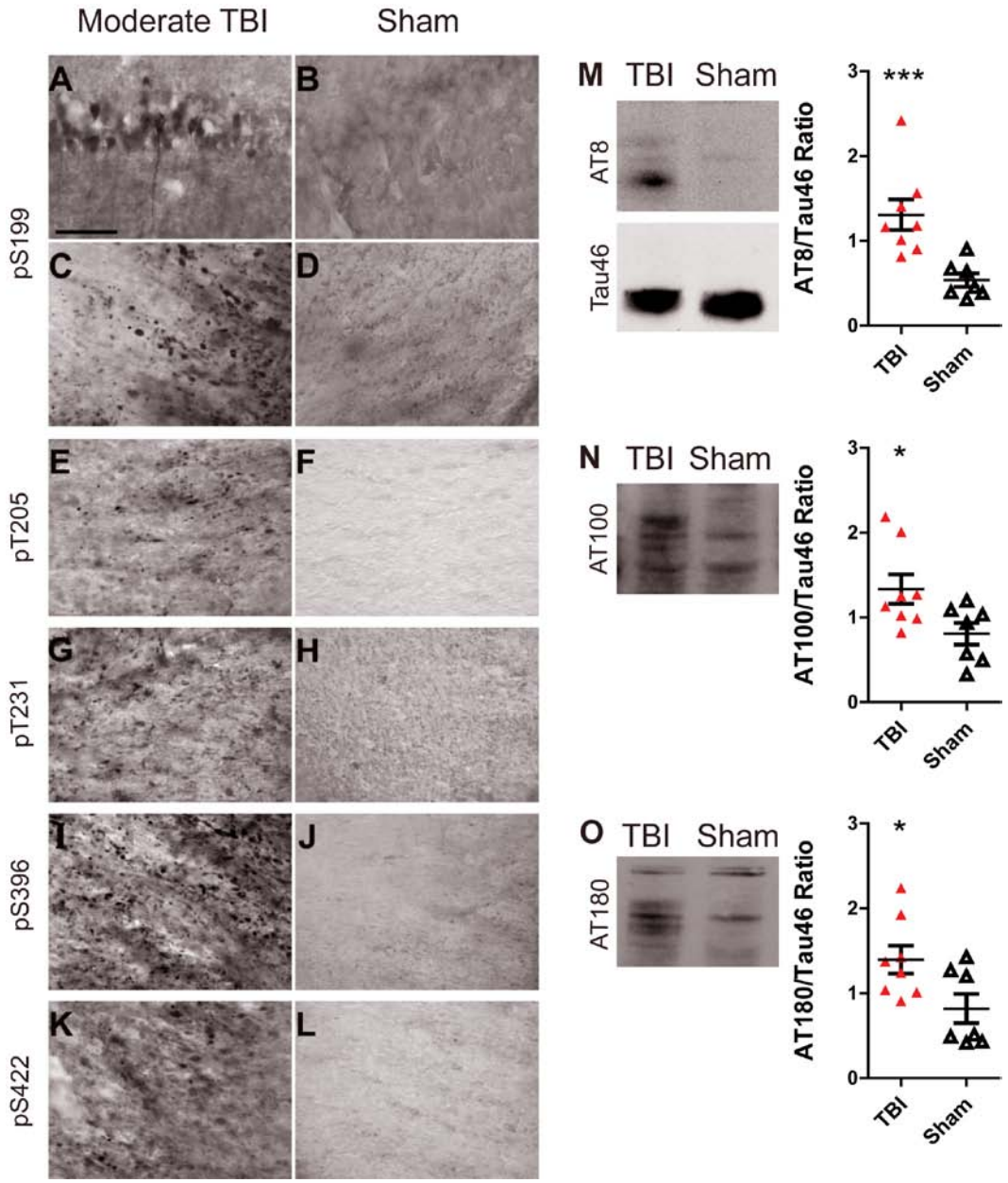

Figure 3.8 Controlled cortical impact TBI increased levels of phospho-tau immunoreactivity in ipsilateral hippocampi and fimbria of young 3xTg-AD mice. **A-D.** Tau staining of moderate TBI (2.0 mm) and sham 3xTg-AD mice using polyclonal antibody against phosphorylated tau at S199. Scale bar: 50 μm. **A-B.** Ipsilateral hippocampal CA1. **C-D.** Ipsilateral fimbria. **E-L.** Phospho-tau staining in fimbria of TBI and sham 3xTg-AD mice using polyclonal antibodies against tau phosphorylated at T205 (**E-F**), T231 (**G-H**), S396 (**I-J**), and S422 (**K-L**). **M.** Representative AT8 western blot of ipsilateral hippocampi from 2.0

mm TBI and sham 3xTg-AD mice. AT8 blots were stripped and reprobed with Tau46 antibody for total tau. A significant increase in ratio of AT8 to Tau46 band densities was observed following TBI. (*** $p = 0.0006$, Mann-Whitney U Test) **N.** Representative AT100 western blot of ipsilateral hippocampi from 2.0 mm TBI and sham 3xTg-AD mice. A significant increase in ratio of AT100 to Tau46 band densities was observed following TBI. (* $p = 0.03$, Student's t-test). **O.** Representative AT180 western blot of ipsilateral hippocampi from 2.0 mm TBI and sham 3xTg-AD mice. A significant increase in ratio of AT180 to Tau46 band densities was observed following TBI. (* $p = 0.03$, Student's t-test.) N = 7-8 mice per group. Bars represent mean ± SEM.

To further confirm these findings, separate groups of sham and moderately injured mice were sacrificed at 24 h by rapid decapitation. Bilateral hippocampi were quickly removed and frozen. Tissue were homogenized in RIPA buffer and subjected to western blotting using the monoclonal AT8 antibody against phosphorylated tau at S199 or S202 and T205, the AT100 antibody against phosphorylated tau at T212 and S214, and the AT180 antibody against phosphorylated tau at T231 (Mercken et al., 1992). Blots were stripped and reprobed with the Tau46 antibody to quantify total tau.

We found marked increases in the densities of AT8, AT100, and AT180 immunoreactive bands in injured compared to sham 3xTg-AD mice, indicating an increase in levels of tau phosphorylation (**Figure 3.8 M-O**). Total tau levels in these samples appeared slightly lower in the injured mice (**Figure 3.8 M**). Overall, there were approximately two-fold increases in the ratio of AT8, AT100, and AT180 immunoreactive phospho-tau band densities to total tau band densities following TBI in 3xTg-AD mice (**Figure 3.8 M-O,** Mann Whitney U-test, $p < 0.05$). No such immunoreactivity for tau was observed when primary antibody was omitted (**Figure 3.9**

A). No increases in tau phosphorylation were detected in contralateral hippocampal lysates (**Figure 3.9 B-C**).

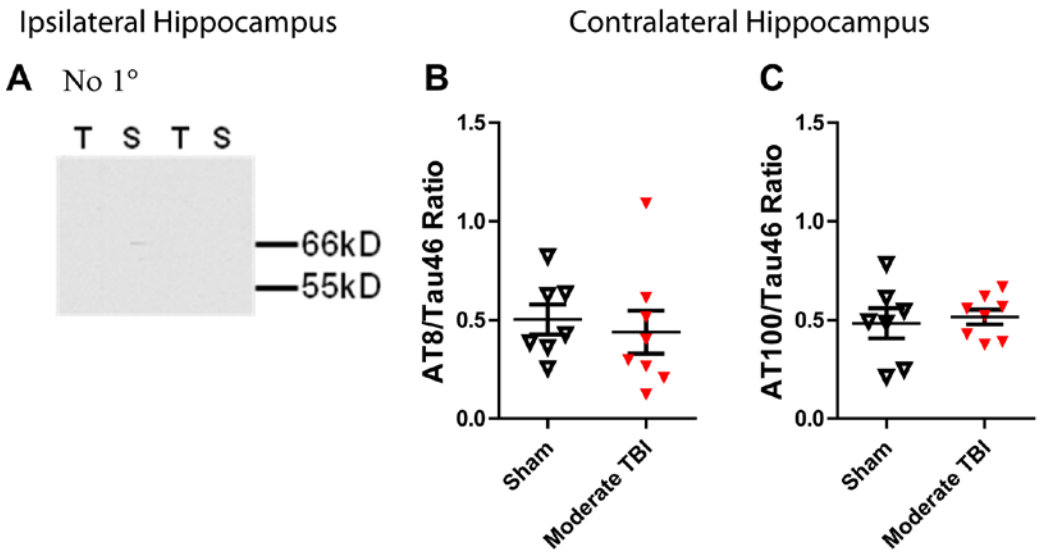

Figure 3.9 Negative control and western blotting of contralateral hippocampal lysates. **A.** Negative control: Western blot of hippocampal lysates from moderate TBI (T) and sham (S) 3xTg-AD mice when primary antibody was omitted and secondary anti-mouse antibody-conjugated to HRP was applied. No signal was observed. **B.** Ratio of AT8 to Tau46 from contralateral hippocampal lysates of injured and sham mice. **C.** Ratio of AT100 to Tau46 from contralateral hippocampal lysates of injured and sham mice. Bars represent mean ± SEM. N=7-8 mice per group. Student's t-tests, not significant.

In summary, experimental TBI caused increased tau immunoreactivity in young 3xTg-AD mice. Notably, the spatial distribution of TBI-related changes in tau immunoreactivity was distinct from those of post-injury Aβ. Levels of tau phosphorylation were significantly increased following TBI, based on both biochemical and immunohistochemical analyses.

3.3.2 Tau Pathology from 1 h to 24 h post TBI in 3xTg-AD Mice

We investigated the temporal patterns of tau accumulation in ipsilateral fimbria, ipsilateral amygdala, and contralateral CA1 using the same mice used to assess the time course of Aβ described above. We quantitatively characterized the time course of tau immunoreactive changes using stereological methods (**Figure 3.10 I, P, W**). In the ipsilateral fimbria, there were significantly elevated numbers of tau-positive puncta at 1 h and 24 h, but not at 6 h – 12 h following injury (**Figure 3.10 C-H**). In sham mice, there were 3,420 ± 919, whereas at 1 h post injury, there were 69,641 ± 8,496 ($p < 0.05$) and at 24 h there were 138,887 ± 35,543 ($p < 0.0001$) tau-stained puncta per cubic millimeter of fimbria (**Figure 3.10 I**).

Tau immunoreactivity in cell bodies of the ipsilateral amygdala exhibited a similar biphasic time course: the numbers of immunoreactive cell bodies were increased at 1 h following injury (**Figure 3.10 K**), came back to sham levels from 6 h to12 h (**Figure 3.10 L-N**), and rose again at 24 h (**Figure 3.10 O**). Since there was substantial tau immunoreactivity in sham 3xTg-AD mice in this region (**Figure 3.10 J**), stereological quantification of numbers of tau-positive somata was expressed as percent of sham. While numbers of tau-positive cell bodies from 6 h to 12 h after injury were similar to sham, significantly more were apparent at 1 h and 24 h in ipsilateral amygdala after injury (**Figure 3.10 P**, $p < 0.05$).

Interestingly, the temporal profile of tau-positive processes in the contralateral hippocampal CA1 region followed a different pattern, with a delayed monophasic rise. Specifically, the extent of tau immunoreactivity in contralateral CA1 in uninjured 3xTg-

AD mice and injured mice sacrificed from 1 h to 9 h following injury appeared similar (**Figure 3.10 Q-T**). From 12 h after TBI, however, tau immunoreactivity in this region increased (**Figure 3.10 U-V**). Stereological quantification of total length of tau-positive process using the spherical probes (also known as 'spaceballs') method indicated a significant increase from sham starting at 12 h following injury (**Figure 3.10 W**, $p < 0.05$); this measure stayed elevated at 24 h (**Figure 3.10 V, W**).

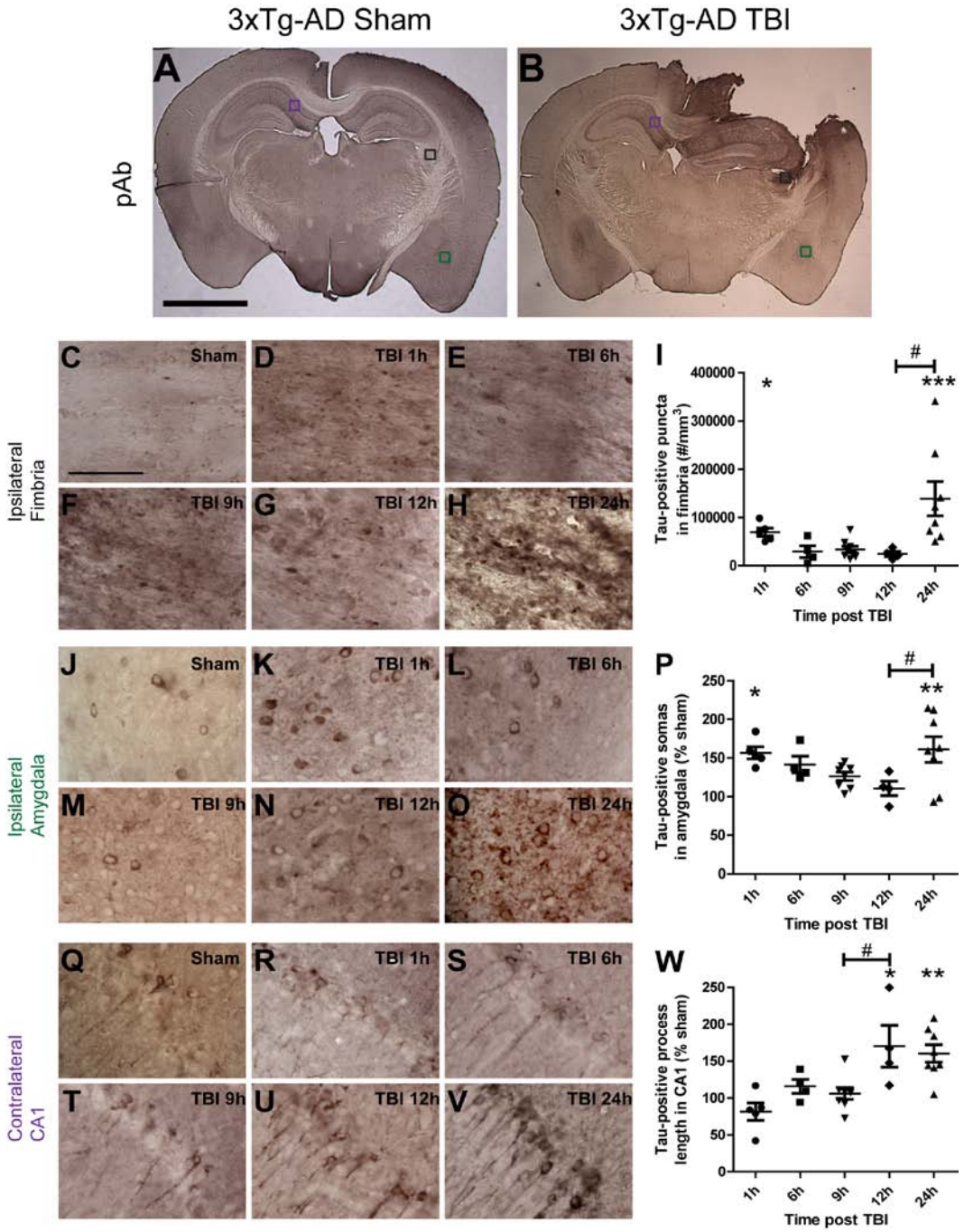

Figure 3.10 Time course of TBI-induced tau pathology was distinct in several brain structures of 3xTg-AD mice.

Tau staining was with polyclonal total tau antibody. **A-B.** Tau staining in a sham (**A**) and an injured (**B**) 3xTg-AD mouse. Three regions with accelerated tau pathology compared to sham at 24 h post TBI were the ipsilateral fimbria/fornix (black box), ipsilateral amygdala (green box),

and contralateral CA1 (purple box). Scale bar: 2 mm. **C-H.** Higher magnification of punctate tau staining in the ipsilateral fimbria (black box in **A-B**) of a sham (**C**) and injured 3xTg-AD mice at 1 h (**D**), 6 h (**E**), 9 h (**F**),12 h (**G**), and 24 h (**H**) following TBI. Scale bar in C: 50 μm. **I.** Stereological quantification of numbers of tau-positive puncta per cubic millimeter in ipsilateral fimbria as a function of time post injury. **J-O.** Perinuclear, cytoplasmic tau staining in somata of the ipsilateral amygdala (green box in **A-B**). **P.** Stereological quantification of numbers of tau-positive somata per cubic millimeter in the ipsilateral amygdala as a function of time post injury. **Q-V.** Tau staining in processes of the contralateral CA1 (purple box in **A-B**). **W.** Stereologcial quantification of tau-positive processes of CA1 pyramidal neurons per cubic millimeter as a function of time post injury. N = 4-8 mice per group per time point. Bars are mean ± SEM in fimbria, and percent of sham ± SEM for amygdala and CA1 region. One-way ANOVA with Newman-Keuls post tests, * $p < 0.05$, ** $p < 0.01$, *** $p < 0.001$: significant increase from sham mice at same time point. # $p < 0.05$: significant increase from injured mice at previous time point.

Thus, experimental TBI increased tau immunoreactivity in a multifocal fashion in the brains of 3xTg-AD mice. A two-phase increase in tau immunoreactivity was observed at 1 hour and 24 hours after TBI in the ipsilateral fimbria and ipsilateral amygdala, while only a single phase was observed at 12-24 hours in the contralateral hippocampal CA1 region. Notably, the spatiotemporal distribution of TBI-related changes in tau immunoreactivity was distinct from those of post-injury Aβ accumulation.

3.3.3 Effects of Injury Severity on Tau Pathology at 24 h post TBI in 3xTg-AD Mice

Next, we examined the effects of varying injury severity on total tau pathology in 3xTg-AD mice (**Figure 3.11 B-D**). Abnormal tau-positive puncta in the ipsilateral fimbria appeared to increase in an injury severity dependent manner (**Figure 3.11 F-H**).

There was minimal tau staining in the same region of sham injured mice (**Figure 3.11 A, E**). Only in the moderate TBI group were there more tau-positive somata in the ipsilateral amygdala and tau-positive neurites in the contralateral CA1 (**Figure 3.11 I-P**). No tau immunoreactivity was observed in injured 3xTg-AD mice when the primary antibody was omitted (data not shown).

Quantitative analyses of tau immunoreactivity in these regions using stereology confirmed the qualitative histological findings. There were significantly more tau-positive puncta in ipsilateral fimbria/fornix as the injury became more severe (**Figure 3.11 Q,** One-way ANOVA, $p < 0.0001$). In the moderately injured group (2.0 mm), there was a significant increase in tau-positive somata in the ipsilateral amygdala compared to other TBI and sham groups (**Figure 3.11 R,** One-way ANOVA, $p = 0.008$). Likewise, tau-positive neurite length density in the contralateral CA1 of these moderately injured mice was significantly greater than the length density in the other groups (**Figure 3.11 S,** One-way ANOVA, $p = 0.0079$).

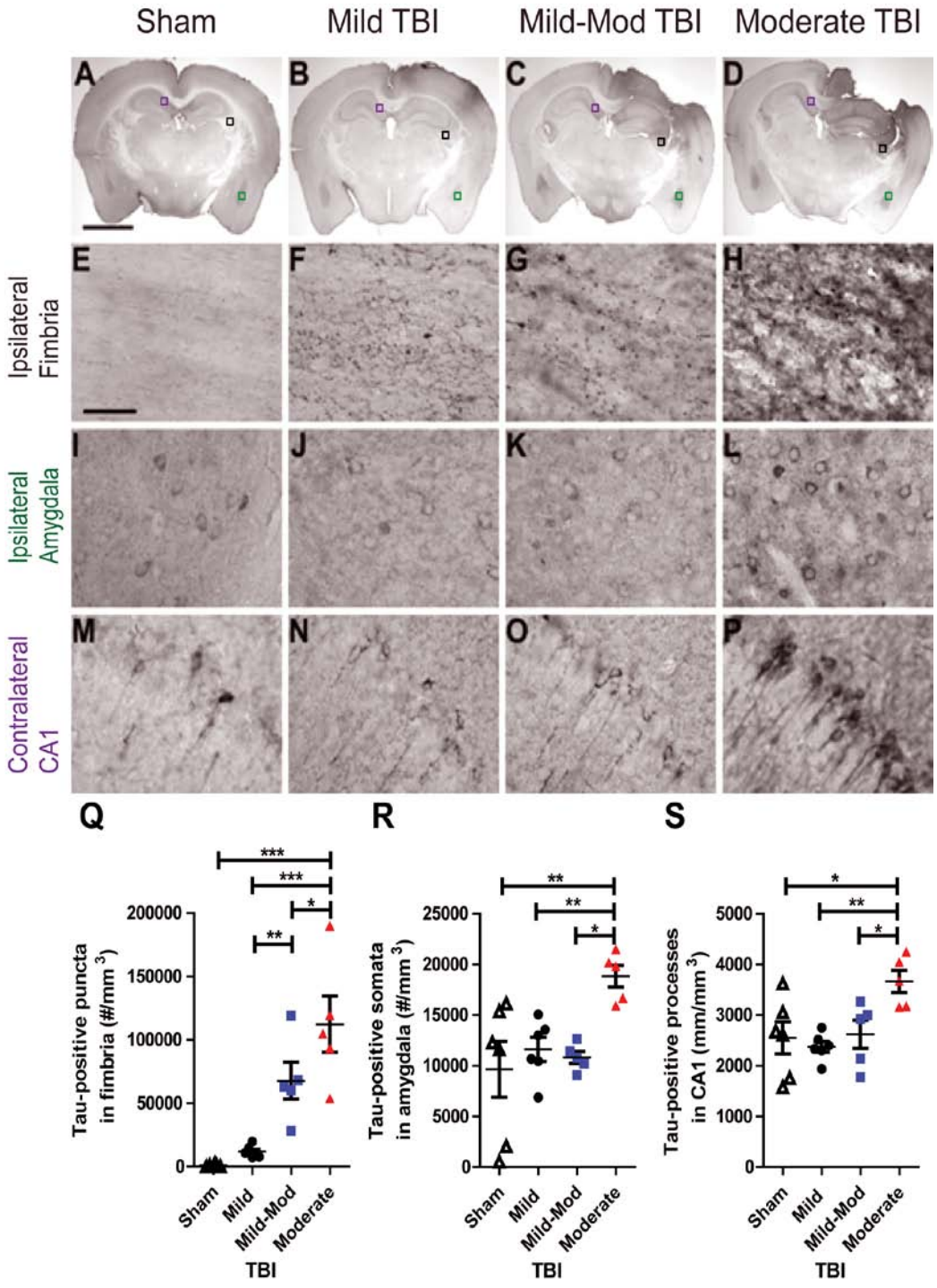

Figure 3.11 Tau pathology varied with injury severity in young 3xTg-AD mice.

A-D. pAb Tau IHC of sham, mildly (1.0 mm), mild-moderately (1.5 mm), and moderately (2.0 mm) injured, young 3xTg-AD mice. Scale bar: 2 mm. **E-H.** Higher magnification of tau staining

in the ipsilateral fimbria (black boxes in **A-D**). Scale bar: 50 μm. **I-L.** Higher magnification of tau staining in the ipsilateral amygdala (green boxes in **A-D**). **M-P.** Higher magnification of tau staining in the contralateral CA1 (purple boxes in **A-D**). **Q.** Stereological quantification of numbers of tau-stained punctate varicosities per cubic mm of the ipsilateral fimbria as a function of injury severity. **R.** Stereological quantification of numbers of tau-stained somata per cubic mm of the ipsilateral amygdala as a function of injury severity. **S.** Stereological quantification of tau-immunoreactive neuritic processes per cubic mm of the contralateral CA1 as a function of injury severity. N = 5-6 mice per injury severity. Bars represent mean ± SEM. One-way ANOVA with Newman-Keuls post-hoc test, * $p < 0.05$, ** $p < 0.01$, *** $p < 0.005$.

In summary, tau pathology in different brain regions of injured 3xTg-AD mice exhibited distinct responses to injury severity.

3.4 Discussion of Acute Aβ and Tau Pathologies Observed in 3xTg-AD Mice post TBI

In summary, controlled cortical impact TBI in 3xTg-AD mice recapitulated two key features observed post TBI in human. First, TBI caused rapid Aβ accumulation in injured axons of young 3xTg-AD mice. This intra-axonal Aβ was detectable at 1 hour post injury, and continued to rise monotonically through 24 hours. This is similar to the intra-axonal Aβ accumulation observed in human TBI patients (Smith et al., 2003c; Ikonomovic et al., 2004; Uryu et al., 2007; Chen et al., 2009). No such accumulation is expected at this age and none was seen in sham-injured mice. Second, TBI increased tau immunoreactivity in three distinct brain regions of moderately injured 3xTg-AD mice. The time course was different across regions. In particular, puntate tau staining the ipsilateral fimbria and perinuclear tau staining in the amygdala had a biphasic response

with peaks at 1 hour and 24 hours post TBI. Instead, the numbers of tau-positive processes in the contralateral CA1 started to increase at 12 h post injury. There was also immunohistochemical and biochemical evidence for increased tau accumulation and phosphorylation induced by TBI at several epitopes.

Axonal injury appears necessary for post-traumatic Aβ accumulation in this model, as the extent of intra-axonal Aβ accumulation correlated well with injury severity and no Aβ was detected immunohistochemically in areas without axonal injury. Aβ was found colocalized with the axonal injury markers APP and NFL-68 in injured 3xTg-AD mice. Histological findings of Aβ accumulation following TBI were further confirmed biochemically; there was approximately twice the amount of insoluble total Aβ and $A\beta_{40}$ in ipsilateral hippocampal tissues of moderately injured as compared to uninjured mice. The significant increase in only $A\beta_{40}$ levels following TBI in these mice may be related to the lack of extracellular Aβ plaques observed by immunohistochemistry.

APP, the precursor protein of Aβ, has been found to accumulate in injured axons within 30 minutes following central nervous system injury (Dikranian et al., 2008). Axonal APP accumulation has in turn been hypothesized to serve as substrate for intra-axonal Aβ generation (Smith et al., 2003c; Chen et al., 2004). Thus, our finding that intra-axonal Aβ was detected starting at 1 hour post TBI in 3xTg-AD mice is in line with the reported time for the earliest APP accumulation following brain trauma.

Our mouse model recapitulates one aspect of post-traumatic Aβ pathology in human TBI: intra-axonal Aβ accumulation. Neither our model nor other small animal experimental TBI models of which we are aware result in acute extracellular plaques. Interestingly, recent findings suggest that intracellular Aβ buildup is an early event in

Alzheimer's disease pathogenesis, preceding plaque formation (Gouras et al., 2000; D'Andrea et al., 2001; Gyure et al., 2001; Mori et al., 2002a). Indeed, animal and cellular Alzheimer models have shown that the accumulation of intracellular Aβ species are neurotoxic and may be linked to synaptic dysfunction, cell loss, and memory impairment (Chui et al., 1999; Wirths et al., 2001; Zhang et al., 2002; Oddo et al., 2003a; Casas et al., 2004). Thus, our TBI mouse model of intra-axonal Aβ accumulation may emerge as an interesting model to study the relationship between TBI and Alzheimer's disease.

In addition to focal injuries, the controlled cortical impact TBI model employed in this study also affected distant regions such as the contralateral hippocampi and ipsilateral amygdala. Evidence for this observation included a significant increase in total tau accumulation in the contralateral CA1 and ipsilateral amygdala of moderately injured mice. Interestingly, there was not a substantial increase in total tau accumulation in the ipsilateral hippocampus. Neuronal loss or injury may have caused release of tau into the extracellular space where it could not be detected by immunohistochemistry.

The biphasic increase in tau immunoreactivity following TBI in ipsilateral fimbria and amygdala of 3xTg-AD mice is intriguing. Changes of tau immunoreactivity at 1 hour post TBI perhaps reflect an immediate response to mechanical injury.

While axonal tau accumulation has been observed in a few cases of acute TBI in humans, the effects of injury severity on axonal tau accumulation, as described in this study, have not been documented. Likewise, the increased somatic tau accumulation in this model is rarely observed in human TBI (Ikonomovic et al., 2004). Thus, the relevance of these pathologies is not known.

In conclusion, this controlled cortical impact model using 3xTg-AD mice reproduced key features of human post-TBI AD-related pathology. It will likely allow many mechanistic hypotheses to be tested and may be useful for preclinical therapeutic development.

Chapter 4

Investigation of the Interaction between Aβ and Tau in the Setting of TBI in 3xTg-AD Mice

4.1 Introduction

Traumatic brain injury (TBI) can increase the risk for subsequent development of dementia of the Alzheimer's type (Mortimer et al., 1991; Nemetz et al., 1999; Plassman et al., 2000; Fleminger et al., 2003). Pathological hallmarks of Alzheimer's disease (AD) are extracellular plaques containing the amyloid-β (Aβ) peptides and neurofibrillary tangles (NFTs) containing hyperphosphorylated tau proteins.

In mouse models of AD, Aβ pathology appears to be upstream of tau pathology. Three lines of experimental evidence support this relationship. First, intracerebral injections of aggregated Aβ increased tau phosphorylation and therefore numbers of NFTs in Tau_{P310L} transgenic mice at both local and distant regions (Gotz et al., 2001). Second, double transgenic mice expressing both mutant APP and tau developed greater tau pathology than single tau transgenic mice (Lewis et al., 2001; Perez et al., 2005; Hurtado et al., 2010). Third, intracerebral injections of anti-Aβ antibodies in 3xTg-AD mice reduced both Aβ and tau pathology. Aβ pathology then recurred followed by later recurrence of tau pathology (Oddo et al., 2004).

On the other hand, the human pathological literature suggests that Aβ and tau pathologies may be independent in the setting of TBI, or at least that the relationship may be more complex. First, in single severe TBI, intra-axonal Aβ and diffuse extracellular plaques occurred in about 30% of subjects (Roberts et al., 1991; Roberts et al., 1994; Uryu et al., 2007). Intra-axonal accumulations of total and phospho-tau, but not true NFT pathology, have been documented in a smaller number of cases (Smith et al., 2003a; Ikonomovic et al., 2004). In repetitive concussive TBI resulting in dementia pugilistica or chronic traumatic encephalopathy, the opposite relationship was found; 100% of cases reported to date have had widespread NFTs, but a smaller subset had Aβ pathology (Corsellis and Brierley, 1959; Corsellis, 1989; Roberts et al., 1990; Tokuda et al., 1991; Geddes et al., 1996; Geddes et al., 1999; Schmidt et al., 2001; McKee et al., 2009). Even when both pathologies were present, there was no indication that they colocalized.

To investigate the relationship between Aβ and tau pathologies in the setting of TBI, we used our experimental TBI model on 3xTg-AD mice. In this section, we showed that controlled cortical impact TBI independently results in intra-axonal Aβ and tau accumulation and increased tau phosphorylation in 3xTg-AD mice. This model may be a useful tool for many mechanistic and preclinical therapeutic investigations into the association between TBI and Alzheimer's disease.

4.2 Effects of Acute (24 h) γ-secretase Inhibition on Post-traumatic Aβ and Tau Abnormalities in 3xTg-AD Mice

4.2.1 Effects of Acute γ-secretase Inhibition on Post-traumatic Aβ Accumulation

The findings that both Aβ and tau pathologies were accelerated by controlled cortical impact allowed us the opportunity to investigate the interaction between Aβ and tau in the setting of TBI.

To investigate the interaction between Aβ and tau pathologies, we blocked Aβ production using a γ-secretase inhibitor. γ-secretase is one of the canonical enzymes required for proteolytic processing of APP to form Aβ (Selkoe, 2001). If tau is downstream of Aβ in the setting of TBI, we expected to see amelioration of tau abnormalities after blocking Aβ production. However, if tau and Aβ are independently affected by trauma, blocking Aβ production should have no effects on tau pathology observed following TBI in these mice.

We first confirmed that inhibition of γ-secretase blocked intra-axonal Aβ buildup in 3xTg-AD mice following moderate TBI. We treated injured mice with compound E (CmpE), a small molecule inhibitor of γ-secretase (Seiffert et al., 2000; Olson et al., 2001; Grimwood et al., 2005; Yang et al., 2008; Yan et al., 2009) or DMSO vehicle. Mice received i.p. injections of 10 mg/kg of CmpE or vehicle at 1 h before injury, then again at 5 h, 11 h, and 17 h post injury. The frequent dosing regimen was employed due to the short half-life of CmpE (Yan et al., 2009)). A relatively high dose

was used due to the presence of a PS1 mutation in 3xTg-AD mice, since such mutations may result in diminished response to γ-secretase inhibition (Czirr et al., 2007).

In our first experiment, mice were sacrificed at 24 h following injury. One group of CmpE and vehicle treated mice was used for immunohistochemical analysis, another group was used for biochemical assessment. For histology, we used polyclonal antibody $A\beta_{40}$ for Aβ immunohistochemistry in this experiment since γ-secretase cleavage of APP is at the C-terminus of Aβ; N-terminal anti-Aβ antibodies would still recognize the longer APP fragments remaining after γ-secretase inhibition. We stained these brains for APP to assess the extent of axonal injury. We also assessed full-length, α-CTFs and β-CTFs (APP fragments resulted from cleavage of APP by α- and β-secretases respectively) in the cerebellar lysates of the same mice via western blot to demonstrate that CmpE was effective at inhibiting brain γ-secretase activity. For the biochemical assessment, we sacrificed mice by rapid decapitation and homogenized ipsilateral hippocampi in RIPA buffers. RIPA lysates of CmpE and vehicle treated mice were used to determine levels of $A\beta_{40}$ by ELISA.

CmpE treatment almost completely prevented intra-axonal Aβ accumulation in ipsilateral fimbria of injured 3xTg-AD mice (**Figure 4.1 A-D**). Stereological quantification of numbers of $A\beta_{40}$-positive axonal varicosities showed ~90% reduction in CmpE vs. vehicle treated mice (**Figure 4.1 E,** 1-sided t-test, $p < 0.0001$). Biochemical quantification of RIPA-soluble $A\beta_{40}$ in ipsilateral hippocampi and surrounding white matter showed similar reduction (**Figure 4.1 F**, 32.5 ± 2.87 pg/mg in CmpE treated mice vs. 217.9 ± 52.1 pg/mg in vehicle treated mice, 1-sided t-test, $p = 0.0013$).

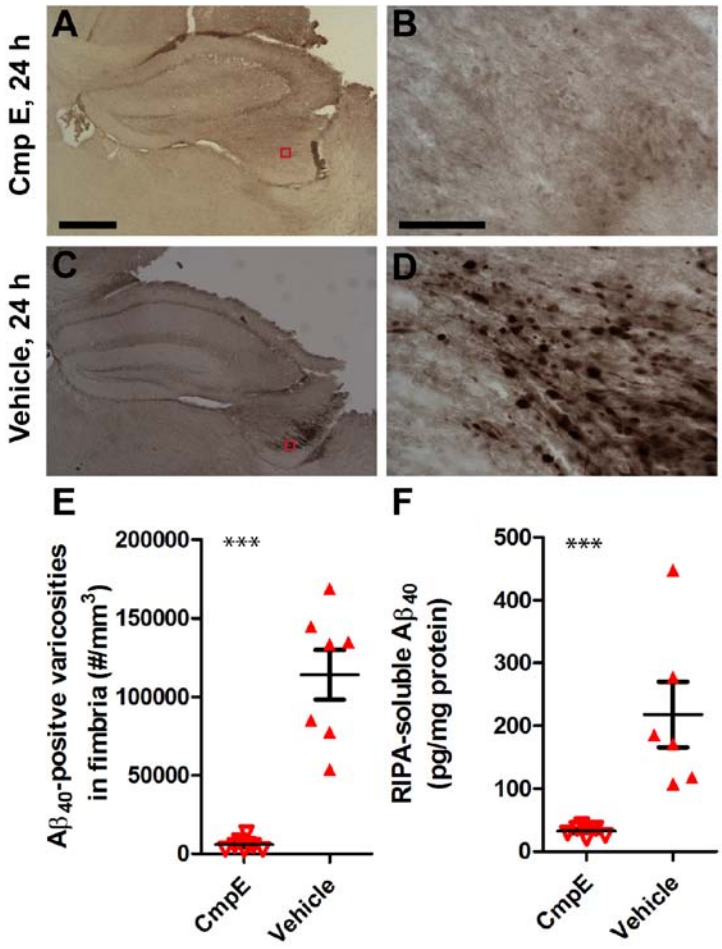

Figure 4.1 Systemic inhibition of γ-secretase activity with Compound E (CmpE) blocked post-traumatic Aβ accumulation in moderately (2.0 mm) injured 3xTg-AD mice.

A. Representative $A\beta_{40}$ IHC for an injured 3xTg-AD mouse receiving CmpE treatment. Scale bar in **A**: 1 mm. **B.** Higher magnification image of the fimbria of a CmpE treated mouse (box in **A**). Scale bar in **B**: 50 μm. **C.** Representative $A\beta_{40}$ IHC for an injured 3xTg-AD mouse receiving DMSO vehicle treatment. **D.** Higher magnification image of the fimbria of a vehicle treated mouse (box in **C**). **E.** Stereological quantification of numbers of $A\beta_{40}$-stained varicosities in the ipsilateral fimbria of injured 3xTg-AD mice receiving either CmpE or vehicle treatment. *** $p < 0.0001$, Student's t-test. N=7-8 mice per group. **F.** RIPA-extracted $A\beta_{40}$ levels in ipsilateral hippocampal tissues of injured 3xTg-AD mice receiving either CmpE or vehicle treatment. *** $p = 0.001$, Student's t-test. N = 6-7 mice per group. These data demonstrated intra-axonal Aβ buildup following TBI could be inhibited by blocking γ-secrectase activity.

CmpE effectively blocked γ-secretase activity in the setting of TBI, as evidenced by similar levels of full-length APP but increased α-CTFs and β-CTFs in cerebellar lysates of mice with CmpE treatment (**Figure 4.2 A-B**). Furthermore, numbers of APP-stained varicosities were similar between treatment groups (**Figure 4.2 C-D**). This finding demonstrated that γ-secretase inhibition by CmpE specifically reduced proteolytic Aβ production, rather than reducing Aβ pathology by affecting extent of axonal injury in these injured mice.

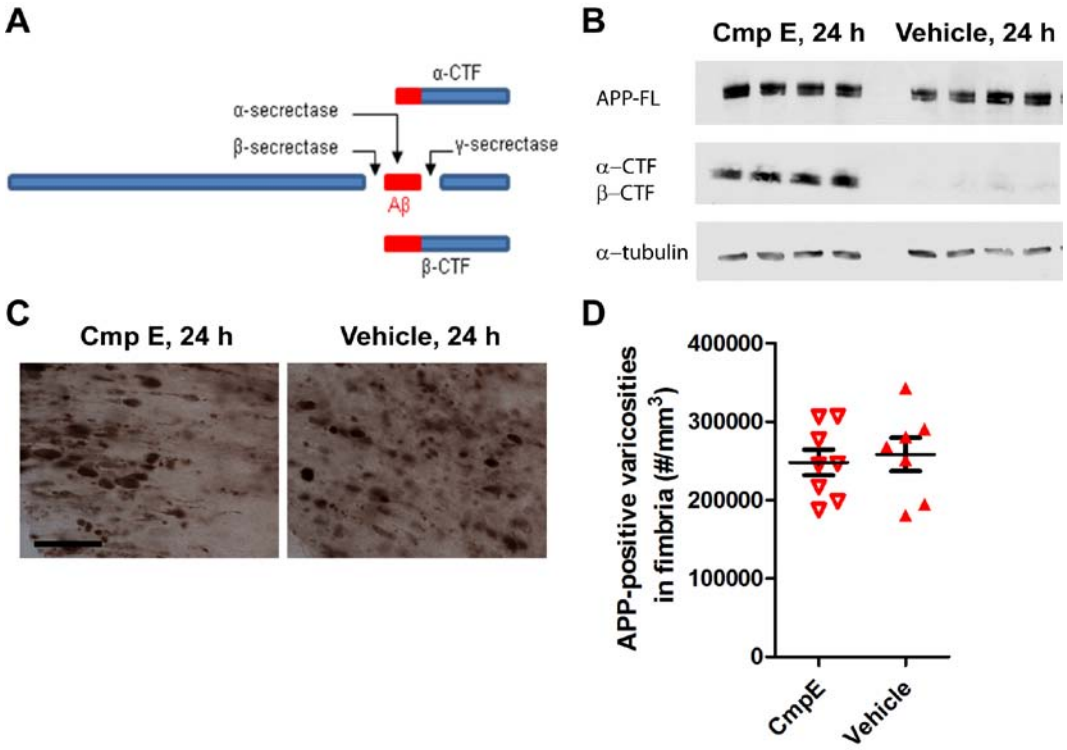

Figure 4.2 Compound E treatment in moderately injured (2.0 mm) 3xTg-AD mice caused accumulation of α- and β- C-terminal fragments (CTFs) but did not alter the extent of axonal injury.

A. Schematic of cleavage sites of full-length APP (APP-FL) by α-, β-, and γ-secretases to generate CTFs and Aβ. **B.** Western blot of APP-FL and CTFs from cerebellar lysates of injured mice treated with CompoundE (CmpE) or vehicle. Full-length APP levels were similar, but there were more CTFs in injured mice treated with CmpE than vehicle control. This

demonstrates systemic CmpE treatment can inhibit γ-secretase activity in the brain. **C.** APP immunohistochemistry of fimbria from injured 3xTg-AD mice treated with CmpE or vehicle. Scale bar: 50 μm. **D.** Stereological quantification of APP-positive axonal varicosities in ipsilateral fimbria of injured mice treated with CmpE or vehicle. Similar numbers of APP-positive axonal varicosities in the two groups indicate CmpE treatment successfully blocked Aβ formation by inhibiting γ-secretase activity, not by affecting the extent of axonal injury in these mice. N=7-8 per group. Bars represent mean ± SEM. Student's t-test, ns: not significant.

In summary, systemic CmpE treatment effectively blocked post-traumatic Aβ accumulation in injured axons of 3xTg-AD mice without affecting severity of axonal injury.

4.2.2 Effects of Acute γ-secretase Inhibition on Post-traumatic Tau Pathology

CmpE treatment had no effect on tau pathologies in 3xTg-AD mice sacrificed at 24 h after TBI, despite the 90% reduction in Aβ accumulation (**Figure 4.3, 4.4**). We assessed total and phosphorylated tau levels in injured 3xTg-AD mice treated with CmpE or vehicle. Specifically, we studied tau pathology histologically with polyclonal total tau antibody, phospho-S199 antibody against tau phosphorylated at S199, and PHF1 antibody against phosphorylated tau at S396 and S404. We also examined tau pathology biochemically via western blots using the AT8, AT100, and Tau46 antibodies. Finally, we investigated total and phospho-S199 levels by ELISA. All assessments were done in a blinded fashion.

Using quantitative stereological methods as described above, we found that the numbers of total tau-positive puncta in the ipsilateral fimbria, the numbers of total tau-stained somata in the ipsilateral amygdala, and total length density of tau-positive CA1

processes were not affected by CmpE treatment in injured 3xTg-AD mice (**Figure 4.3 A-I**). Total tau levels in the ipsilateral hippocampal tissues of injured mice treated with CmpE were not statistically different from those of vehicle treated mice, as assessed by human tau ELISA (819.7 ± 99.38 pg/mg in CmpE treated mice vs. 796.6 ± 161.1 pg/mg in vehicle treated mice, Student's t test, p = 0.9).

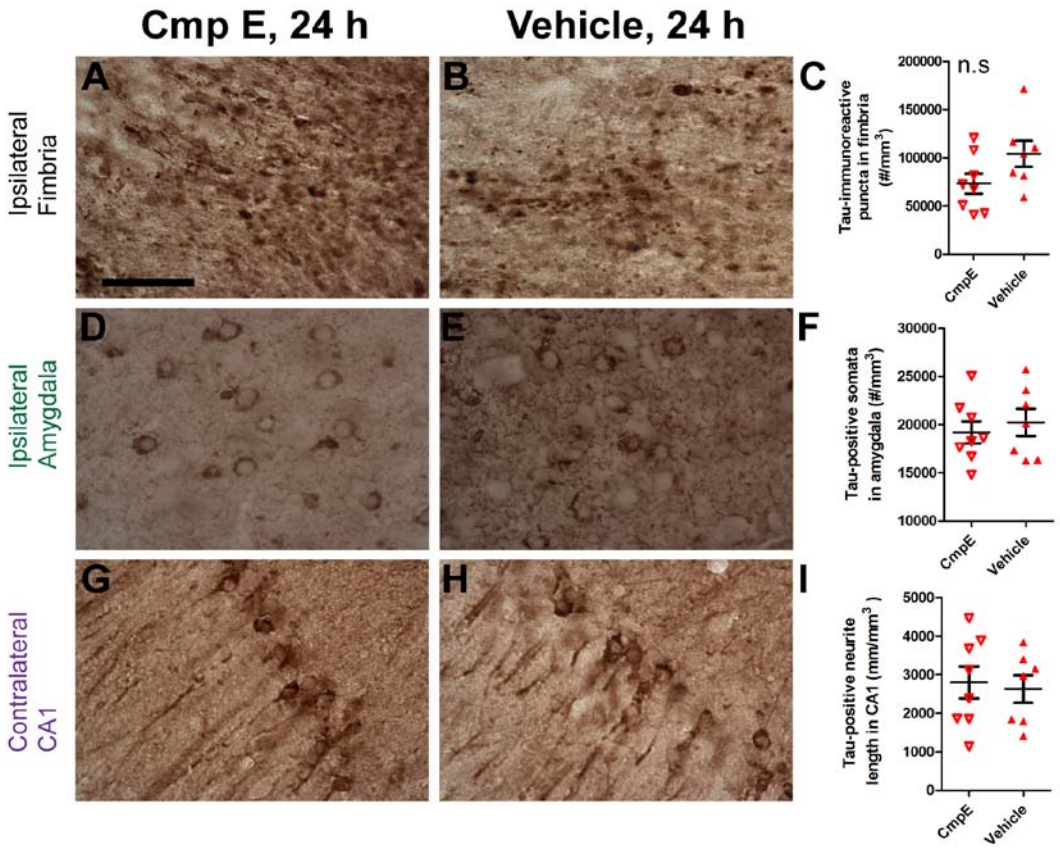

Figure 4.3 Systemic γ-secretase inhibition with CmpE did not affect total tau pathology in injured 3xTg-AD mice killed at 24 h post injury.

Total tau staining using polyclonal tau antibody in the ipsilateral fimbria (**A-B**), ipsilateral amygdala (**D-E**), and contralateral CA1 (**G-H**) of mice treated with CmpE (**A, D, G**) or vehicle DMSO (**B, E, H**). Scale bar in A: 50 μm. Stereological quantifications revealed similar numbers of total tau-positive puncta in the fimbria (**C**), amygdala (**F**), and CA1 (**I**) of CmpE and vehicle treated mice. Student's t-tests, n.s: not significant. N = 7-8 mice per group. Bars are means ± SEM.

The increases in tau phosphorylation following TBI were not affected by CmpE treatment. There were similar numbers of pS199- and PHF1-positive tau puncta in ipsilateral fimbria of injured mice treated with CmpE compared to vehicle treated mice (**Figure 4.4 A-F**). Phospho-tau S199 levels in ipsilateral hippocampi assessed by ELISA revealed similar levels in CmpE and vehicle treated mice (CmpE group: 61.1 ± 9.2 pg/mg vs. vehicle group: 57.9 ± 13.9 pg/mg, Student's t-test, $p = 0.85$). Ipsilateral hippocampi of CmpE and vehicle treated mice subjected to western blotting using AT8 and AT100 antibodies also corroborated these findings (**Figure 4.4 G-H**). Tau pathologies in these experimental groups were qualitatively and quantitatively similar to those seen in the moderately injured mice that received neither vehicle nor CmpE (**Figure 3.7, 3.8, 3.11**). Thus, it was unlikely that there were any effects of DMSO vehicle treatment or the additional handling required for the injections.

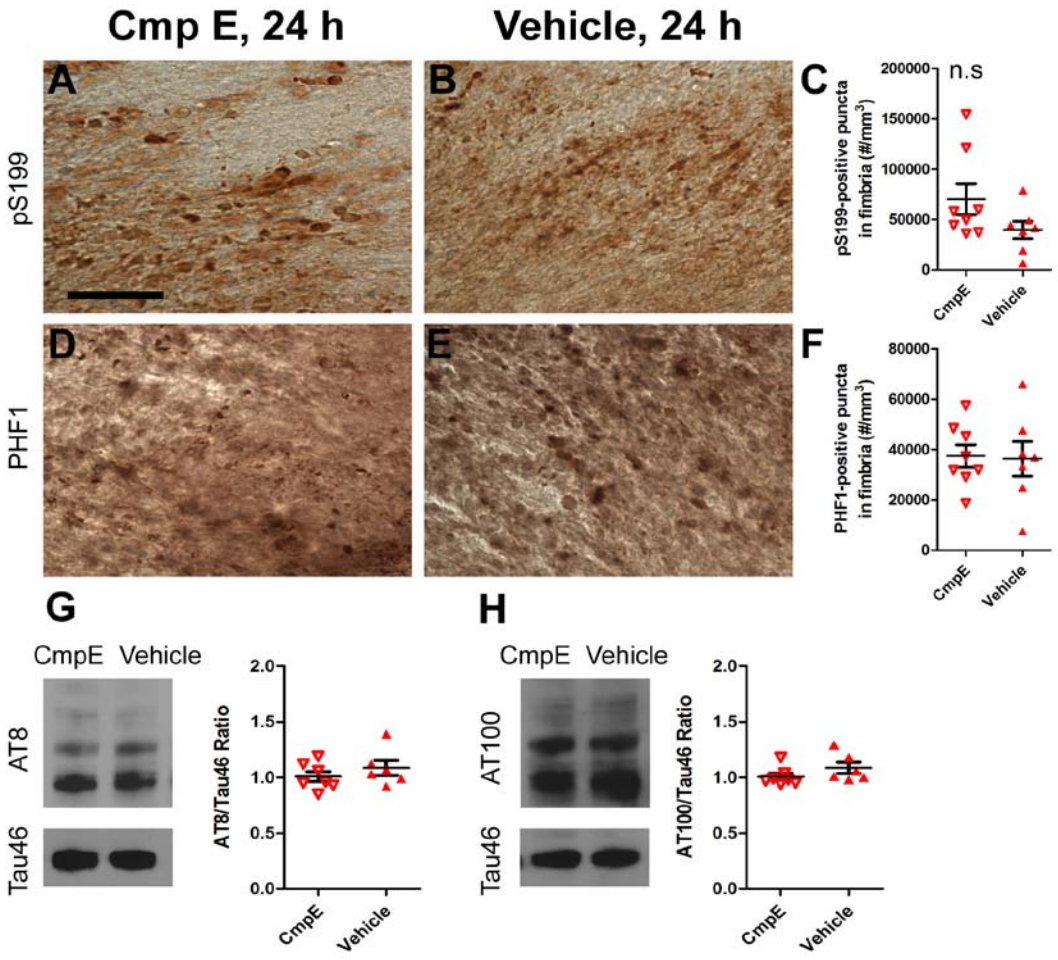

Figure 4.4 Inhibition of post-traumatic Aβ accumulation did not affect tau phosphorylation in injured 3xTg-AD mice.

Phospho-tau staining using antibodies against tau phosphorylated at S199 (pS199, **A-B**) and at S396 and S404 (PHF1, **D-E**) in the ipsilateral fimbria of CmpE and vehicle treated mice. Stereological quantification showed similar numbers of pS199- (**C**) and PHF1-positive puncta (**F**) in the fimbria of mice treated with CmpE and vehicle. Student's t-tests, n.s: not significant. N = 7-8 mice per group. **G-H.** AT8 (**G**) and AT100 (**H**) western blots of ipsilateral hippocampal lysates of mice received CmpE or vehicle. No significant difference was observed. Student's t-tests. N = 6-7 mice per group. Bars are means ± SEM.

To summarize, tau pathology was unaltered in injured 3xTg-AD mice, even though more than 90% of post-traumatic Aβ pathology was blocked.

4.3 Effects of Subacute (7 d) γ-secretase Inhibition on Post-traumatic Aβ and Tau Abnormalities in 3xTg-AD mice

4.3.1 Effects of Subacute γ-secretase Inhibition on Post-traumatic Aβ Accumulation

We examined the effects of CmpE or vehicle treatment on injured mice up to 7 days post TBI. We chose this survival period because we found that both Aβ and tau abnormalities persisted in untreated, injured mice at 7 days post TBI, though to a lesser extent than those observed at 24 h following TBI. Mice received CmpE or vehicle injections 4 times in the first 24 hours as described above, then twice daily until they were sacrificed at 7 days post injury. We stained brain sections for $A\beta_{40}$ and APP to assess the effects of CmpE treatment on Aβ accumulation.

Extended CmpE treatment successfully blocked the accumulation of the Aβ in the ipsilateral fimbria/fornix of injured 3xTg-AD mice at 7 days (**Figure 4.5 A-C,** 1-sided t-test, $p = 0.001$). In vehicle treated mice, there were still numerous Aβ positive (**Figure 4.5 B**) and APP positive (**Figure 4.5 E**) varicosities at 7 days, though the extent of staining was reduced compared to 24 h post TBI (**Fig 4.1, 4.2**). Similar to the acute CmpE treatment experiments, extended CmpE treatment did not alter the extent of axonal injury as assessed by numbers of APP-positive varicosities in the ipsilateral fimbria/fornix (**Figure 4.5 D-F**).

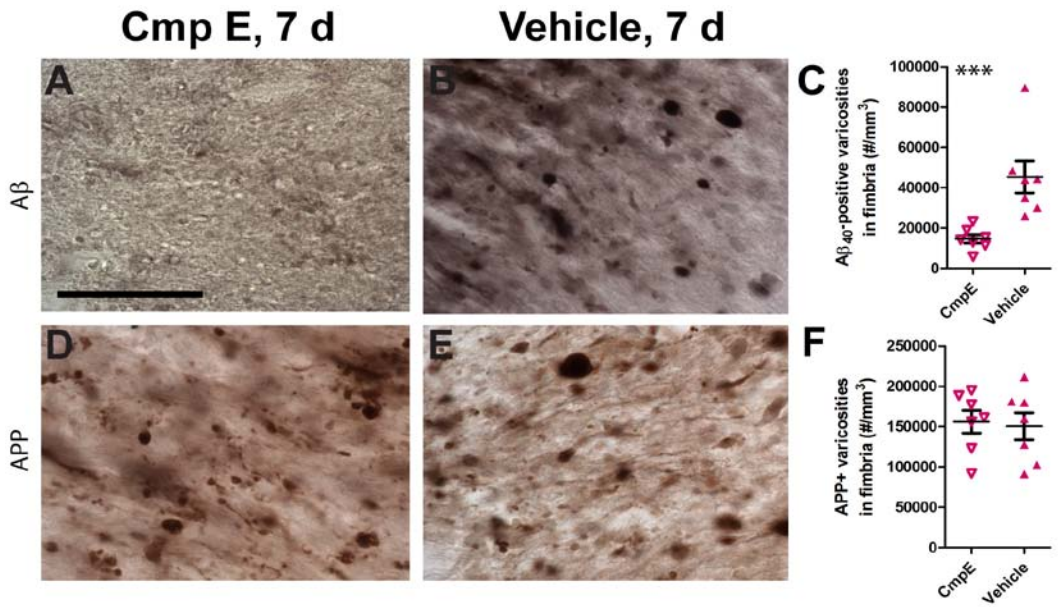

Figure 4.5 CmpE treatment for 7 d blocked post-traumatic Aβ accumulation but did not affect extent of axonal injury in injured 3xTg-AD mice.

A-B. Aβ staining using $A\beta_{40}$ antibody in the ipsilateral fimbria of injured mice treated with CmpE or vehicle. **C.** Stereological quantification showed significant reduction of $A\beta_{40}$-positive varicosities in the fimbria of mice received extended CmpE treatment, as compared to vehicle. *** $p < 0.0001$, Studen's t-test. **D-E.** APP staining in the ipsilateral fimbria. **F.** Stereological quantification showed similar APP-positive varicosities. N = 7 mice per group. Bars are mean ± SEM.

In summary, extended CmpE treatment for 7 days blocked more than 70% of post-traumatic Aβ accumulation in 3xTg-AD mice, but did not affect the extent axonal injury.

4.3.2 Effects of Subacute γ-secretase Inhibition on Post-traumatic Tau Pathology

We next stained brains of CmpE and vehicle treated mice for total tau using polyclonal antibody (pAb), and phospho-tau using pS199 and PHF1 antibodies. Total tau immunoreactivity in the fimbria, amygdala and CA1 were not statistically different in mice received CmpE and vehicle for 7 days post injury (**Figure 4.6 A-I**). Importantly, tau phosphorylation at phospho-S199 and PHF1 epitopes was also unaffected following 7 days of CmpE treatment (**Figure 4.6 J-O**). Thus, we did not observe a delayed effect of inhibition of Aβ accumulation on tau pathology after TBI.

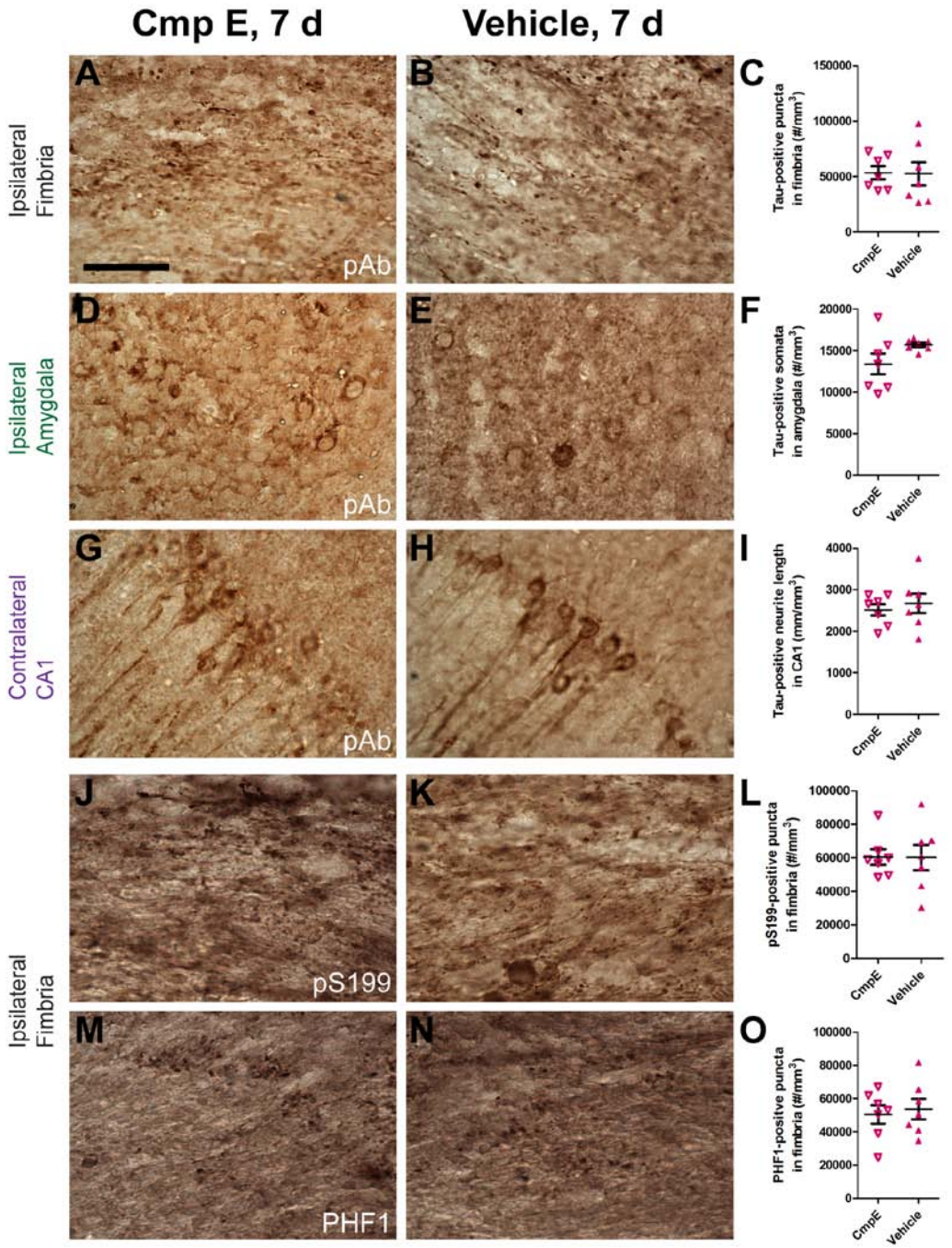

Figure 4.6 Extended CmpE treatment did not affect tau pathology in injured 3xTg-AD mice.

Total tau staining using polyclonal antibody (pAb) in the ipsilateral fimbria (**A-B**), ipsilateral amygdala (**D-E**), and contralateral CA1 (**G-H**) of mice treated with CmpE or vehicle for 7 d. Scale bar in **A**: 50 μm. **C, F, I.** Stereological quantifications showed similar levels of total tau

between treatment groups. Phospho-tau staining using pS199 antibody (**J-K**) and PHF1 antibody (**M-N**) in the fimbria of mice treated with CmpE or vehicle for 7 d. **L, O.** Stereological quantifications showed similar levels of pS199- and PHF1-positive puncta in the fimbria of CmpE and vehicle treated mice. Student's t-tests. N = 7 mice per group. Bars are mean ± SEM.

In summary, inhibition of γ-secretase activity with CmpE successfully blocked post-traumatic Aβ generation and buildup in injured axons in 3xTg-AD mice but did not affect either local or distant tau immunoreactivity. This provides experimental evidence that post-traumatic acceleration of Aβ and tau pathologies occur independently in this animal model.

4.4 Discussion of γ-secretase Inhibition in Injured 3xTg-AD Mice and the Utility and Limitations of This Experimental TBI model

In summary, we found that systemic inhibition of γ-secretase activity by CmpE effectively blocked the post-traumatic Aβ accumulation in 3xTg-AD mice at both 24 h and 7 d post injury. However, Aβ blockade did not affect tau pathology accelerated by TBI at either time points.

The subacute effects of TBI are evidenced in the persistent immunoreactivity of APP, Aβ, total and phospho-tau in injured 3xTg-AD mice sacrificed at 7 days post injury. However, there was less APP, Aβ, and total tau immunoreactivity at 7 days compared to 24 h following TBI, presumably due to progressive cell death and tissue

loss at the affected regions at the later time point. Interestingly, tau phosphorylation at phospho-S199 and PHF1 epitopes remained elevated at 7 days post injury. This suggests a possible role for pathological tau on longer-term outcomes following TBI in vivo.

Importantly, inhibition of enzymatic activity of γ-secrectase, one of the canonical enzymes involved in cleaving APP to form Aβ under physiological conditions, almost completely eliminated post-traumatic Aβ aggregation in injured 3xTg-AD. However, accelerated tau abnormalities observed following trauma in these mice appear likely to be independent of Aβ, since inhibition of intra-axonal Aβ buildup did not alter tau pathology. These findings were consistent during the acute (24 h) as well as the subacute (7 d) periods following TBI. This demonstrates the utility of this controlled cortical impact 3xTg-AD model in the mechanistic investigation of the association between TBI and AD-related pathology.

Taken together, these results support a causal relationship between TBI and acceleration of Aβ and tau pathologies. Our mouse model is the first small animal model of which we are aware which reliably and rapidly reproduces these key features of acute human post-TBI Aβ and tau pathologies. This could be due to a number of reasons. First, previous TBI models using transgenic mice only utilized those which overexpress either mutated forms of APP or tau, not both (Smith et al., 1998; Uryu et al., 2002; Yoshiyama et al., 2005). Second, 3xTG-AD mice also have a knock-in PS1 mutation, which shifts Aβ accumulation to mostly intracellular (Mastrangelo and Bowers, 2008), and possibly increases tau phosphorylation (Baki et al., 2004; Dewachter et al., 2008). Furthermore, methodological differences between our stereotaxic

electromagnetically driven controlled cortical impact device-based protocol and previously used injury paradigms could have resulted in different distributions of axonal injury or other subtle differences in post-injury physiology.

However, there are several limitations of our TBI model. First, this model produces a central contusion and pericontusional axonal injury. Humans often do sustain contusions with pericontusional axonal injury, but many injuries in humans are diffuse or multifocal. Nonetheless, axonal injury appears to be a virtually ubiquitous sequela of TBI (Adams, 1982; Gennarelli et al., 1982; Gennarelli, 1983; Adams et al., 1984; Gennarelli, 1993; Blumbergs et al., 1994, 1995; Geddes et al., 2000) and many types of injuries in humans have been reported to result in Aβ and tau pathology (Roberts et al., 1991; Schmidt et al., 2001; Smith et al., 2003a; Smith et al., 2003c; Ikonomovic et al., 2004; Uryu et al., 2007; McKee et al., 2009). Injured axons appear to be a major source of Aβ following TBI in humans (Smith et al., 2003c; Ikonomovic et al., 2004; Uryu et al., 2007; Chen et al., 2009), pigs (Smith et al., 1999b; Chen et al., 2004), rats (Pierce et al., 1996; Iwata et al., 2002), and now mice. Therefore, robust axonal injury and intra-axonal Aβ accumulation lends support to the validity of our model. An additional mouse injury paradigm such as fluid percussion or impact acceleration injury that produces more diffuse axonal injury will be required in order to generalize our findings.

Second, most humans with TBI do not have a known genetic predisposition to developing AD-related pathologies, while the 3xTg-AD line has 3 mutations implicated in familial dementia. This limitation applies to this and other mouse models of age-related AD pathology as well. The introduction of these mutations seems to be required

either because of fundamental differences between mouse and human coding sequences, differences in gene regulation, the short life span of the mouse, or a combination of these. Mice with human wild-type APP, PS1 and tau alleles "knocked in" to the mouse loci would be useful to differentiate these possibilities.

Third, while axonal tau accumulation has been observed in a few cases of acute TBI in humans, the effects of injury severity on axonal tau accumulation, as described in this study, have not been documented. Likewise, the increased somatic tau accumulation in this model is rarely observed in human TBI (Ikonomovic et al., 2004). Thus, the relevance of these pathologies is not known.

Fourth, neither this animal model, nor any other small animal of which we are aware, develops acute post-traumatic extracellular Aβ plaque pathology. The relative importance of extracellular vs. intracellular Aβ pathologies in the setting of TBI is not known. Nonetheless, the opportunity to investigate one form of acute post-traumatic Aβ pathology, acute post-traumatic tau abnormalities, and the interaction of these two pathologies makes the model presented here a significant advance. Ultimately, full validation will require predictions made based on the model that are subsequently confirmed in humans.

The question of whether these pathologies trigger chronic, progressive neurodegeneration remains to be addressed. Similarly, future studies should be performed to determine if these Aβ and tau abnormalities adversely affect behavioral outcomes in 3xTg-AD mice subjected to TBI. If so, preclinical therapeutic trials would be required to determine whether clinically realistic interventions could ameliorate these deficits (Abrahamson et al., 2006; Loane et al., 2009). The long-term goal would be to

develop treatments that block the adverse effects of AD-related pathophysiological processes after acute TBI in humans.

Based on our findings, it is most likely that Aβ does not play a critical role in TBI-induced tau pathology. However, a small fraction of Aβ remained following γ-secrectase inhibition in injured 3xTg-AD mice. Thus, there may be minor yet toxic Aβ species which could ultimately affect tau pathology. Additional studies should be carried out to identify if such species exist and if they do in fact accelerate tau pathology in the setting of TBI. Experiments involving Tau_{P301L} only transgenic mice or 3xTg-AD, BACE -/- mice subjected to TBI would provide further insights into effects of TBI on tau pathology. If, as seems likely, tau pathology is truly independent of Aβ in the setting of TBI, the underlying mechanisms will require investigation in order to elucidate additional therapeutic targets. Possible involvement of GSK3β, calpain, JNK and cdk5 cascades on tau pathology could be considered (Querfurth and LaFerla, 2010).

Apart from its effects on Aβ production, mutant PS1 has been implicated in other functions such as neuronal calcium dyshomeostasis and regulation of synaptic plasticity (Thinakaran and Parent, 2004; Mattson, 2010). Since dysregulation of calcium signaling is thought to play an important role in glutamate-induced excitotoxicity following brain injury (Tymianski and Tator, 1996; Arundine and Tymianski, 2004; Szydlowska and Tymianski, 2010), it is possible that the mutant PS1 in the 3xTg-AD mouse model may exacerbate TBI-induced neurodegeneration, in addition to its effects on both Aβ and tau pathologies. Future experiments subjecting PS1 single transgenic mouse to brain trauma will be required to elucidate its role in the context of TBI.

In conclusion, this controlled cortical impact model using 3xTg-AD mice reproduced key features of human post-TBI AD-related pathology. It will likely allow many mechanistic hypotheses to be tested and may be useful for preclinical therapeutic development.

Chapter 5

Aβ Pathology in APP/PS1 and Tau Pathology in Tau_{P301L} Mice following TBI

5.1 Introduction

To test whether the findings in 3xTg-AD mice can be generalized, we subjected two additional transgenic mouse lines to controlled cortical impact TBI. We found that TBI caused acute Aβ accumulation in young APP/PS1 mice (Jankowsky et al., 2004), which harbor a different PS1 mutation from 3xTg-AD mice. Furthermore, TBI acutely accelerated tau pathology in Tau_{P301L} transgenic mice (Gotz et al., 2001). Overall, our TBI models represent a useful tool for future investigation into the link between TBI and AD.

5.2 Axonal Aβ Pathology in Young APP/PS1 Mice at 24 h Post Injury

To test whether the findings of acute Aβ accumulation post TBI in 3xTg-AD mice can be generalized to another mouse model, we subjected a different transgenic line, APP/PS1 mice to experimental TBI of similar injury severity. These mice overexpress the Swedish (K670M/N671L) mutation of the human APP gene and the human PS1 gene with exon 9 deleted (Jankowsky et al., 2004). They were injured at 2

months of age; extensive extracellular Aβ pathology normally develops by approximately 6 months of age in this line. They were sacrificed at 24 h post TBI; their brains were stained for APP to assess the extent of axonal injury, and for Aβ using both panAβ and HJ3.4 antibodies. TBI resulted in comparable degree of axonal injury in pericontusional white matter in both APP/PS1 and 3xTg-AD mice, as evidenced by similar patterns of APP staining (**Figure 5.1 B-C**). Stereological quantification of APP-positive axonal varicosities corroborated the qualitative observation (3xTg-AD: 295,579 ± 36,388 APP-positive axonal varicosities per cubic mm, n = 8 vs. APP/PS1: 272,212 ± 43,249, n = 5, p = 0.69). Likewise, the pattern of Aβ accumulation detected by panAβ and HJ3.4 antibodies appeared similar in injured 3xTg-AD and APP/PS1 mice (**Figure 5.1 E-F, H-I**). Quantification also confirmed this histological finding (3xTg-AD: 65,437 ± 8,458 HJ3.4-positive varicosities vs. APP/PS1: 47,257 ± 11,763, p = 0.23). Uninjured APP/PS1 mice at 2 months of age had neither APP nor Aβ accumulation in the ipsilateral fimbria/fornix (**Figure 5.1 A, D, G**).

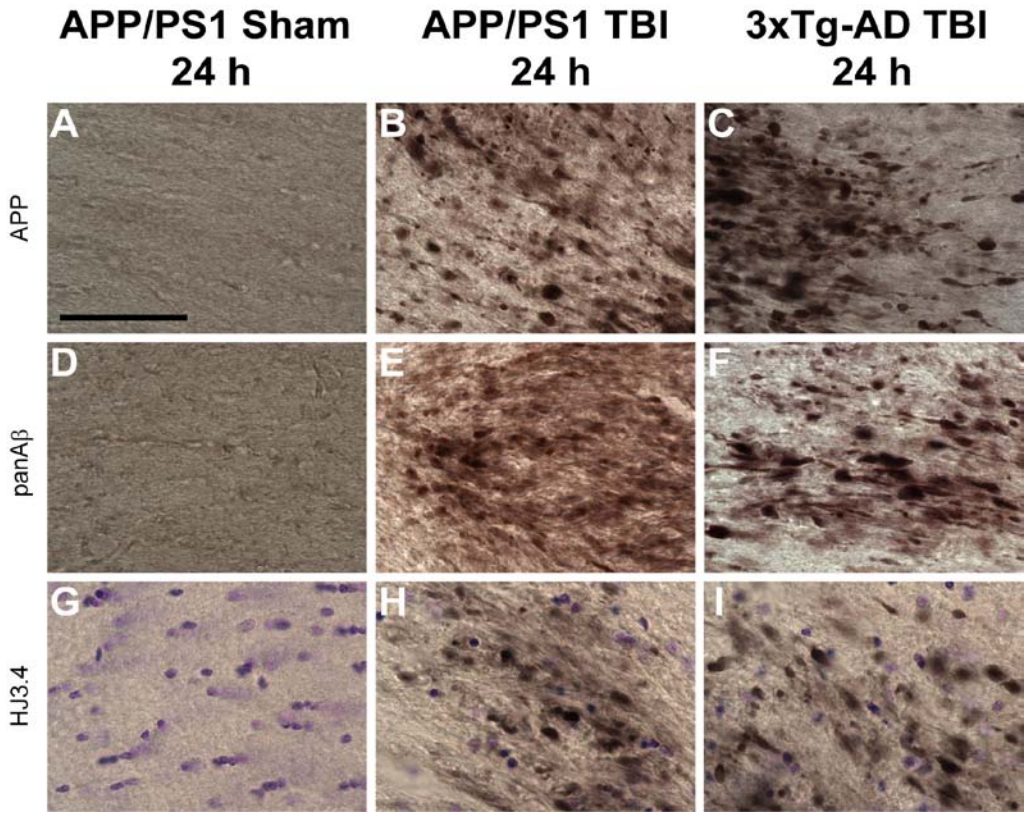

Figure 5.1 Aβ accumulated in fimbria/fornix axons of 2 month-old APP/PS1 mice at 24 hours post TBI.

A-C. APP staining in the ipsilateral fimbria/fornix of a sham APP/PS1 mouse (**A**), an injured APP/PS1 mouse (**B**), and an injured 3xTg-AD mouse (**C**). Scale bar: 50 μm. Similar extent of axonal injury as detected by APP staining was seen in injured APP/PS1 and 3xTg-AD mice. **D-F**. Aβ staining with panAβ antibody. **G-I**. Aβ staining with HJ3.4 antibody. Histological and stereological quantification showed similar extent of Aβ accumulation in injured APP/PS1 and 3xTg-AD mice: 47,257 ± 11,763 HJ3.4-positive varicosities per cubic mm in APP/PS1 (n = 5) vs. 65,437 ± 8,458 in 3xTg-AD mice (n = 8), Student's t-test, p = 0.23.

These data suggest post-traumatic Aβ accumulation in 3xTg-AD mice is not unique to the genetic constructs carried by these mice.

5.3 Tau Pathology at 24 h following TBI in Single Transgenic Tau_{P301L} Mice

To provide further evidence for the independent relationship between Aβ and tau in the setting of TBI, we performed controlled cortical impact TBI on transgenic mice expressing only human tau mutant gene, Tau_{P301L} (Gotz et al., 2001). Expression of the transgene in these mice was under transcriptional control of the Thy1.2 promoter, the same promoter which drives transgenes expression in 3xTg-AD mice. Tau pathology was investigated at 24 h post TBI in 6 month old Tau_{P301L} mice by immunohistochemistry with an antibody against total human tau. We found that controlled cortical impact TBI also caused acute tau accumulations with punctate morphologies in the ipsilateral fimbria/fornix of injured Tau_{P301L} mice (**Figure 5.2 A-B**). Quantification indicated there were substantial numbers of tau-positive puncta in the ipsilateral fimbria/fornix of injured Tau_{P30L} mice; approximately half as many as in injured 3xTg-AD mice (Tau_{P301L}: 63,180 ± 9,636 tau-positive puncta per cubic mm of fimbria, n = 6, vs. 3xTg-AD mice: 138,887 ± 35,543, n = 8, p = 0.1). This result is not surprising, as the 3xTg-AD mice were homozygous for human mutant tau whereas the Tau_{P301L} mice were heterozygous. Furthermore, total tau staining in the ipsilateral amygdala and contralateral CA1 of injured Tau_{P301L} was increased relative to sham Tau_{P301L} mice, similar to the effects in injured 3xTg-AD mice (**Figure 5.2 C-F** vs. **Figure 3.8**).

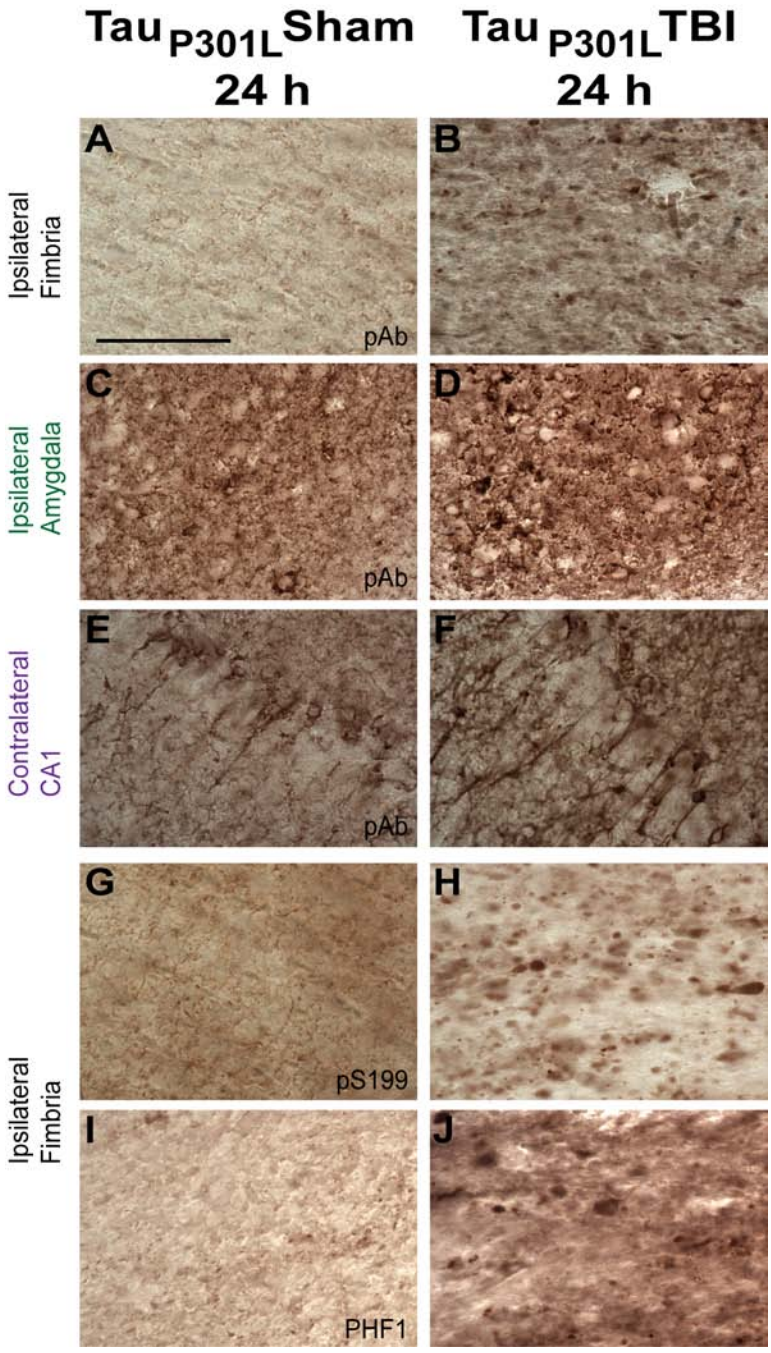

Figure 5.2 TBI acutely accelerated tau pathology in TauP301L mice.

A-B. Punctate total tau staining (pAb) in the ipsilateral fimbria of injured but not sham Tau_{P301L} mice. Scale bar in A: 50 μm. Stereological quantification showed similar numbers of tau-positive puncta in this region in Tau_{P301L} and 3xTg-AD mice: Tau_{P301L}: 63,180 ± 9,636 tau-positive puncta per cubic mm of fimbria, n = 6, vs. 3xTg-AD mice: 138,887 ± 35,543, n = 8, Student's

t-test, p = 0.1. **C-D.** Increased tau immunoreactivity in the cell bodies of the ipsilateral amygdala of injured compared to sham Tau_{P301L} mice. **E-F.** Increased tau immunoreactivity in processes of the contralateral CA1 of injured compared to sham Tau_{P301L} mice. **G-H.** Phospho-tau staining using pS199 antibody against tau phosphorylated at S199. **I-J.** Phospho-tau staining using PHF1 antibody against tau phosphorylated at S396 and S404. Both phospho-tau antibodies detect punctate axonal tau accumulations in the ipsilateral fimbria of injured but not sham Tau_{P301L} mice.

Since TBI acutely affects tau phosphorylation in 3xTg-AD mice at several sites (**Chapter 3.3**), we tested whether TBI increased tau phosphorylation in injured Tau_{P301L} mice by staining with antibodies against tau phosphorylated at S199 (pS199) and at S396 and S404 (PHF1). Abnormal, punctate phospho-tau staining was observed in the ipsilateral fimbria/fornix of injured but not uninjured Tau_{P301L} mice (**Figure 5.2 G-J**). Similar results were found in all 6 injured Tau_{P301L} mice.

In summary, controlled cortical impact TBI consistently increased tau pathology in both young 3xTg-AD mice and Tau_{P301L} mice. The spatial and temporal pattern of tau pathology was distinct from that of Aβ.

5.4 Discussions of Findings in APP/PS1 and Tau_{P301L} Mice

In summary, we showed that the finding of post-traumatic Aβ accumulation in 3xTg-AD mice was recapitulated in a different transgenic mouse model of Alzheimer's disease, APP/PS1. Furthermore, accelerated tau pathology was also observed in transgenic mice carrying only Tau_{P301L} mutation at 24 hours following TBI.

We have previously presented evidence that TBI can independently alter Aβ and tau abnormalities in 3xTg-AD mice (**Chapter 4**). Specifically, systemic inhibition of γ-secretase activity, an enzyme required for Aβ generation from its precursor, APP, successfully blocked post-traumatic Aβ accumulation in injured mice. However, tau pathology was unaffected following blockade of Aβ generation and accumulation. The finding that TBI can accelerate tau pathology in single transgenic Tau_{P301L} mice further supports the hypothesis that Aβ and tau pathologies are independent in the setting of TBI. As such, future studies will be required to investigate the mechanisms underlying TBI-induced tau hyperphosphorylation.

PS1 mutations are thought to drive intracellular Aβ generation (Chui et al., 1999). Additionally, transgenic mice which have both PS1 mutations and APP mutations exhibit accelerated Aβ pathology compared to those with only APP mutations (Borchelt et al., 1997; Holcomb et al., 1998; Wirths et al., 2001; Blanchard et al., 2003; Jankowsky et al., 2004; Wirths et al., 2006). In the setting of TBI, these mutations also appear necessary for rapid intra-axonal Aβ accumulations. Acute Aβ accumulation in axons of injured 3xTg-AD and APP/PS1 mice in the present study and the lack of such pathology in previous experimental TBI models using wildtype and mutant APP mice without PS1 mutations support this observation (Johnson et al., 2010).

However, our TBI mouse models have several limitations. First, we utilized transgenic mice with mutations implicated in familial dementia, while most human with TBI are not genetically predisposed to developing such Aβ and tau pathologies. Nevertheless, these mutations seem to be required for post-traumatic human

pathologies to be recapitulated in mice. Other genetic differences between human and mice may be one of the underlying reasons. Second, the majority of brain injuries in human are mild and diffuse (Cassidy et al., 2004), while our TBI model produces a relatively severe, focal contusion with pericontusional axonal injury. Thus, to generalize our findings, other TBI paradigms such as fluid percussion injury and closed-skull impact, which result in more diffuse axonal injury, will be required. Lastly, the current study focuses only on the acute period post injury. Future studies will therefore be required to assess the long-term effects of intra-axonal buildup of Aβ and tau on neuronal survival, synaptic integrity, and behavioral outcomes following TBI in these mice.

In summary, our experimental TBI model using 3xTg-AD, APP/PS1, and Tau_{P301L} mice confirms the causal role of TBI in acceleration of acute Alzheimer-related pathological abnormalities. These models may provide useful tools to study therapeutic strategies to prevent adverse effects mediated by these pathologies following brain injury.

Chapter 6

Investigation of Potential Mechanisms underlying TBI-induced Tau Hyperphosphorylation

6.1 Introduction

Progressive accumulation of hyperphosphorylated microtubule-associated protein tau into neurofibriallry tangles (NFTs) and neuropil threads is a common feature of many neurodegenerative tauopathies, including Alzheimer's disease (AD) and frontal temporal lobar degeneration (FLTD) (Ballatore et al., 2007). Tau pathology has also been documented in individuals who suffered from a single severe traumatic brain injury (TBI) or multiple mild, concussive injuries (Ikonomovic et al., 2004; Uryu et al., 2007; McKee et al., 2009; Johnson et al., 2011). Tau pathologies in AD and TBI share similar immunohistochemical and biochemical features (Tokuda et al., 1991; Schmidt et al., 2001). In both conditions, somatodendritic tau immunoreactivity is prominent, However, tau-immunoreactive neurites observed in TBI have been suggested to have an axonal origin, which may be distinct from the threadlike forms in AD suggested to be dendritic in origin (Tokuda et al., 1991; Braak et al., 1994; Anderton et al., 1998; Ikonomovic et al., 2004; Uryu et al., 2007; McKee et al., 2009). Furthermore, the anatomical distribution of NFTs may be different following TBI than is typically seen in

AD (McKee et al., 2009). As such, the exact mechanisms leading to tau hyperphosphorylation in TBI may differ from those in AD.

Multiple studies suggest tau pathology results in part from loss-of-function of tau (Ballatore et al., 2007). Abnormally phosphorylated tau has reduced microtubule (MT) binding, which result in MT destabilization. This compromises normal cytoskeletal function, ultimately leading to axonal- and neuronal- degeneration (Bramblett et al., 1993; Alonso et al., 1994; Merrick et al., 1997). Two major mechanisms proposed to underlie tau hyperphosphorylation are aberrant activation of kinases and downregulation of protein phosphatases. Cyclin-dependent kinase-5 (CDK5) and its co-activator p25 (Patrick et al., 1999; Tseng et al., 2002; Noble et al., 2003), glycogen synthase kinase-3β (GSK-3β) (Lucas et al., 2001; Hernandez et al., 2002), and protein phosphatase 2A (Gong et al., 1993; Gong et al., 1995; Kins et al., 2001) have been implicated in hyperphosphorylation of tau *in vivo*. Others such as protein kinase A (PKA)(Litersky and Johnson, 1992; Wang et al., 2007), extracellular signal-regulated kinase 1/2 (ERK1/2) (Drewes et al., 1992; Goedert et al., 1992), and c-jun N-terminal kinase (JNK) (Goedert et al., 1997; Buee-Scherrer and Goedert, 2002; Yoshida et al., 2004; Vogel et al., 2009) have only been shown to regulate tau phosphorylation *in vitro*. It is unknown whether these kinases and phosphatase contribute to TBI-induced tau pathology.

We have previously reported that controlled cortical impact TBI accelerated tau pathology in young 3xTg-AD and Tau_{P301L} mice (Tran et al., 2011). Importantly, the post-traumatic tau pathology appeared to be independent of Aβ. Furthermore, TBI-induced tauopathy in these mice resembled tau pathology observed in humans in that

tau immunoreactivity was evident in both axonal and somatodendritic compartments. In this study, we used these experimental TBI mouse models to investigate mechanisms responsible for increased tau phosphorylation following brain trauma. We found JNK to be critically involved in this process. This suggests targeting JNK pathway may be beneficial in amelioration adverse effects of tau pathology in the setting of TBI.

6.2 Examination of Various Kinase and Phosphatase Activities in Hippocampal Homogenates of TBI and Sham 3xTg-AD Mice at 24 h

Aberrant activation of tau kinase(s) (Patrick et al., 1999; Lucas et al., 2001; Hernandez et al., 2002; Tseng et al., 2002; Cruz et al., 2003; Noble et al., 2003) or inhibition of protein phosphatases (Gong et al., 1993; Gong et al., 1995; Arendt et al., 1998; Kins et al., 2001) are the major proposed mechanisms underlying tau hyperphosphorylation in many tauopathies. We therefore tested whether these mechanisms could account for the observed trauma-induced tau phosphorylation in our experimental TBI model. Toward this end, we subjected young 3xTg-AD mice to sham or controlled cortical impact TBI. After 24 hours, ipsilateral hippocampi and surrounding white matter, including the fimbria/fornix, were dissected, immediately frozen, and homogenized in RIPA buffer. We studied overall tissue levels of the following tau kinases via western blots: protein kinase A (PKA), extracellular signal-regulated kinase 1 and 2 (ERK1/2), glycogen synthase kinase-3β (GSK-3β), and the stress activated kinase, c-jun N-terminal kinase (JNK) (Drewes et al., 1992; Goedert et

al., 1992; Robertson et al., 1993; Sperber et al., 1995; Litersky et al., 1996; Goedert et al., 1997; Buee-Scherrer and Goedert, 2002; Yoshida et al., 2004; Virdee et al., 2007). Phosphorylation of the catalytic subunit of PKA is essential for its activity (Adams et al., 1995; Smith et al., 1999a), while ERK1/2 and JNK are activated via phosphorylation (Anderson et al., 1990; Lisnock et al., 2000; Wada et al., 2001). Thus, blots were probed with phospho-specific antibodies to assess the levels of active PKA, ERK1/2, and JNK (**Figure 6.1 A**). GSK-3β activity, on the other hand, is controlled via inhibitory phosphorylation of GSK-3β at Ser-9 by Akt/protein kinase B pathways (Cross et al., 1995). Thus, blots were probed with an antibody against phosphorylated Ser-9 of GSK-3β (**Figure 6.1 A**). Another well-characterized tau kinase is the cyclin-dependent kinase 5 (CDK5). Physiological activity of CDK5 is regulated by its association to the regulatory subunit p35, while association of CDK5 to p25 results in abnormal kinase activation and contributes to neurodegeneration (Patrick et al., 1999; Cruz et al., 2003; Noble et al., 2003). Therefore, we also measured CDK5, p35, and p25 levels via western blot to probe for CDK5 activity following TBI (**Figure 6.1 C**). Western blot analyses showed no difference in the total and activated levels of all examined kinases from the homogenates of TBI compared to sham mice ($p > 0.05$**, Figure 6.1 B, D**).

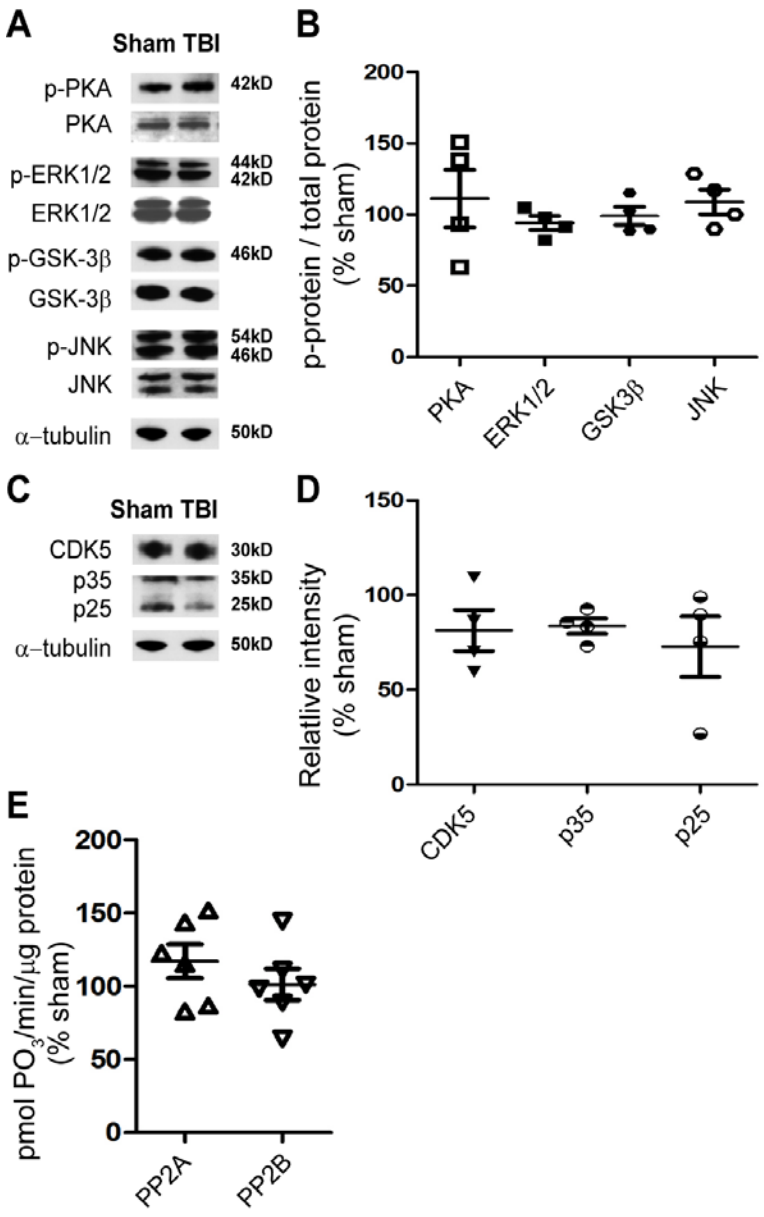

Figure 6.1 TBI did not affect hippocampal levels of tau kinases and activities of tau phosphatases at 24 h.

A. Representative western blots of ipsilateral hippocampal lysates of a sham and an injured (TBI) mouse detected with antibodies against phosphorylated PKA (p-PKA), p-ERK1/2, p-GSK3β at Ser9, and p-JNK. Blots were stripped and reprobed with antibodies against total PKA, ERK1/2, GSK3β, and JNK. The same blots were finally stripped and reprobed with α-tubulin for loading control. **B.** Densitometric quantification of ratios of phosphorylated protein over total protein of each examined kinase from hippocampal lysates of TBI mice, expressed as

% of sham. None were significantly different from 100%. **C.** Representative western blots of ipsilateral hippocampal lysates of a sham and a TBI mouse probed with antibodies against total CDK5 and its regulatory subunits, p35/p25. CDK5 blots were reprobed with α-tubulin for loading control. **D.** Densitometric quantification of bands immunoreactive for CD5, p35, and p25 from hippocampal lysates of TBI mice, expressed as % sham. No significant difference was observed between TBI (n = 4) and sham (n = 4) samples, Student's t-test. **E.** Activity of protein phosphatase 2A (PP2A) and 2B (PP2B, calcineurin) from hippocampal lysates of TBI mice, expressed as % sham. No significant difference was observed between TBI (n = 6) and sham (n = 6) samples, Student's t-test.

Protein phosphatase 2A (PP2A) and protein phosphatase 2B (PP2B) are two major tau phosphatases (Gong et al., 1995; Wang et al., 1995; Gong et al., 2000). Thus, we measured the activities of these phosphatases from the same hippocampal homogenates of TBI and sham mice using a phosphatase activity assay kit. We found that TBI did not significantly affect activities of PP2A and PP2B when compared to sham mice ($p > 0.05$, **Figure 6.1 E**).

To summarize, changes in tau kinases and phosphatases could not be detected at the whole tissue homogenate level 24 h following injury in 3xTg-AD mice.

6.3 Immunohistochemical Analyses of Activated Kinases in Injured and Sham 3xTg-AD Mice at 24 h

Traumatic axonal injury (TAI) is a prominent feature of TBI in many contexts (Gennarelli et al., 1982; Gentleman et al., 1995; Geddes et al., 2000; Smith et al., 2003b), including pericontusional axonal injury in our mouse model (Tran et al., 2011). TAI is thought to disrupt axonal transport and therefore alter the localizations of many

proteins (Povlishock and Christman, 1995). As such, it is probable that TAI causes mislocalizations of tau and tau kinases, resulting in the observed TBI-induced tauopathy in our model. We tested this hypothesis by subjecting separate 3xTg-AD mice to TBI or sham injuries, and examining their brains immunohistochemically. We stained their brains for activated forms of PKA, ERK1/2, and JNK, and for total CDK5 using the same antibodies used for western blotting. In a pilot experiment, we did not observe any immunoreactivity in our tissues using antibody directed against phospho-S9 of GSK-3β (not shown). Therefore, we used an antibody against phosphorylated tyrosine residues of GSK-3 in this experiment; tyrosine phosphorylation of GSK-3 is necessary for its functional activity and is enhanced following various insults (Hughes et al., 1993; Bhat et al., 2000; Leroy et al., 2002).

We found that TBI resulted in activation of most of the kinases examined, primarily in injured axons of the ipsilateral fimbria/fornix (**Figure 6.2**). JNK (**Figure 6.2 K-L**) appeared markedly activated compared to the rest of the examined kinases (**Figure 6.2 A-J**). JNK activation was also observed in the ipsilateral cortex and thalamus of injured mice (**Figure 6.3 A-D**), while increased immunoreactivity for activated PKA and GSK-3 was observed in the ipsilateral CA1 (**Figure 6.3 E-H**).

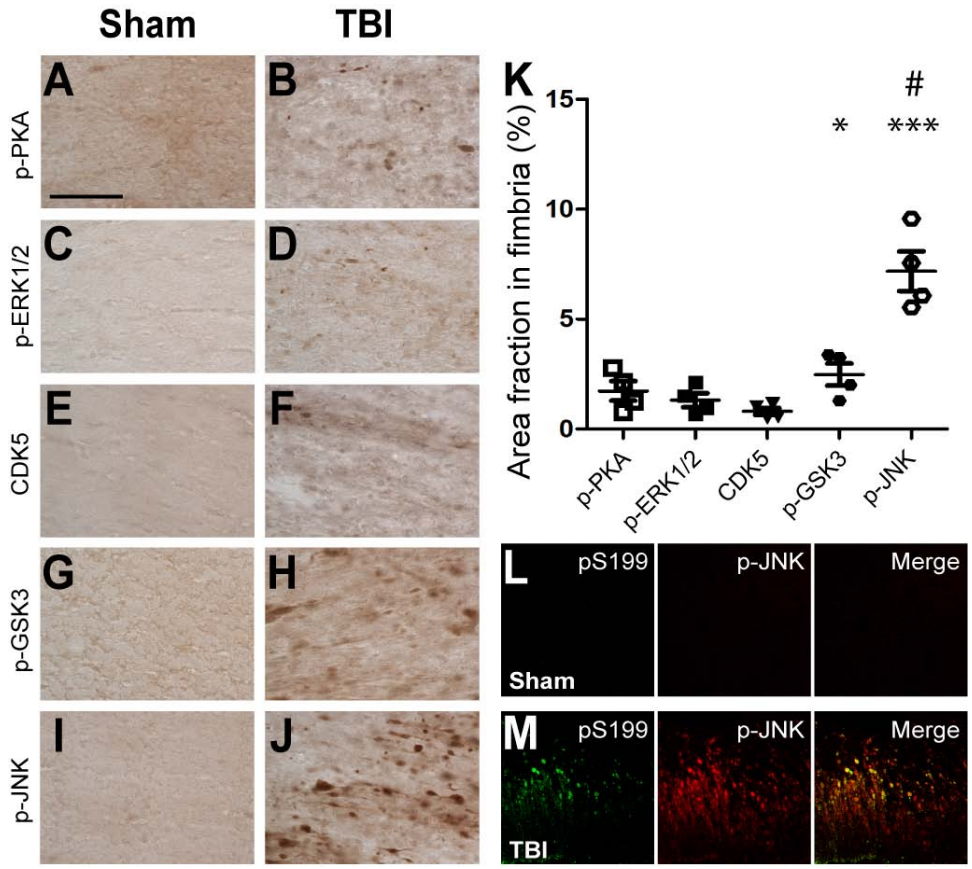

Figure 6.2 JNK was markedly activated in the ipsilateral fimbria/fornix of injured 3xTg-AD mice and colocalized with phospho-tau.

Representative brain sections from a sham and a TBI mouse stained with p-PKA (**A-B**), p-ERK1/2 (**C-D**), CDK5 (**E-F**), p-GSK3 at Y279 and Y216 (**G-H**), and p-JNK (**I-J**). Scale bar in **A**: 50 μm. **K.** Percentage of fimbria area occupied by p-PKA, p-PKC, p-ERK1/2, CDK5, p-GSK3, and p-JNK staining. Areas occupied by p-GSK3 and p-JNK were significantly different from sham. * $p < 0.05$, *** $p < 0.001$, Student's t-test. p-JNK-positive area was significantly more than the rest of the examined kinases. # $p < 0.0001$, One-way ANOVA with Neuman Keuls post-test. N = 4 mice per group. **L-M.** Colocalization of tau phosphorylated at S199 (pS199) and phosphorylated JNK (p-JNK) in a TBI (**M**) but not sham (**L**) mouse.

Densitometric analyses showed 7.6 ± 0.8% area with p-JNK-positive staining and 2.5 ± 0.5% area with p-GSK-3 in the fimbria/fornix of TBI mice vs. 0.38 ± 0.1% area in sham mice. Areas covered by p-JNK ($p < 0.0001$) and p-GSK-3 ($p < 0.05$) were

significantly greater in TBI compared to sham mice (**Figure 6.2 M**). In comparisons with other examined kinases, p-JNK staining in the fimbria/fornix was the most prominent ($p < 0.0001$, Neuman Keuls post-test following one-way ANOVA). Furthermore, double immunofluorescence and confocal microscopy revealed that p-JNK colocalized with tau phosphorylated at Ser-199 (pS199) in the fimbria/fornix of injured but not sham mice (**Figure 6.2 N-O**).

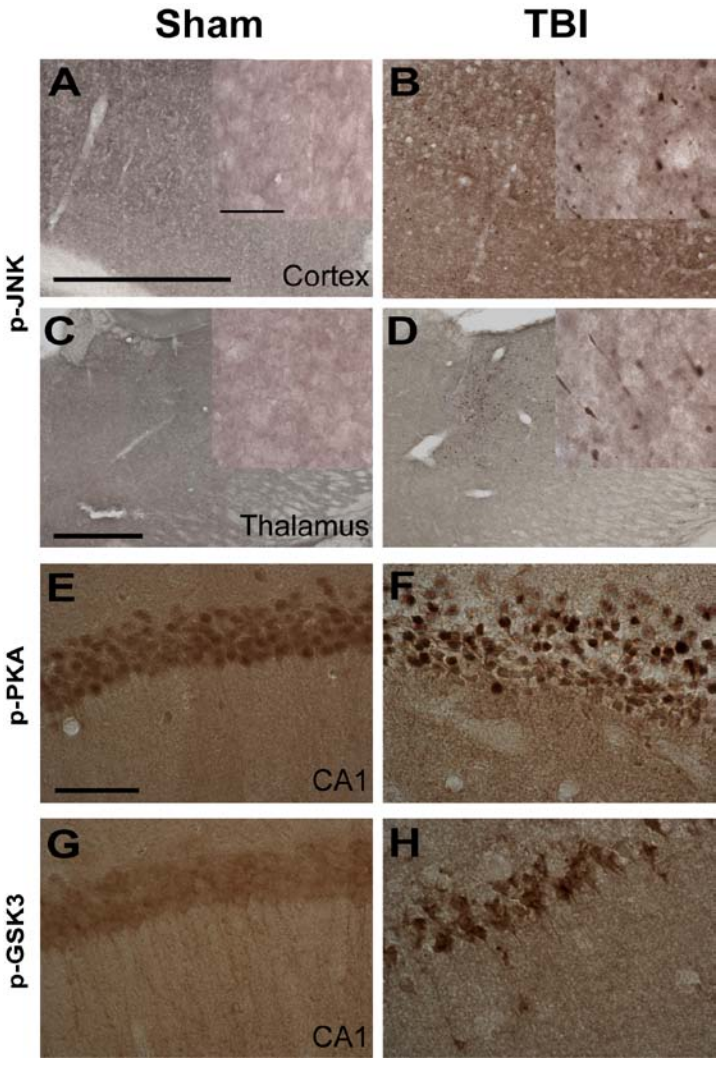

Figure 6.3 Activated JNK, PKA, and GSK-3 localized in distinct brain regions of injured 3xTg-AD mice at 24 h.

A-D. Phopho-JNK staining (p-JNK) for activated JNK was observed in the ipsilateral cortex (**B**) and thalamus (**D**) of injured but not sham 3xTg-AD mice (**A**, **C**). Scale bars in **A** and **C**: 500 μm. **Insets** in **A-D**: Higher magnification of p-JNK staining. Scale bar: 50 μm. **E-F.** Phospho-PKA (p-PKA) for activated PKA. **G-H.** Phospho-GSK3 (p-GSK3) for activated GSK-3 in ipsilateral CA1 of injured 3xTg-AD mice. Scale bar in **C**: 50 μm.

Taken together, these data suggest that mislocalizations of tau and tau kinases, particularly JNK, following TBI may be responsible for post-traumatic axonal tau pathology in 3xTg-AD mice.

6.4 JNK Inhibition by D-JNKi1 Peptide in 3xTg-AD and TauP301L Mice following controlled cortical impact TBI

6.4.1 D-JNKi1 Peptide (5 μg) Inhibited JNK Activity and Reduced TBI-induced Tauopathy in 3xTg-AD mice

To test the hypothesis that JNK is involved in increasing axonal tau phosphorylation and accumulation following TBI in 3xTg-AD mice, we treated mice with a specific peptide inhibitor of JNK, D-JNKi1, or control peptide, D-TAT via i.c.v injection immediately following TBI. D-JNKi1 was chosen over an alternative, the ATP-competitive inhibitor of JNK, SP600125, because of its high specificity to JNK and its long half-life (Bonny et al., 2001; Borsello et al., 2003b). We sacrificed mice at 24 h post injury and examined their brains immunohistochemically. Since c-jun is a major target of JNK (Hibi et al., 1993), we stained for c-jun phosphorylated at Ser-63 (p-c-jun) to determine the extent to which JNK activity was inhibited by D-JNKi1 treatment.

TBI resulted in c-jun activation in many pericontusional regions, most consistently the ipsilateral thalamus (**Figure 6.4 A-D**). We therefore quantified p-c-jun nuclear staining in this region, and found that D-JNKi1 treatment reduced p-c-jun immunoreactivity approximately 40% when compared with D-TAT treated mice ($p < 0.0001$, **Figure 6.5 A-C**).

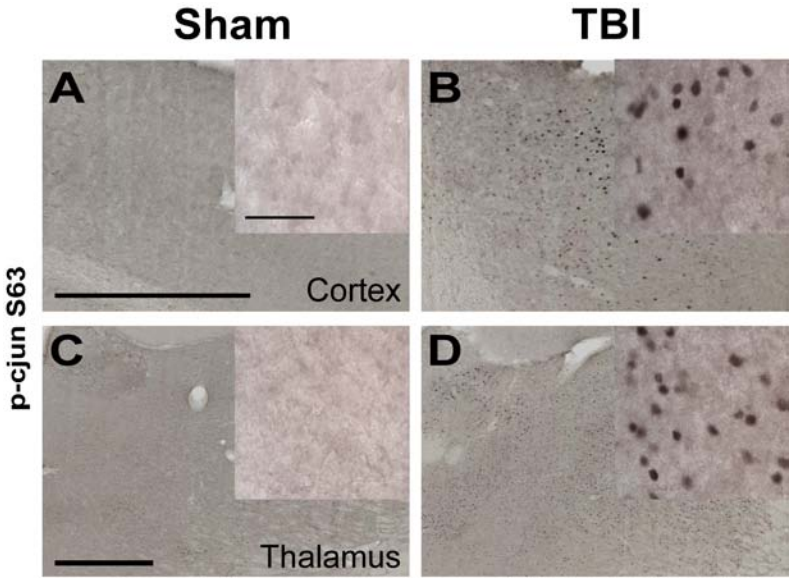

Figure 6.4 TBI caused c-jun activation in the ipsilateral cortex and thalamus of 3xTg-AD mice.

A-D. Phospho-cjun staining against activated cjun in the cortex and thalamus of injured mice. Scale bars: 500 μm. **Insets:** Higher magnification of nuclear c-jun staining. Scale bar: 50 μm.

APP is a robust marker of axonal injury (Sherriff et al., 1994b; Graham et al., 1995; Stone et al., 2000, 2001). Thus, we stained these brains for APP to assess the effects of JNK inhibition on the extent of axonal injury. We also stained for APP proteolytic product, Aβ using the 3D6 antibody, which does not recognize APP (Johnson-Wood et al., 1997). D-JNKi1 treatment did not significantly affect the degree

of axonal injury as determined by the numbers of APP-positive axonal varicosities in the fimbria/fornix ($p = 0.31$, **Figure 6.5 D-F**). D-JNKi1 treatment appeared to reduce the numbers of 3D6-positive varicosities in the fimbria, but the reduction did not reach statistical significance when compared to D-TAT treated mice ($p = 0.07$, **Figure 6.5 G-I**). This finding is not surprising because D-JNKi1 has been shown to reduce Aβ production *in vitro* (Colombo et al., 2007).

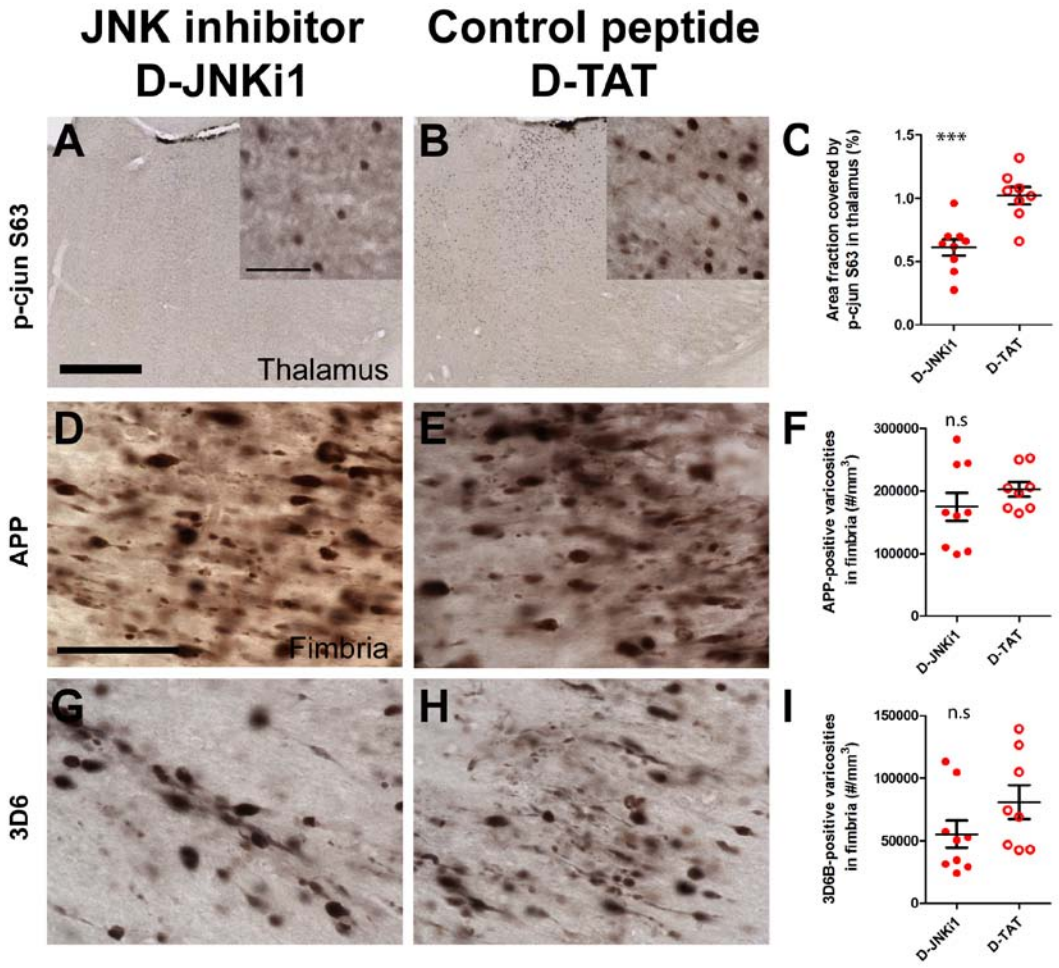

Figure 6.5 D-JNKi1 treatment blocked c-jun phosphorylation but did not affect axonal injury and Aβ accumulation in injured 3xTg-AD mice at 24 h.

A-B. Nuclear staining of phosphorylated c-jun at S63 (p-cjun S63) in the thalamus of injured 3xTg-AD mice received i.c.v. injection of D-JNKi1 and D-TAT control peptide. Scale bar in **A**: 500 μm. **Insets** in **A** and **B**: Higher magnification of p-cjun S63 staining. Scale bar: 50 μm. **C.**

Percentage of area occupied by p-cjun S63 staining in D-JNKi1 and D-TAT treated mice. JNK inhibition by D-JNKi1 significantly reduced extent of c-jun phosphorylation in the thalamus of injured 3xTg-AD mice: 40% reduction, *** $p < 0.001$. **D-E.** APP staining in the ipsilateral fimbria of injured 3xTg-AD mice treated with D-JNKi1 or D-TAT. Scale bar in D: 50 μm. **F.** Stereological quantification showed similar numbers of APP-stained varicosities in mice treated with D-JNKi1 compared to D-TAT. **G-H.** Aβ staining using N-terminal antibody 3D6 in the ipsilateral fimbria of injured 3xTg-AD mice treated with D-JNKi1 or D-TAT. **I.** Stereological quantification showed a nonsignificant 20% reduction in the numbers of Aβ-stained axonal varicosities between groups. n.s: not significant. Student's t-tests. N = 8-9 mice per treatment group. Bars are mean ± SEM.

Although our D-JNKi1 treatment regimen did not fully block c-jun phosphorylation, we nevertheless asked if partial JNK inhibition was sufficient to affect post-traumatic tau pathology in our TBI mouse model. We assessed total tau pathology by staining with a polyclonal antibody which recognizes tau independent of its phosphorylation state (**Figure 6.6 A-B, D-E, G-H**). Stereological quantification showed a moderate but significant reduction (35%) of total tau-positive puncta in the ipsilateral fimbria/fornix ($p = 0.025$, **Figure 6.6 C**). As controls, we also quantified total tau-positive somata in the ipsilateral amygdala and tau-positive neurites in the contralateral CA1. These two regions exhibited increased total tau immunoreactivity (**Section 3.3, Figure 3.7 and 3.8**) but lacked p-JNK staining following TBI (not shown). As expected, stereological quantifications showed similar numbers of tau-positive somata and neurites in the amygdala and CA1 of D-JNKi1 and D-TAT treated mice ($p > 0.05$, **Figure 6.6 F, I**).

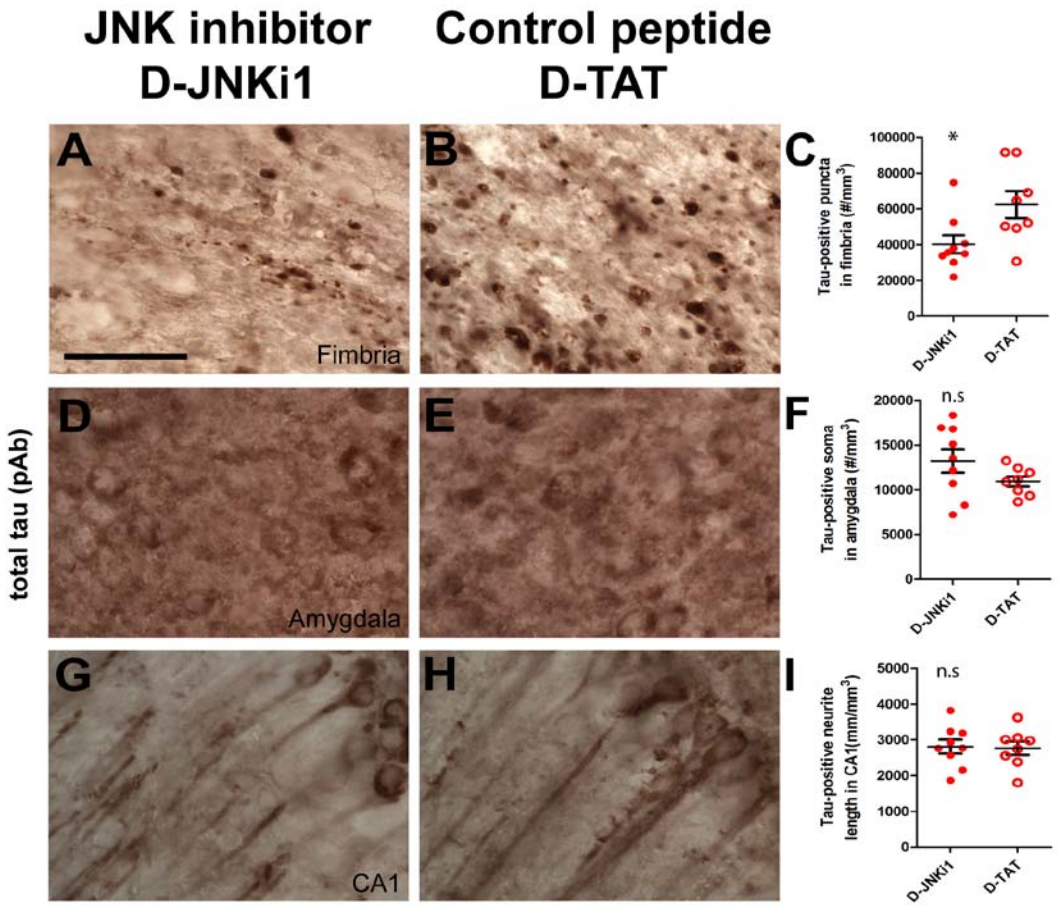

Figure 6.6 JNK inhibition by D-JNKi1 peptide reduced axonal tau accumulation but did not affect somatodendritic tau accumulation.

Total tau staining using polyclonal antibody (pAb) in the ipsilateral fimbria (**A-B**), ipsilateral amygdala (**D-E**), and caontralateral CA1 (**G-H**) of mice received D-JNKi1 or D-TAT i.c.v injection. Scale bar in **A**: 50 μm. **C, F, I.** Stereological quantifications showed D-JNKi1 treatment reduced axonal tau accumulation in the fimbria (**C**), but did not affect somatic tau staining in the amygdala (**F**) nor tau-positive process length in the CA1 region (**I**). * $p < 0.025$, n.s: not significant. Student's t-tests. N = 8-9 mice per group. Bars are mean ± SEM.

We next studied effects of JNK inhibition on tau phosphorylation using phospho-specific antibodies against tau phosphorylated at Ser-199 (pS199), Ser-396 and Ser-404 (PHF1), and Thr-231 (pT231) (**Figure 6.7 A-B, D-E, G-H**). There were also significant reductions of numbers of pS199-positive (55%, $p < 0.0001$, **Figure 3.26 C**)

and PHF1-positive (34%, p = 0.014, **Figure 6.7 F**) puncta in the ipsilateral fimbria/fornix of D-JNKi1 compared to D-TAT treated mice. Numbers of pT231-positive puncta were not statistically different between treatment groups (p = 0.12, **Figure 6.7 I**). This is consistent with in vitro findings that JNK preferentially phosphorylates tau at Ser-199 and Ser-396, but not at Thr-231 (Reynolds et al., 1997).

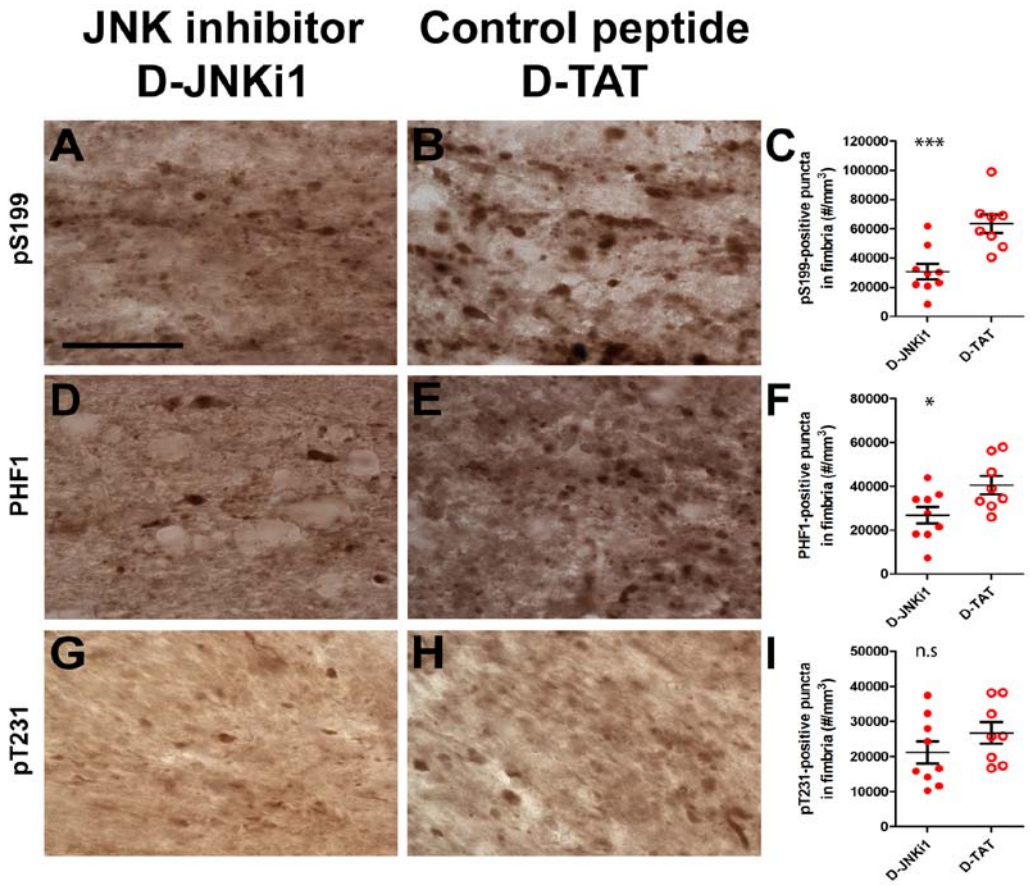

Figure 6.7 D-JNKi1 treatment reduced tau pathology in injured axons of 3xTg-AD mice. Phospho-tau staining using polyclonal antibodies against tau phosphorylated at S199 (pS199, **A-B**), at S396 and S404 (PHF1, **D-E**), and T231 (pT231, **G-H**) in the ipsilateral fimbria/fornix of injured 3xTg-AD mice treated with D-JNKi1 or D-TAT peptide. **C, F, I.** Stereological quantification of pS199-, PHF1-, and pT213-tau puncta in the ipsilateral fimbria of injured mice treated with D-JNKi1 or D-TAT. D-JNKi1 treatment significantly reduced numbers of pS199- and PHF1-tau puncta but had no effect of pT231-tau puncta in the ipsilateral fimbria of injured

mice. * $p < 0.025$, ** $p < 0.001$, ns: not significant. 1-sided t-tests. N = 8-9 mice per treatment group. Bars are mean ± SEM.

In summary, we found that moderate reduction of JNK activity could effectively block the axonal accumulations of total, pS199, and PHF1-tau in injured axons of 3xTg-AD mice.

6.4.2 Similar Dose of D-JNKi1 Peptide (5 μg) Was Ineffective in Blocking JNK Activity in injured TauP301L Mice

Since TBI caused acute increase in tau phosphorylation and accumulation in young Tau_{P301L} mice at 24 hours (**Chapter 5.3**), we asked if JNK is also involved in TBI-induced tau pathology in these mice. We thus treated injured Tau_{P301L} mice with similar dose (5 μM) of D-JNKi1 or D-TAT control peptide via i.c.v injection immediately following TBI. When we assessed phospho-c-jun staining in the thalamus, we did not observe an effect of D-JNKi1 treatment on c-jun phosphorylation (**Figure 6.8**).

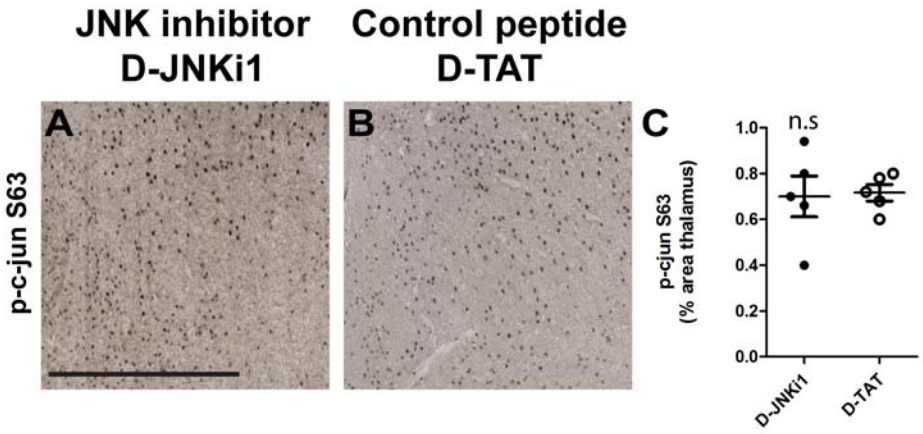

Figure 6.8 D-JNKi1 treatment failed to block c-jun phosphorylation in injured Tau_{P301L} mice at 24 hours.

A-B. Representative photomicrographs showing p-c-jun S63 IHC in the ipsilateral thalamus of injured Tau_{P301L} mice which received i.c.v. injection of D-JNKi1 or D-TAT control peptides (5 μM). Scale bar in **A**: 500 μm. **C.** Quantitative histochemical analysis showed similar levels of p-c-jun S63 staining in the thalamus of treated mice. N = 5 mice per group. Student's t-test. n.s: not significant. Bars are mean ± SEM.

6.5 Discussion of Findings on JNK Inhibition

The current section shows that TBI resulted in different regional patterns of activation of a number of tau kinases. The primary site of kinase activation and accumulation was within injured axons, particularly the ipsilateral fimbria/fornix. JNK was markedly activated in this region compared to the rest of the examined kinases. JNK was also activated in cortical and thalamic regions surrounding the impact site. Notably, JNK appeared to play a critical role in TBI-induced tau hyperphosphorylation, as activated JNK colocalized with phospho-tau, and inhibition of JNK activity reduced tau phosphorylation in injured axons.

Traumatic axonal injury (TAI) is thought to cause axonal transport deficits, resulting accumulations of various organelles and proteins, including neurofilaments and

APP (Povlishock and Christman, 1995). Our data suggest that axonal transport deficits induced by TAI may be responsible for the accumulation and activation of the examined tau kinases and tau. The observations that sciatic nerve ligation resulted in accumulation of total and phosphorylated ERK1/2 and JNK (Averill et al., 2001; Reynolds et al., 2001; Middlemas et al., 2003) lend support to this hypothesis. Nonetheless, this hypothesis can be further tested by treatment of TBI mice with drugs that rescue or reduce transport deficits, such as the microtubule stabilizer epothilone D. Epothilone D has been shown to reduce fast axonal transport defects in CNS axons and lessen axonal degeneration in tau transgenic mice (Brunden et al., 2010b).

The distinct spatial distributions of activated kinases, particularly JNK, GSK-3 and PKA are indicative of the heterogeneous responses of different brain structures and cellular compartments to TBI. Such selective responses may be better documented using immunohistochemical techniques, and thus in part accounts for the mismatch between our immunohistochemical and western blotting data. Nevertheless, it is possible that our semiquantitative densitometric approach used to quantify the levels of total and activated protein kinases in hippocampal homogenates may not be sensitive enough to detect modest but functionally important changes. It is also likely that these kinases exhibit transient pattern of activation, which our analysis at 24 h post TBI failed to capture. In fact, a study using fluid percussion TBI in rats has reported that activated ERK1/2 and JNK in hippocampal lysates were evident within minutes but no longer detectable within hours post injury (Otani et al., 2002b). As such, a more thorough analysis in which mice are sacrificed at different time points post injury will be necessary to resolve the temporal profiles of activation of these kinases.

Importantly, JNK activation has been documented in contusional TBI in human (Ortolano et al., 2009). This supports the validity of our TBI model. JNK was also reported to be activated in a number of studies using the fluid percussion TBI model in rats (Mori et al., 2002b; Otani et al., 2002a; Otani et al., 2002b; Raghupathi et al., 2003; Ortolano et al., 2009) . Together, these data suggest that JNK activation is a general response to brain trauma, which is consistent with the role of JNK in signalling stress signals (Kyriakis and Avruch, 2001). Furthermore, ours and findings from Raghupathi et al. suggest that JNK signalling is complex and may have distinct functions in somata vs. axons (Rapughathi et al., 2003). In support of this notion, many studies provide evidence for the unequivocal roles of JNK and c-jun activation in programmed cell death in neurons (Silva et al., 2005). Although JNK function in axons has gotten less attention, recent investigations implicate JNK in signaling axonal injury (Cavalli et al., 2005) and in mediating axonal degeneration (Miller et al., 2009). Since hyperphosphorylated tau is associated with axon degeneration, our findings of JNK role in tau phosphorylation is in line with previous reports.

Nonetheless, our study bears a number of limitations. First, we have not tested the therapeutic windows during which D-JNKi1 can be administered. Borsello et al. showed that D-JNKi1 treatment can have beneficial effects if given up to 6 hours following ischemic injury (Borsello et al., 2003). Meanwhile, findings from Miller et al. indicated that JNK inhibition within 3 hours following axotomy of dorsal roots ganglion axons can effectively block JNK-mediated axon degeneration (Miller et al., 2009). The latter time window of JNK inhibition is perhaps more applicable to our model, since axonal injury is a major pathology observed following TBI. Second, we

have not systematically tested other doses and methods of delivery of this peptide inhibitor. This may in part explain the negative result we observed with D-JNKi1 treatment in injured Tau_{P301L} mice. Third, we have yet to determine which JNK isoform is responsible for induction tau phopshoryalation post injury. $JNK1^{-/-}$, $JNK2^{-/-}$ and $JNK3^{-/-}$ knockout mice subjected to similar injury paradigm will be useful for this purpose. Fourth, even though hyperphosphorylation of tau has been observed following a single severe injury in human, the majority of tauopathy appears to occur in individuals suffering from multiple concussions, which result in a condition known as dementia pugilistica or chronic traumatic encephalopathy. As such, it would be important to test the role of JNK in tau phosphorylation in a different injury paradigm which more closely resembles human cases. In fact, our recently developed repetitive closed-skull injury model (Shitaka et al., 2011) is a good candidate model. Fifth, although our study supports JNK activation as a probable mechanism underlying TBI-induced tau pathology, we cannot rule out other mechanisms that may result in tau hyperphosphorylation, such as changes in tau conformation (Kanaan et al., 2011) and other post-translational modifications of tau (Min et al., 2010; Cohen et al., 2011). As such, future studies will be required to assess these alternative mechanisms.

Additionally, roles of GSK-3 and PKA in tau phosphorylation will require further investigation, as activated forms of these kinases were found to localize in both axons and ipsilateral CA1 regions of injured mice. Interestingly, inhibition of GSK-3 was recently found to protect dorsal ganglion root axons from degeneration following axotomy (Gerdts et al., 2011). Thus, it is possible that a combined therapy involving

JNK, GSK-3, and possibly PKA inhibition may be required to observe functional benefits of blocking tau hyperphosphorylation and axon degeneration.

In summary, we identified JNK as a likely kinase that phosphorylates tau in vivo in the setting of TBI. We propose that targeting the JNK pathway should be tested extensively to determine whether this is beneficial in amelioration of deficits induced by TBI.

Chapter 7

Long-term Behavioral and Neurodegenerative Consequences of Acute Post-traumatic Aβ and Tau Pathologies in 3xTg-AD Mice

7.1 Introduction

Traumatic brain injury (TBI) is a major environmental risk factor for subsequent development of dementia of the Alzheimer's type (Mortimer et al., 1991; Nemetz et al., 1999; Plassman et al., 2000; Fleminger et al., 2003). Pathological hallmarks of AD include extracellular plaques containing the amyloid-beta (Aβ) peptides and neurofibirllary tangles containing microtubule-associated tau protein. Studies from human TBI, experimental TBI models in pigs (Smith et al., 1999b; Chen et al., 2004), and rodents (Iwata et al., 2002; Tran et al., 2011) support the link between TBI and AD at the pathological level. For instance, acute depositions of Aβ in diffuse plaques and inside axons have been documented in approximately 30% human TBI cases (Roberts et al., 1991; Roberts et al., 1994; Uryu et al., 2007). Acute accumulations of total and hyperphosphorylated tau inside axons and neurites, and less frequently tangle pathology, have also been reported in these patients (Smith et al., 2003c; Ikonomovic et al., 2004; Uryu et al., 2007; Johnson et al., 2011). Experimental TBI in pigs readily reproduced pathological features observed post TBI in human (Smith et al., 1999b), while TBI in

rats only recapitulated the intra-axonal Aβ accumulation aspect (Iwata et al., 2002). Our recently published TBI model using transgenic 3xTg-AD mice, which had mutant APP_{swe}, Tau_{P301L}, and $PS1_{M146V}$ knock-in, displayed acute intra-axonal total and phosphorylated tau accumulation, in addition to axonal Aβ pathology (Tran et al., 2011). Taken together, these findings support the hypothesis that TBI is causally related to AD. The questions of whether these acute pathologies negatively contribute to long-term neurodegenerative and behavioral deficits, act as a protective response, or play a neutral role following TBI remained to be studied. We therefore tested these hypotheses in this study. Furthermore, we sought to investigate the roles of mutant $PS1_{M146V}$ in TBI-induced neurodegeneration. Mutant PS1 is not only known to affect Aβ generation and tau phosphorylation (Baki et al., 2004; Koo and Kopan, 2004; Dewachter et al., 2008), but is also thought to disrupt calcium homeostasis (Mattson et al., 2000; LaFerla, 2002; Mattson, 2010). As such, PS1 mutant alone can have detrimental effects on neuronal and behavioral outcomes following TBI. Since differences in genetic background strains may influence behavioral performance (Owen et al., 1997; Holmes et al., 2002), we generated homozygous 3xTg and $PS1_{M146V}$ littermates and used them for all experiments in this study. 3xTg mice are homozygous for APP_{swe}, Tau_{P301L}, and $PS1_{M146V}$ mutations, while PS1 mice are homozygous for only $PS1_{M146V}$ mutation. We subjected young mice to controlled cortical impact TBI, tested them on the Morris water maze task at 1 month and 6 months post injury, and assessed their brains histologically. We found that the acute post-traumatic Aβ and tau pathologies played a neutral role in long-term outcomes: TBI-induced degeneration and long-term cognitive deficits in injured mice were similar between genotypes. Furthermore, while persistent axonal Aβ

pathology was observed up to 6 months post injury in 3xTg-AD mice, chronically abnormal tau phosphorylation was a common feature in both injured 3xTg-AD and PS1 mice. Taken together, our data demonstrate that TBI can initiate chronic neurodegenerative processes but that these processes do not appear to contribute negatively to behavioral outcomes in mice.

7.2 Spatial Learning as Assessed by the Morris Water Maze Task in 3xTg and PS1 Littermate Controls at 1 and 6 months post TBI

To study the long-term neurodegenerative and behavioral consequences of the acute Aβ and tau pathologies observed in 3xTg mice post TBI and to investigate the roles of mutant $PS1_{M146V}$ in TBI-induced neurodegeneration, we performed controlled cortical impact TBI on 3xTg and PS1 littermates. 3xTg mice are homozygous for APP_{swe}, Tau_{P301L}, and $PS1_{M146V}$ mutations, while PS1 mice are homozygous for only $PS1_{M146V}$ mutation. Mice were moderately injured at 2.0 mm below the dura, since this injury severity has been previously shown to result in robust and acute Aβ and tau abnormalities in young 3xTg mice (Tran et al., 2011).

To test for learning and memory, we used the Morris water maze task. One sham and one TBI group were tested at 1 month post TBI or sham surgeries, while another TBI group was tested at 6 months post injury. Overall, injured PS1 and 3xTg mice were significantly impaired in this task. For escape latencies in the visible platform

testing at 1 month post injury, there were significant main effects of injury status ($F = 17.28$, $p = 0.00026$, repeated measures ANOVA), day of testing ($p < 0.00001$), but no interaction between injury status and day of testing ($p = 0.17$). There were also significant main effects of genotype ($F = 6.94$, $p = 0.01$), in which 3xTg mice took 37% longer time to locate the visible platform than PS1 mice (14.57 ± 1.07 vs 10.61 ± 1.05 seconds). There was a significant interaction between genotype and day of training ($p = 0.0041$): latencies on day 1, but not days 2-3, were longer in 3xTg mice than PS1 mice. However, there was no interaction between injury status and genotype and day of testing ($p = 0.95$).

In the hidden platform testing, injured PS1 and 3xTg mice took longer time and swam longer distance than respective sham mice (**Figure 7.1A-B**). There were significant main effects of injury status (**Figure 7.1A**, $F = 19.06$, $p < 0.00001$), day of training ($F = 11.31$, $p < 0.00001$), but there was no interaction between injury status and day of training ($p = 0.77$). There were no effects of genotype ($F = 0.04$, $p = 0.85$), genotype x injury status ($p = 0.76$), nor day x genotype x injury status ($p = 0.84$). Performance of TBI mice at 1 month was equally impaired compared to 6 months post injury ($p = 0.57$). Similar results were found for escape distances, in that significant main effects were only observed for injury status (**Figure 7.1B**, $F = 14.63$, $p = 0.00001$). In pre-specified post hoc tests, mean escape time and escape distance over 4 days of training were not statistically different between injured PS1 and 3xTg mice at either 1 month or 6 months post injury (**Figure 7.1 C-D**, $p > 0.05$, Dunn's post hoc test). Injured mice at both time points performed worse than respective sham mice ($p <$

0.001). There was no difference in probe performance between injured and sham mice of either genotype at either time points (**Figure 7.1E**).

In summary, TBI caused long-term cognitive deficits in PS1 and 3xTg littermates. The impairments in visible platform could result from reduced motivation, motor and visual dysfunctions, or a combination of these factors. Notably, expression of all 3 transgenes in 3xTg mice appears to influence their performance in this portion of the task. The longer time and distance injured mice took to reach the hidden platform are likely due to deficits in spatial learning. All mice performed well on the probe trial, though it is possibly due to overlearning. Most intriguingly, TBI negatively affected PS1 and 3xTg to the same extent.

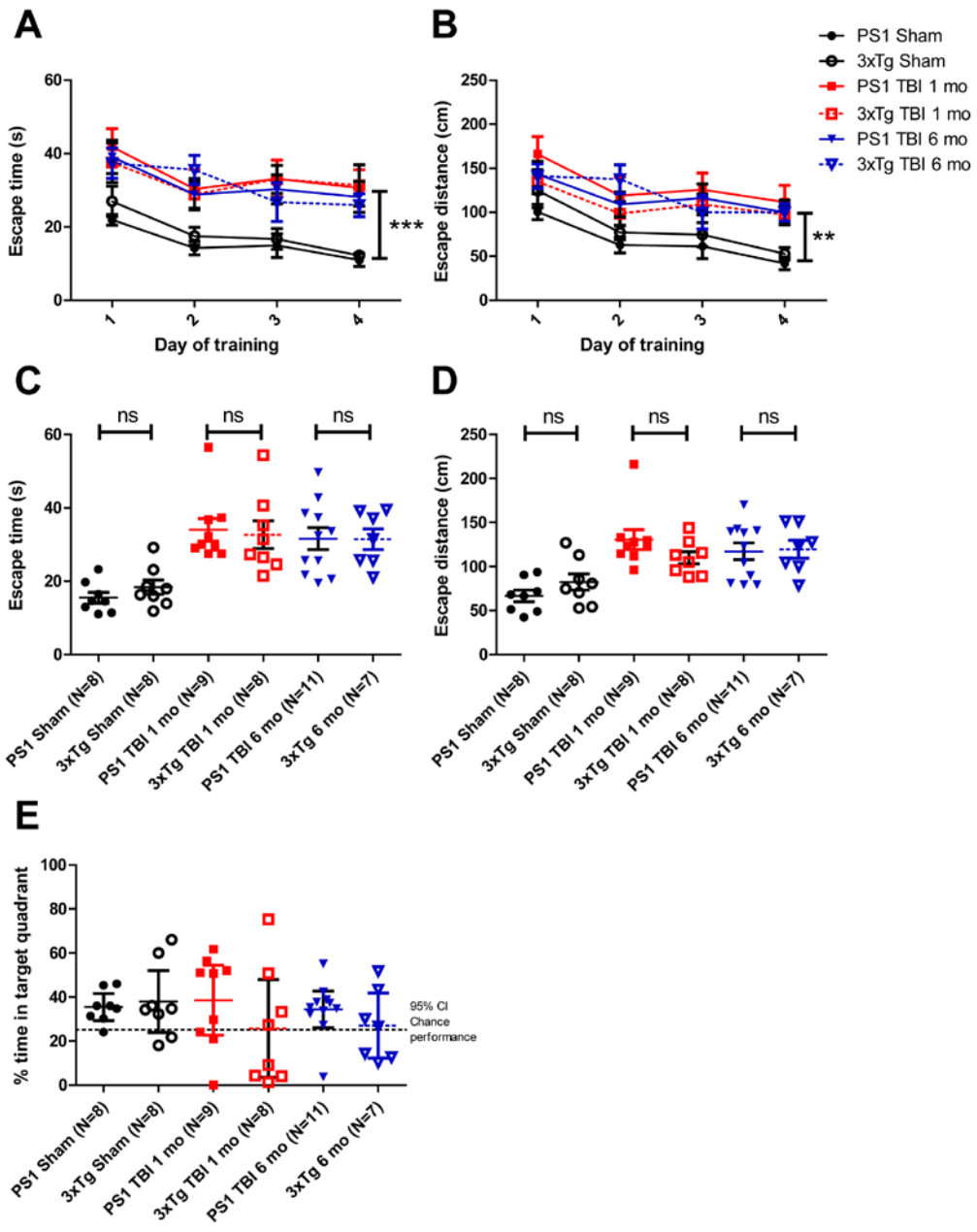

Figure 7.1 Injured 3xTg and PS1 littermate controls were equally impaired in spatial learning at 1 and 6 months post TBI.

A. Escape time mice took locate hidden platform by day of training. Repeated measures ANOVA. There is no statistical difference between genotype, genotype x injury status, day x genotype x injury status, $p > 0.05$. Statistical difference was only observed between injury status, *** $p < 0.0001$. **B.** Escape distance mice took to locate hidden platform. Statistical difference was only observed between injury status, ** $p < 0.001$. **C.** Mean time mice swam to find the

hidden platform. Each data point represents average time of 4 trials per day, and over 4 days of training. **D.** Mean distance mice swam to find the hidden platform. Each data point represents average time of 4 trials per day, and over 4 days of training. Kruskal-Wallis test with Dunn's post-hoc test. Bars are mean ± SEM. **E.** Probe trial at 24 h post the last training session; bars are 95% CI.

7.3 Neurodegeneration in 3xTg and PS1 Littermate Controls at 1 and 6 months post TBI

Following Morris water maze testing, all mice were sacrificed. Their brain sections were stained with cresyl violet for cytoarchitecture delineation. The remaining volumes of the hippocampus and fimbria ipsilateral to the injury site were quantified to determine the extent of degeneration following TBI. There were progressive atrophies of the ipsilateral hippocampus and fimbria of injured PS1 and 3xTg mice over time (**Figure 7.2 A-F**). Quantitative analyses corroborated the histological observations (**Figure 7.2 G-H**). Specifically, hippocampus and fimbria volumes of sham injured mice were significantly greater than those of injured mice (**Figure 7.2 G-H**, $p < 0.0001$). There were no significant difference in these measures between genotypes at 1 or 6 months post TBI (**Figure 7.2 G-H**, $p > 0.05$, Dunn's post hoc test).

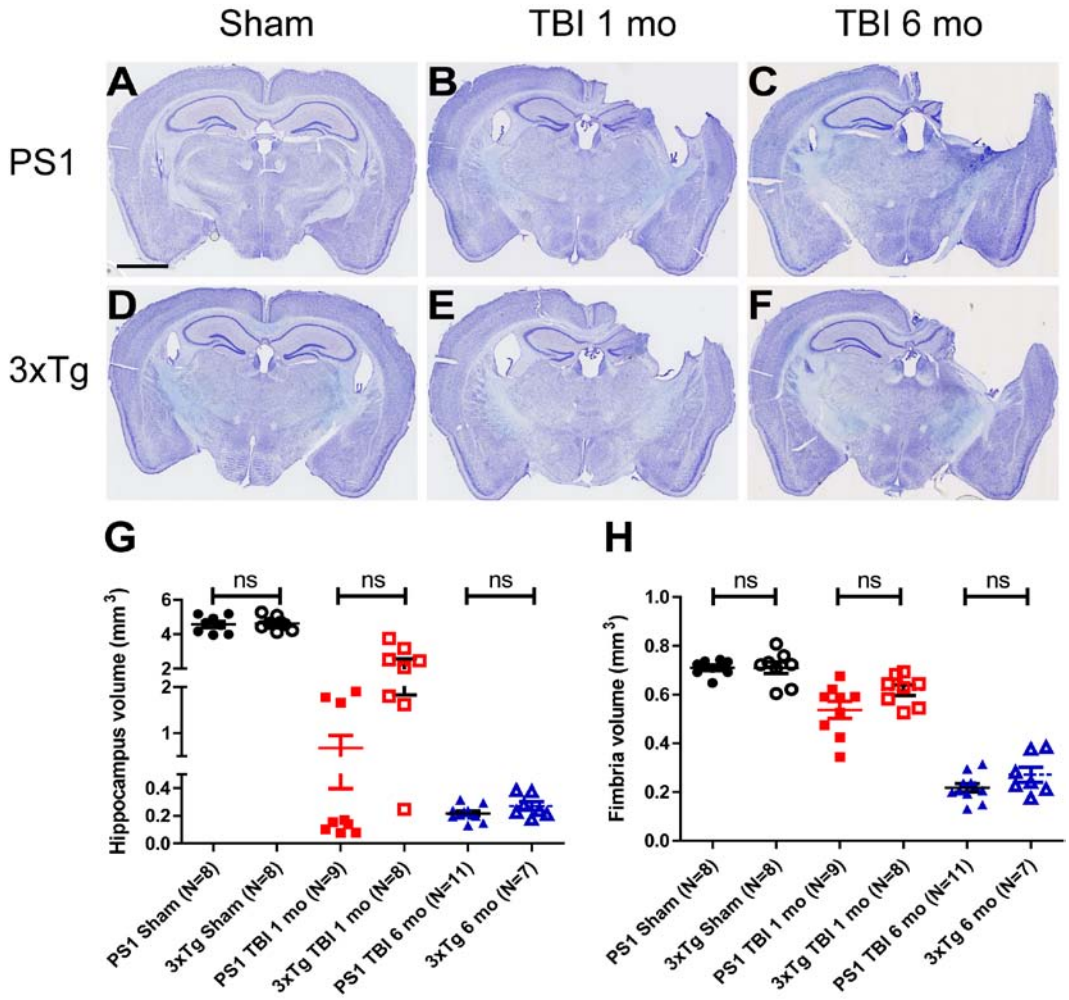

Figure 7.2 Ipsilateral hippocampus and fimbria of PS1 and 3xTg-AD littermates atrophied at similar rates following TBI.

Cresyl violet staining for cytoarchitechture. **A-C.** Representative photomicrographs of brains of PS1 mice sacrificed after sham surgery at 1 mo (**A**), and after TBI at 1 mo (**B**) and 6 mo (**C**). Scale bar: 2mm. **D-F.** 3xTg-AD mice. **G.** Quantification of the hippocampus volume of PS1 and 3xTg-AD littermates subjected to sham or TBI and sacrificed at indicated time points. **H.** Quantification of the fimbria volume of PS1 and 3xTg-AD littermates subjected to sham or TBI and sacrificed at indicated time points. Kruskal-Wallis test with Dunn's post-hoc test. ns: not significant.

7.4 Histopathologies of 3xTg and PS1 Littermate Controls at 1 and 6 months post TBI

7.4.1 Long-term Consequences of TBI on Axonal Injury and Axonal Aβ Pathology

To assess the long-term effects of TBI on axonal injury, we stained brain sections of 4 randomly chosen mice in each group with APP, a robust marker of axonal injury. Since we have previously reported that the ipsilateral fimbria/fornix of injured 3xTg mice exhibited extensive APP staining at 24 h and up to 7 d post TBI (Tran et al., 2011), we focused on this pericontusional axonal tract for our chronic study. There were still numerous APP-stained axonal bulbs in the ipsilateral fimbria/fornix of injured mice at 1 mo post TBI (**Figure 7.3 B, E, H**). This staining persisted up to 6 months following injury, though to a lesser extent (**Figure 7.3 C, F, I**). APP axonal bulbs at these chronic time points still had the spheroidal morphology, which is typical of injured axons. As expected, axonal APP-stained varicosities were not observed in sham injured mice (**Figure 7.3 A, D, G**). Interestingly, the extent of APP staining was qualitatively similar in both injured PS1 and 3xTg littermates.

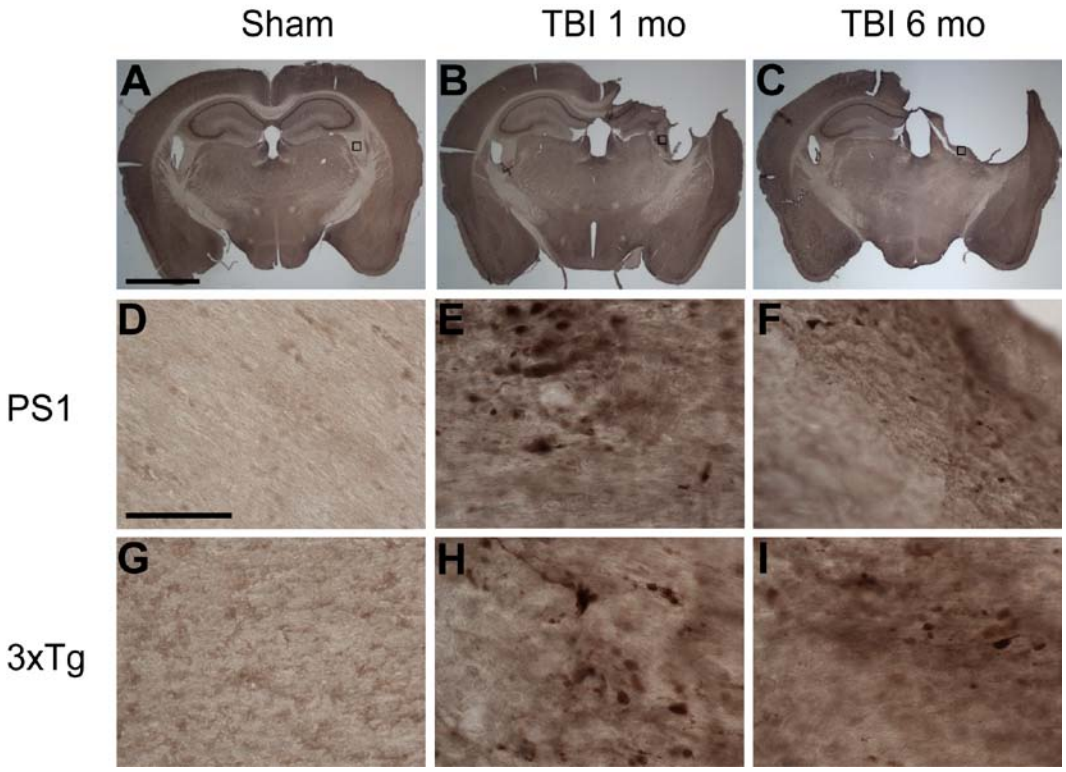

Figure 7.3 Persistent axonal injury as detected by APP immunohistochemistry in PS1 and 3xTg littermates at 1 month and 6 months post injury.
A-C. APP staining of a section from a sham (**A**) and injured PS1 mouse sacrificed at 1 mo (**B**) or 6 mo (**C**) post surgery. Scale bar: 2 mm. **D-F.** Higher magnification of the fimbria/fornix (boxes in **A-C**) shows APP positive varicosities.

We next studied the long-term effects of TBI on Aβ pathology in these mice. PanAβ antibody (against amino acids 15-30) and 3D6 antibody (against amino acids 1-5) were used for Aβ immunohistochemistry. We found axonal Aβ accumulation in the ipsilateral fimbria/fornix of all examined injured 3xTg mice at both 1 month and 6 months post injury (**Figure 7.4 B-C, K-L, N-O**). Similar to APP staining, there were much less Aβ accumulations at 6 months as compared to 1 month post TBI. Axonal Aβ pathology was not observed in injured PS1 mice (**Figure 7.4 E-F, H-I**), sham PS1 and 3xTg mice (**Figure 7.4 D, J**), or in brain sections of injured 3xTg mice when primary

antibody was omitted (**Figure 7.4 Q**). No extracellular Aβ plaques were observed in injured PS1 or 3xTg mice at either time points, even though the staining method used is capable of detecting Aβ plaques in an 8 month-old APP/PS1 mice (Jankowsky et al., 2004) (**Figure 7.4 R**).

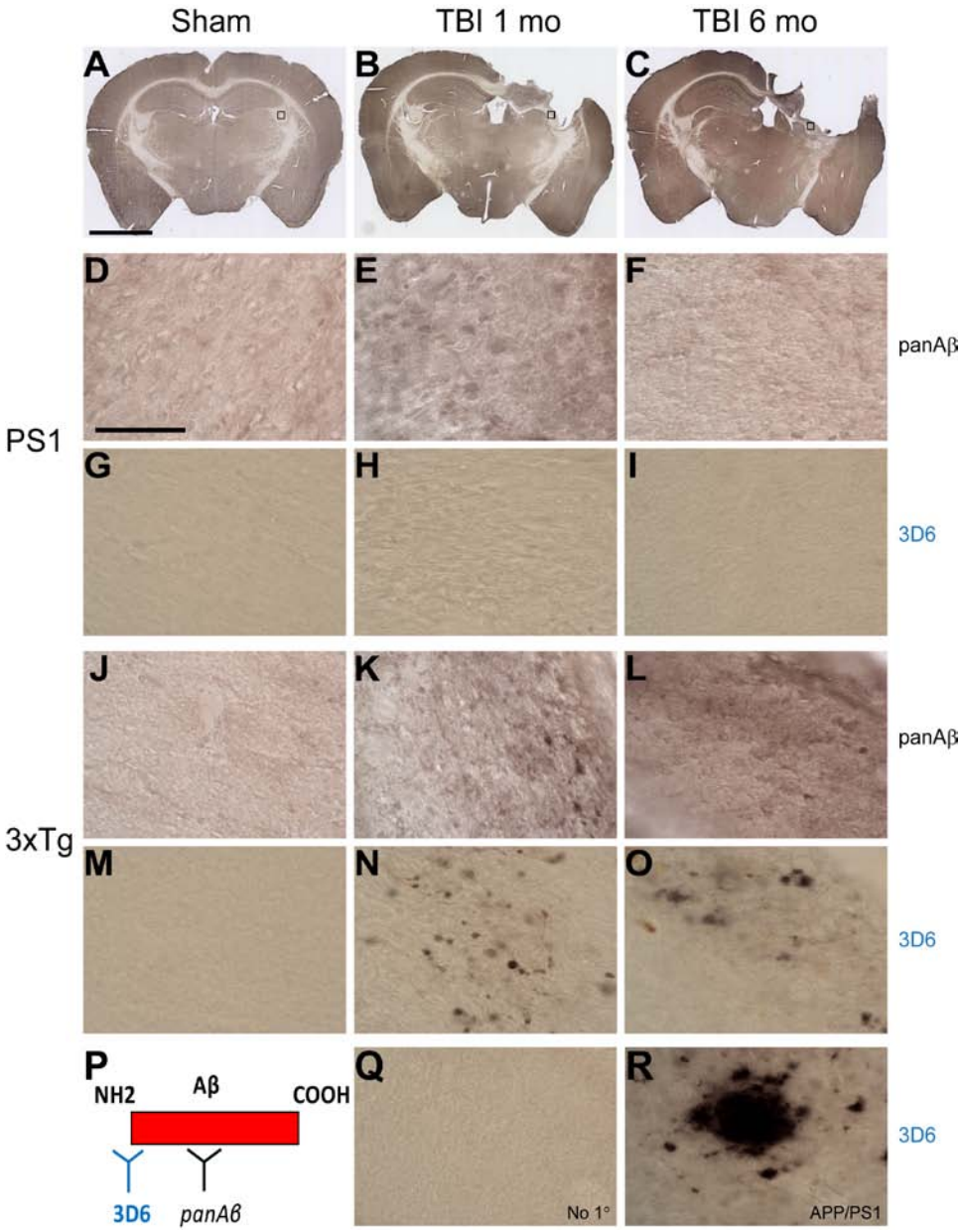

Figure 7.4 TBI did not result in the formation of Aβ plaques but caused persistent intraa-xonal Aβ accumulations at 1 and 6 months post injury in 3xTg-AD mice.

A-C. Low magnification image of a section from a sham (**A**) and injured 3xTg-AD mouse sacrificed at 1 mo (**B**) or 6 mo (**C**) post surgery. Scale bar: 2 mm. **D-I.** Aβ staining in the ipsilateral fimbria/fornix (boxes in **A-C**) of injured PS1 mice using panAβ (**D-F**) or 3D6 (**G-I**) antibody. Scale bar: 50 μm. No intra-axonal Aβ accumulation was detected. **J-O.** Intra-axonal Aβ accumulation in injured axons of 3xTg-AD mice. **P.** Schematic of anti-Aβ antibodies used. **Q.** No immunoreactivity is observed in injured fimbria of 3xTg-AD mouse when primary antibody (3D6) was omitted. **R.** Extracellular plaques from a positive control, 8 month-old APP/PS1 mouse, detected by 3D6 antibody.

7.4.2 Tau Pathology in 3xTg and PS1 Littermate Controls at 1 and 6 months post TBI

Next, we examined the long-term effects of TBI on tau pathology in these mice, since we have shown that TBI can acutely affect tau phosphorylation in 3xTg mice. Brain sections from the same mice used for Aβ staining were stained with antibody against phospho-tau at S396 and S404 (PHF1 antibody). Intra-axonal punctate PHF1 tau staining was observed in the ipsilateral fimbria/fornix of both injured PS1 and 3xTg mice at 1 month (**Figure 7.5 B, E, K**), and to a lesser extent at 6 months post injury (**Figure 7.5 C, F, L**). While minute staining was observed in sham 3xTg mice (**Figure 7.5 J**), no staining was observed in sham PS1 mice (**Figure 7.5 D**) and injured 3xTg mice when the primary antibody was omitted (**Figure 7.5 Q**). Perinuclear PHF1 staining was observed in the ipsilateral amygdala of injured mice at both time points but not sham injured mice (**Figure 7.5 G-I, M-O**).

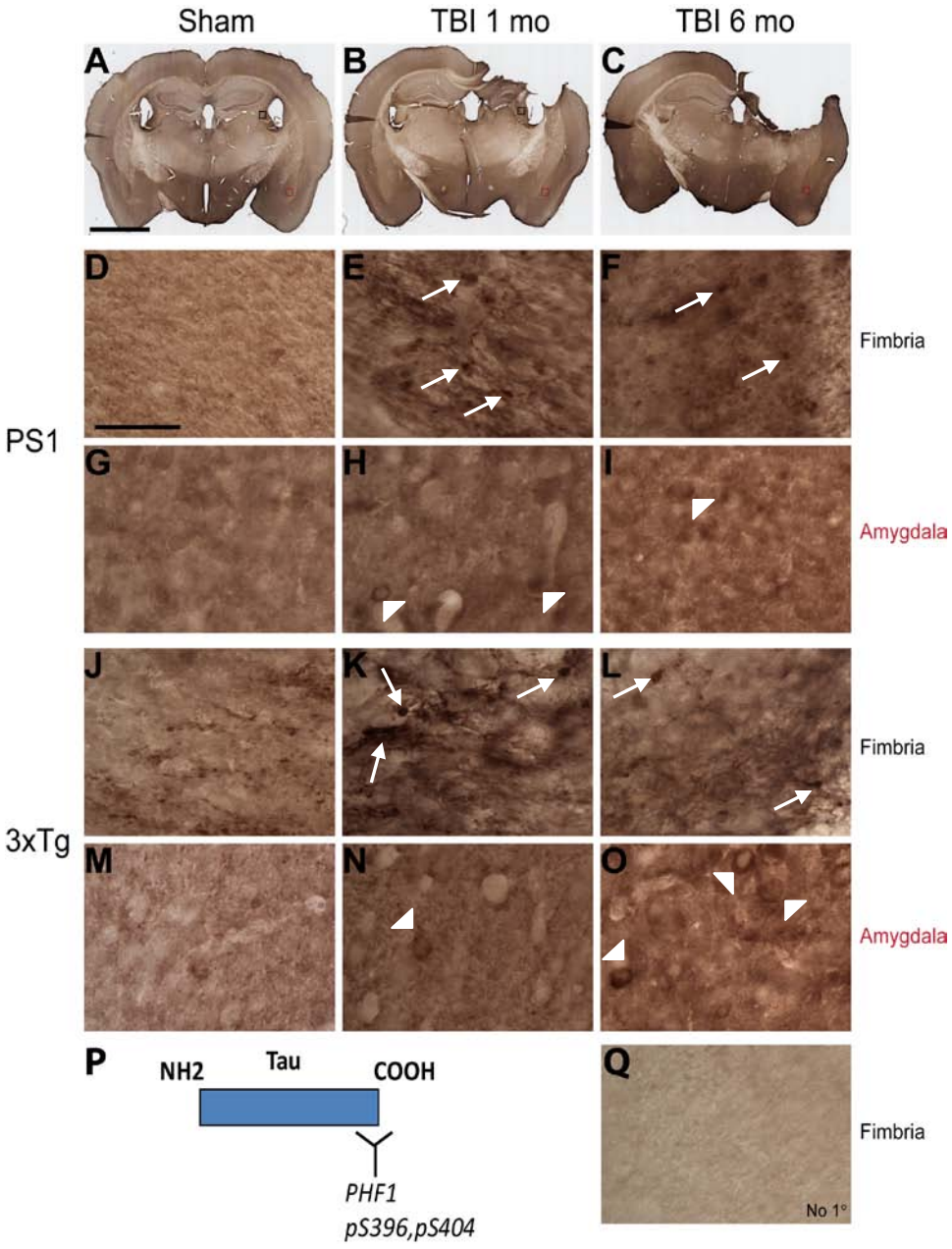

Figure 7.5 TBI did not result in neurofibrillary tangles but caused persistent phopho-tau accumulation as detected by PHF1 antibody in the ipsilateral fimbria and amygdala of injured mice.

A-C. Low magnification image of a section from a sham (**A**) and injured 3xTg-AD mouse sacrificed at 1 mo (**B**) or 6 mo (**C**) post surgery. Scale bar: 2 mm. **D-F.** High magnification images of the ipsilateral fimbria/fornix (black box in **A-C**) of PS1 littermates. Scale bar: 50 μm. **G-I.** High magnification of the ipsilateral amygdala (red box in **A-C**) of PS1 littermates. **J-L.**

Ipsilateral fimbria of 3xTg-AD mice. **M-O.** Ipsilateral amygdala of 3xTg-AD mice. **P.** Schematic of epitope at which PHF1 antibody detects of full-length tau. **Q.** Ipsilateral fimbria of an injured 3xTg-AD mouse when primary antibody is omitted. Punctate tau staining is present in the ipsilateral fimbria of injured PS1 and 3xTg-AD mice (arrows). Cytoplasmic, perinuclear tau staining is observed in the ipsilateral amygdala of injured mice (arrow head).

7.4.3 No Formation of Fibrillar Structures in 3xTg and PS1 Littermate Controls at 1 and 6 months post TBI

We further asked if TBI could lead to formation of fibrillar structures such as plaques and neurofibrillary tangles in the long-term following injury in these mice. Thus, X-34 staining was employed. We did not detect any positive X-34 staining in all mice examined, even though signal was observed for the positive control APP/PS1 brain sections (data not shown).

7.5 Discussion

In summary, we found that controlled cortical impact TBI results in long-term behavioral deficits and progressive neuro- and axonal- degeneration in 3xTg and PS1 littermates. Learning deficits were evidenced by impaired performance of injured 3xTg and PS1 mice compared to sham in the hidden platform Morris water maze task. Moreover, these impairments persisted up to 6 months following TBI. Hippocampus and fimbria ipsilateral to the injury significantly atrophied over 6 months post trauma. Interestingly, both the rate and extent of degeneration were similar in injured 3xTg and PS1 mice. Furthermore, TBI causes persistent axonal injury as detected by APP in both injured 3xTg and PS1 mice. 3xTg mice subjected to TBI also had persistent axonal Aβ and phospho-tau pathology in the ipsilateral fimbria, and somatic phospho-tau staining

in the ipsilateral amygdala, though the immunoreactivity was markedly reduced compared to the acute phase post injury (Tran et al., 2011). Meanwhile, PS1 mice subjected to TBI did not exhibit any Aβ pathology, but had persistent phospho-tau accumulation in the axonal (fimbria) and somatic (amygdala) compartments.

It appears unlikely that axonal Aβ pathology contributes to TBI-induced neurodegeneration and behavioral deficits in 3xTg mice. The evident neuronal atrophy and cognitive impairments of injured PS1 mice in the absence of axonal Aβ pathology support this claim. Tau hyperphosphorylation affects its ability to bind and stabilize microtubule. This in turn affects normal structural and regulatory functions of the cytoskeleton, and ultimately leads to neuronal dysfunction, degeneration, and death. Interestingly, chronic accumulation of hyperphosphorylated tau was observed to be a common pathological feature in injured 3xTg and mutant PS1 mice. As such, tau pathology, but not Aβ, may mediate the progressive neurodegeneration and behavioral deficits observed in these mice. Future studies will be required to determine the mechanisms underlying TBI-induced tau hyperphosphorylation and whether reducing tau phosphorylation is beneficial in the setting of TBI.

The interaction between TBI and mutant PS1 is intriguing. Various mutants PS1, including $PS1_{M146V}$, have been implicated in neuronal calcium dyshomeostasis, which renders neurons more vulnerable to various insults (Koo and Kopan, 2004; Mattson, 2010). Thus, our findings that TBI causes similar impairments in 3xTg and PS1 mice, though surprising, is not unprecedented.

APP, which is normally transported along axons via the fast axonal transport mechanism, is a robust marker of traumatic axonal injury (Grady et al., 1993; Christman

et al., 1994; Graham et al., 1995; Stone et al., 2000, 2001). As such, all injured mice examined had positive axonal APP staining. The presence of APP within injured axons up to 6 months post injury is also in accord with findings in human TBI (Chen et al., 2009).

APP accumulation in injured axons appears necessary but not sufficient for axonal Aβ pathology. This is corroborated by extensive APP accumulations observed in both injured 3xTg and PS1, but only in injured 3xTg were there axonal Aβ accumulations. These results also highlight the importance of the interaction between mutant PS1 and APP to generate Aβ the setting of trauma in mice.

Previous studies from human TBI cases (Smith et al., 2003c) and an experimental TBI study in pigs (Smith et al., 1999b) have often found Aβ containing plaque-like profiles to be in proximity to Aβ-positive axonal bulbs. These data thus leads to the proposal that axonal Aβ accumulation and subsequent release from injured axons may contribute to formation of extracellular Aβ plaques in the setting of brain trauma. In contrast to this hypothesis, one human TBI study shows that axonal Aβ pathology can exist for years following TBI in humans without any effects on extracellular plaques (Chen et al., 2009). Our findings of persistent axonal Aβ pathology and absence of extracellular plaques at 6 months post trauma in 3xTg mice lends further evidence against this hypothesis. Our study did not address, however, the origin of these chronically accumulated Aβ species. It is possible that these are remnants of the acute axonal Aβ accumulations observed in these mice at 1 d and 7 d post injury. They could also be newly formed Aβ, since long-term co-localizations of Aβ, APP and APP

cleaving enzymes, BACE and PS-1, have been previously reported (Chen et al., 2004; Uryu et al., 2007; Chen et al., 2009).

Another possible mechanism through which TBI could induce long-term deficits in these mice is via modulation of the inflammatory responses (Loane and Byrnes, 2010; Czlonkowska and Kurkowska-Jastrzebska, 2011). Consequently, additional studies will be required to determine the roles of astrogliosis in this setting.

Taken together, our study shows that a single episode of TBI can initiate long-term degenerative processes and have detrimental effects on behavioral performance, but these may be unrelated.

Chapter 8

Conclusions and Future Directions

8.1 Conclusions

In summary, we found that controlled cortical impact TBI in 3xTg-AD mice recapitulated two key features observed post TBI in human. First, TBI caused rapid Aβ accumulation in injured axons of young 3xTg-AD mice. This intra-axonal Aβ was detectable at 1 hour post injury, and continued to rise monotonically through 24 hours. This is similar to the intra-axonal Aβ accumulation observed in human TBI patients (Smith et al., 2003c; Ikonomovic et al., 2004; Uryu et al., 2007; Chen et al., 2009). No such accumulation is expected at this age and none was seen in sham-injured mice. Second, TBI increased tau immunoreactivity in three distinct brain regions of moderately injured 3xTg-AD mice. The time course was different across regions. In particular, puntate tau staining the ipsilateral fimbria and perinuclear tau staining in the amygdala had a biphasic response with peaks at 1 hour and 24 hours post TBI. Instead, the numbers of tau-positive processes in the contralateral CA1 started to increase at 12 h post injury. Total tau immunoreactivity in the ipsilateral CA1 was not significantly affected by TBI. This may be because of substantial damage to this region, which could have caused tau release into the extracellular space, where it could not be detected immunohistochemically. Further, there was also immunohistochemical and biochemical evidence for increased tau phosphorylation induced by TBI at several epitopes.

Next, we found that systemic inhibition of γ-secretase activity by CmpE effectively blocked the post-traumatic Aβ accumulation in 3xTg-AD mice at both 24 h and 7 d post injury. However, Aβ blockade did not affect tau pathology accelerated by TBI at either time points. These data suggest that Aβ and tau do not interact in the setting of brain trauma.

Furthermore, we showed that the finding of post-traumatic Aβ accumulation in 3xTg-AD mice was recapitulated in a different transgenic mouse model of Alzheimer's disease, APP/PS1. We also found TBI to accelerate tau pathology in transgenic mice carrying only Tau_{P301L} mutation at 24 hours. This finding further supports the independent relationship between Aβ and tau in the setting of TBI.

Additionally, we showed that TBI resulted in different regional patterns of activation of a number of tau kinases. The primary site of kinase activation and accumulation was within injured axons, particularly the ipsilateral fimbria/fornix. The stress activated kinase, c-jun-N-termnial kinase (JNK) was markedly activated in this region compared to the rest of the examined kinases. JNK was also activated in cortical and thalamic regions surrounding the impact site. Notably, JNK appeared to play a critical role in TBI-induced tau hyperphosphorylation, as activated JNK colocalized with phospho-tau, and inhibition of JNK activity reduced tau phosphorylation in injured axons.

Lastly, we found that controlled cortical impact TBI resulted in long-term behavioral deficits and progressive neuro- and axonal- degeneration in 3xTg-AD mice. However, these deficits cannot be attributed to the Aβ and tau pathologies observed

acutely in these mice post TBI, since injured PS1 littermate controls exhibited similar degree of neurodegeneration and cognitive impairments.

8.2 Future Directions

Traumatic axonal injury (TAI) may contribute greatly to morbidity and cognitive dysfunction following TBI. TAI is thought to cause axonal transport deficits, resulting accumulations of various organelles and proteins, including neurofilaments and APP (Povlishock and Christman, 1995). Our data provide further evidence that axonal transport deficits induced by TAI may be responsible for the accumulation of Aβ, tau, and tau kinases. As a result, future studies aiming at reducing axonal transport deficits will likely prove beneficial in the setting of TBI. The use of microtubule-stabilizing drugs such as paclitaxel and epothilone D (EpoD) has been shown to improve microtubule density, ameliorate axonal transport defects, and improve motor and cognitive deficits in tau transgenic mice (Zhang et al., 2005; Brunden et al., 2010b). Notably, mice which received either 1 mg/kg or 3 mg/kg of EpoD weekly for 3 months did not exhibit any overt side-effects (Brunden et al., 2010b). Therefore, similar dosages and treatment regimen of this compound could be employed to treat both transgenic and wildtype mice following controlled cortical impact TBI. It will also be important to evaluate the effectiveness of this drug in a milder injury model, since the majority of TBI cases are mild. In fact, the repetitive closed-skull impact model recently developed by me and characterized by Dr. Shitaka from our lab is a good candidate model. We have reported that 2 consecutive impacts 24 hours apart can cause persistent axonal injury and microglial activation in absence of gross parenchymal damage and

overt cell death (Shitaka et al., 2011). Electron microscopic and electrophysiological studies can be used to assess structural and functional integrity of CNS axonal tracts such as the corpus callosum, fimbria/fornix, and optic nerve following EpoD or vehicle treatment in injured mice. Further, since abnormal signal in diffusion tensor magnetic resonance imaging, which detects water diffusion along white matter, has been shown to correlate with TAI in alive but injured mice (Mac Donald et al., 2007a), this imaging modality could be used as an additional outcome measures of the effectiveness EpoD treatment in rescuing transport deficits in experimental TBI.

The role of JNK in TBI-induced tau pathology will require rigorous testing in future studies. First, a more detailed time course of JNK activation following controlled cortical impact in 3xTg-AD mice will provide useful information for determination of therapeutics windows of JNK inhibition. For this purpose, separate groups of injured mice could be sacrificed at 0.5, 1, 3, 6, and 12 hours, and at 3 and 7 days post injury. JNK activation can be assessed via IHC or WB with antibody against phospho (activated) JNK, or by western blotting against phospho c-jun, or by pull down kinase assay as described (Barr et al., 2002).

Second, we initially used the D-stereoisomer of the JNK inhibiting peptide (D-JNKi1) because of its reported long half-life: FITC-labeled D-JNKi1 peptides were present up to two weeks following application to insulin-secreting cell line (Bonny et al., 2001). However, since JNK has been reported to involve in both axon degeneration (Miller et al., 2009) and regeneration (Nix et al., 2011) following axotomy, it may be better to inhibit JNK during the time when its activity is detrimental. As such, the use of

L-JNKi1 (L-stereoisomer), which has a shorter half-life (less than 24 hours in cell culture) (Bonny et al., 2001), should be tested.

Third, delivery of these peptide inhibitors via intraperitoneal injections should be considered, since this delivery method has been shown to effectively inhibit JNK activity in the mouse models of ischemia (Borsello et al., 2003b; Nijboer et al., 2010).

Next, it will be interesting to determine the upstream signals that activate JNK in the setting of TBI. As a stress-activated kinase, JNK is readily activated by various cytokines (Kyriakis and Avruch, 2001). Furthermore, glutamate has been shown to activate JNK (Borsello et al., 2003a; Choi, 2010), and JNK3-/- protected hippocampal cells from glutamate-induced excitoxicity (Yang et al., 1997). Both glutamate and cytokines such as TNF-α and IL-1β (Lu et al., 2009) are also highly upregulated following brain trauma. Therefore, glutamate receptor antagonists, TNF-α, and IL-1β inhibitors could be employed to determine if these molecules are activators of JNK.

In a pilot study, I found that controlled cortical impact TBI significantly increase caspase-6 but not caspase-3 activity in injured wildtype and 3xTg-AD mice. I also found cleaved (activated) caspase 6 to localize in injured axons of 3xTg-AD mice. Since stress-activated p38 kinase, but not JNK, has been shown to activate caspase 3 in neurons treated with nitric oxide (Ghatan et al., 2000), a product of glutatmate-induced excitotoxicity, it is probable that JNK, but not p38, may be involved in caspase 6 activation in axons. Interestingly, caspase 6 activation has been implicated in axonal degeneration in developing neuronal cultures (Nikolaev et al., 2009). Thus, it will be interesting to determine if similar signaling pathway is involved in axon degeneration in adult mice following TBI. Toward this end, brain homogenates from injured mice

treated with JNK inhibitor peptide could be used to examine caspase activity using VEID-pNA colorimetric assay kit (R&D Systems). Alternatively, treatment of injured mice with a caspase 6 specific inhibitor, VEID-fmk (Calbiochem), could be studied to determine if it could prevent or delay axon degeneration.

Tau pathology is a major pathological hallmark of dementia pugilistica or chronic traumatic encephalopathy (Roberts et al., 1990; Schmidt et al., 2001; McKee et al., 2009), which results from a life-long history of concussive injuries. Thus, it will be important to determine if JNK mediates tau phosphorylation and accumulation in repetitive TBI. JNK activation can be assessed in post-mortem tissues of athletes and boxers. JNK roles in acceleration tau pathology in tau only transgenic mice subjected to repetitive closed-skull impacts will be an important future direction. Moreover, although there exists a strong link between ApoE genotypes and TBI outcomes (Sorbi et al., 1995; Teasdale et al., 1997; Friedman et al., 1999; Lichtman et al., 2000; Diaz-Arrastia et al., 2003; Teasdale et al., 2005; Zhou et al., 2008), differential interaction between ApoE genotypes and microtubule and tau (Horsburgh et al., 2000), and TBI and tau pathology, there is virtually no experimental model which investigates the interaction between tau, ApoE genotypes and TBI. As such, it will be important and will significantly advance the field to study the chronic effect of repetitive TBI in tau and ApoE-2, -3, and -4 knockin or tau and ApoE knockout double transgenic mice.

Lastly, future research should also focus on the roles of GSK-3 on tau phosphorylation and axon degeneration. I found activated GSK-3 to localize to pericontusional CA1 and white matter structures of injured 3xTg-AD mice. It will be important to determine if TBI increases GSK-3 activity using GSK-3 kinase activity as

described (Noble et al., 2005), and if inhibition of GSK-3 activity using lithium or small molecule inhibitor of GSK-3 will reduce TBI-induced tau pathology and axon degeneration. It may be possible that a combined GSK-3 and JNK inhibition regimen will be required to see functional and behavioral benefits of reduction tau pathology in the setting of TBI.

Concluding Remarks:

TBI is a major environmental risk factor for subsequent development of AD. Thus, it is important to understand the underlying link between TBI and AD. During my thesis, I have found that controlled cortical impact TBI caused acute accumulation of Aβ, tau, and phospho-tau. While it is unlikely that acute Aβ pathology contributes negatively to behavioral outcomes, the role of tau pathology is still to be determined. While much work will be required in future studies, identification of JNK as a possible tau kinase in the setting of TBI provides a starting point for research into mechanisms underlying TBI-induced tau pathology, and for determination of whether reducing tau pathology would ameliorate adverse outcomes following TBI.

References

Abbott A (2011) Dementia: a problem for our age. Nature 475:S2-4.

Abrahamson EE, Ikonomovic MD, Ciallella JR, Hope CE, Paljug WR, Isanski BA, Flood DG, Clark RS, DeKosky ST (2006) Caspase inhibition therapy abolishes brain trauma-induced increases in Abeta peptide: implications for clinical outcome. Experimental neurology 197:437-450.

Adams JA, McGlone ML, Gibson R, Taylor SS (1995) Phosphorylation modulates catalytic function and regulation in the cAMP-dependent protein kinase. Biochemistry 34:2447-2454.

Adams JH (1982) Diffuse axonal injury in non-missile head injury. Injury 13:444-445.

Adams JH, Doyle D, Graham DI, Lawrence AE, McLellan DR (1984) Diffuse axonal injury in head injuries caused by a fall. Lancet 2:1420-1422.

Alonso AC, Grundke-Iqbal I, Iqbal K (1996) Alzheimer's disease hyperphosphorylated tau sequesters normal tau into tangles of filaments and disassembles microtubules. Nature medicine 2:783-787.

Alonso AC, Zaidi T, Grundke-Iqbal I, Iqbal K (1994) Role of abnormally phosphorylated tau in the breakdown of microtubules in Alzheimer disease. Proceedings of the National Academy of Sciences of the United States of America 91:5562-5566.

Alonso AD, Grundke-Iqbal I, Barra HS, Iqbal K (1997) Abnormal phosphorylation of tau and the mechanism of Alzheimer neurofibrillary degeneration: sequestration of microtubule-associated proteins 1 and 2 and the disassembly of microtubules by the abnormal tau. Proceedings of the National Academy of Sciences of the United States of America 94:298-303.

Anderson NG, Maller JL, Tonks NK, Sturgill TW (1990) Requirement for integration of signals from two distinct phosphorylation pathways for activation of MAP kinase. Nature 343:651-653.

Anderton BH, Callahan L, Coleman P, Davies P, Flood D, Jicha GA, Ohm T, Weaver C (1998) Dendritic changes in Alzheimer's disease and factors that may underlie these changes. Progress in neurobiology 55:595-609.

Arendt T, Holzer M, Fruth R, Bruckner MK, Gartner U (1998) Phosphorylation of tau, Abeta-formation, and apoptosis after in vivo inhibition of PP-1 and PP-2A. Neurobiology of aging 19:3-13.

Arundine M, Tymianski M (2004) Molecular mechanisms of glutamate-dependent neurodegeneration in ischemia and traumatic brain injury. Cell Mol Life Sci 61:657-668.

Averill S, Delcroix JD, Michael GJ, Tomlinson DR, Fernyhough P, Priestley JV (2001) Nerve growth factor modulates the activation status and fast axonal transport of ERK 1/2 in adult nociceptive neurones. Mol Cell Neurosci 18:183-196.

Baki L, Shioi J, Wen P, Shao Z, Schwarzman A, Gama-Sosa M, Neve R, Robakis NK (2004) PS1 activates PI3K thus inhibiting GSK-3 activity and tau overphosphorylation: effects of FAD mutations. The EMBO journal 23:2586-2596.

Ballatore C, Lee VM, Trojanowski JQ (2007) Tau-mediated neurodegeneration in Alzheimer's disease and related disorders. Nature reviews Neuroscience 8:663-672.

Ballatore C, Brunden KR, Piscitelli F, James MJ, Crowe A, Yao Y, Hyde E, Trojanowski JQ, Lee VM, Smith AB, 3rd (2010) Discovery of brain-penetrant, orally bioavailable aminothienopyridazine inhibitors of tau aggregation. Journal of medicinal chemistry 53:3739-3747.

Barr RK, Kendrick TS, Bogoyevitch MA (2002) Identification of the critical features of a small peptide inhibitor of JNK activity. The Journal of biological chemistry 277:10987-10997.

Bhat RV, Shanley J, Correll MP, Fieles WE, Keith RA, Scott CW, Lee CM (2000) Regulation and localization of tyrosine216 phosphorylation of glycogen synthase kinase-3beta in cellular and animal models of neuronal degeneration. Proceedings of the National Academy of Sciences of the United States of America 97:11074-11079.

Blanchard V, Moussaoui S, Czech C, Touchet N, Bonici B, Planche M, Canton T, Jedidi I, Gohin M, Wirths O, Bayer TA, Langui D, Duyckaerts C, Tremp G, Pradier L (2003) Time sequence of maturation of dystrophic neurites associated with Abeta deposits in APP/PS1 transgenic mice. Experimental neurology 184:247-263.

Blennow K (2011) Dementia in 2010: Paving the way for Alzheimer disease drug development. Nature reviews Neurology 7:65-66.

Blumbergs PC, Scott G, Manavis J, Wainwright H, Simpson DA, McLean AJ (1994) Staining of amyloid precursor protein to study axonal damage in mild head injury. Lancet 344:1055-1056.

Blumbergs PC, Scott G, Manavis J, Wainwright H, Simpson DA, McLean AJ (1995) Topography of axonal injury as defined by amyloid precursor protein and the sector scoring method in mild and severe closed head injury. Journal of neurotrauma 12:565-572.

Bonny C, Oberson A, Negri S, Sauser C, Schorderet DF (2001) Cell-permeable peptide inhibitors of JNK: novel blockers of beta-cell death. Diabetes 50:77-82.

Borchelt DR, Ratovitski T, van Lare J, Lee MK, Gonzales V, Jenkins NA, Copeland NG, Price DL, Sisodia SS (1997) Accelerated amyloid deposition in the brains of transgenic mice coexpressing mutant presenilin 1 and amyloid precursor proteins. Neuron 19:939-945.

Borsello T, Croquelois K, Hornung JP, Clarke PG (2003a) N-methyl-d-aspartate-triggered neuronal death in organotypic hippocampal cultures is endocytic, autophagic and mediated by the c-Jun N-terminal kinase pathway. The European journal of neuroscience 18:473-485.

Borsello T, Clarke PG, Hirt L, Vercelli A, Repici M, Schorderet DF, Bogousslavsky J, Bonny C (2003b) A peptide inhibitor of c-Jun N-terminal kinase protects against excitotoxicity and cerebral ischemia. Nature medicine 9:1180-1186.

Braak E, Braak H, Mandelkow EM (1994) A sequence of cytoskeleton changes related to the formation of neurofibrillary tangles and neuropil threads. Acta neuropathologica 87:554-567.

Bramblett GT, Goedert M, Jakes R, Merrick SE, Trojanowski JQ, Lee VM (1993) Abnormal tau phosphorylation at Ser396 in Alzheimer's disease recapitulates development and contributes to reduced microtubule binding. Neuron 10:1089-1099.

Bramlett HM, Kraydieh S, Green EJ, Dietrich WD (1997) Temporal and regional patterns of axonal damage following traumatic brain injury: a beta-amyloid precursor protein immunocytochemical study in rats. Journal of neuropathology and experimental neurology 56:1132-1141.

Brody DL, Mac Donald C, Kessens CC, Yuede C, Parsadanian M, Spinner M, Kim E, Schwetye KE, Holtzman DM, Bayly PV (2007) Electromagnetic controlled cortical impact device for precise, graded experimental traumatic brain injury. Journal of neurotrauma 24:657-673.

Brunden KR, Trojanowski JQ, Lee VM (2009) Advances in tau-focused drug discovery for Alzheimer's disease and related tauopathies. Nat Rev Drug Discov 8:783-793.

Brunden KR, Ballatore C, Crowe A, Smith AB, 3rd, Lee VM, Trojanowski JQ (2010a) Tau-directed drug discovery for Alzheimer's disease and related tauopathies: a focus on tau assembly inhibitors. Experimental neurology 223:304-310.

Brunden KR, Zhang B, Carroll J, Yao Y, Potuzak JS, Hogan AM, Iba M, James MJ, Xie SX, Ballatore C, Smith AB, 3rd, Lee VM, Trojanowski JQ (2010b) Epothilone D improves microtubule density, axonal integrity, and cognition in a transgenic mouse model of tauopathy. The Journal of neuroscience : the official journal of the Society for Neuroscience 30:13861-13866.

Buee-Scherrer V, Goedert M (2002) Phosphorylation of microtubule-associated protein tau by stress-activated protein kinases in intact cells. FEBS letters 515:151-154.

Carter MD, Simms GA, Weaver DF (2010) The development of new therapeutics for Alzheimer's disease. Clin Pharmacol Ther 88:475-486.

Casas C, Sergeant N, Itier JM, Blanchard V, Wirths O, van der Kolk N, Vingtdeux V, van de Steeg E, Ret G, Canton T, Drobecq H, Clark A, Bonici B, Delacourte A, Benavides J, Schmitz C, Tremp G, Bayer TA, Benoit P, Pradier L (2004) Massive CA1/2 neuronal loss with intraneuronal and N-terminal truncated Abeta42 accumulation in a novel Alzheimer transgenic model. The American journal of pathology 165:1289-1300.

Cassidy JD, Carroll LJ, Peloso PM, Borg J, von Holst H, Holm L, Kraus J, Coronado VG (2004) Incidence, risk factors and prevention of mild traumatic brain injury: results of the WHO Collaborating Centre Task Force on Mild Traumatic Brain Injury. J Rehabil Med:28-60.

Castellano JM, Kim J, Stewart FR, Jiang H, Demattos RB, Patterson BW, Fagan AM, Morris JC, Mawuenyega KG, Cruchaga C, Goate AM, Bales KR, Paul SM, Bateman RJ, Holtzman DM (2011) Human apoE Isoforms Differentially Regulate Brain Amyloid-{beta} Peptide Clearance. Sci Transl Med 3:89ra57.

Cavalli V, Kujala P, Klumperman J, Goldstein LS (2005) Sunday Driver links axonal transport to damage signaling. The Journal of cell biology 168:775-787.

Chartier-Harlin MC, Crawford F, Houlden H, Warren A, Hughes D, Fidani L, Goate A, Rossor M, Roques P, Hardy J, et al. (1991) Early-onset Alzheimer's disease

caused by mutations at codon 717 of the beta-amyloid precursor protein gene. Nature 353:844-846.
Chen S, Pickard JD, Harris NG (2003) Time course of cellular pathology after controlled cortical impact injury. Experimental neurology 182:87-102.
Chen XH, Johnson VE, Uryu K, Trojanowski JQ, Smith DH (2009) A lack of amyloid beta plaques despite persistent accumulation of amyloid beta in axons of long-term survivors of traumatic brain injury. Brain pathology (Zurich, Switzerland) 19:214-223.
Chen XH, Siman R, Iwata A, Meaney DF, Trojanowski JQ, Smith DH (2004) Long-term accumulation of amyloid-beta, beta-secretase, presenilin-1, and caspase-3 in damaged axons following brain trauma. The American journal of pathology 165:357-371.
Chen XH, Meaney DF, Xu BN, Nonaka M, McIntosh TK, Wolf JA, Saatman KE, Smith DH (1999) Evolution of neurofilament subtype accumulation in axons following diffuse brain injury in the pig. Journal of neuropathology and experimental neurology 58:588-596.
Choi HJ, Kang, K.S., Fukui, M., and Zhu, B.T. (2010) Critical role of the JNK-p53-GADD45 apoptotic cascade in mediating oxidative cytotoxicity in hippocampal neurons. British Journal of Pharmacolog 162:175-192.
Christman CW, Salvant JB, Jr., Walker SA, Povlishock JT (1997) Characterization of a prolonged regenerative attempt by diffusely injured axons following traumatic brain injury in adult cat: a light and electron microscopic immunocytochemical study. Acta neuropathologica 94:329-337.
Christman CW, Grady MS, Walker SA, Holloway KL, Povlishock JT (1994) Ultrastructural studies of diffuse axonal injury in humans. Journal of neurotrauma 11:173-186.
Chui DH, Tanahashi H, Ozawa K, Ikeda S, Checler F, Ueda O, Suzuki H, Araki W, Inoue H, Shirotani K, Takahashi K, Gallyas F, Tabira T (1999) Transgenic mice with Alzheimer presenilin 1 mutations show accelerated neurodegeneration without amyloid plaque formation. Nature medicine 5:560-564.
Cirrito JR, May PC, O'Dell MA, Taylor JW, Parsadanian M, Cramer JW, Audia JE, Nissen JS, Bales KR, Paul SM, DeMattos RB, Holtzman DM (2003) In vivo assessment of brain interstitial fluid with microdialysis reveals plaque-associated changes in amyloid-beta metabolism and half-life. J Neurosci 23:8844-8853.
Citron M, Oltersdorf T, Haass C, McConlogue L, Hung AY, Seubert P, Vigo-Pelfrey C, Lieberburg I, Selkoe DJ (1992) Mutation of the beta-amyloid precursor protein in familial Alzheimer's disease increases beta-protein production. Nature 360:672-674.
Citron M, Vigo-Pelfrey C, Teplow DB, Miller C, Schenk D, Johnston J, Winblad B, Venizelos N, Lannfelt L, Selkoe DJ (1994) Excessive production of amyloid beta-protein by peripheral cells of symptomatic and presymptomatic patients carrying the Swedish familial Alzheimer disease mutation. Proceedings of the National Academy of Sciences of the United States of America 91:11993-11997.
Citron M et al. (1997) Mutant presenilins of Alzheimer's disease increase production of 42-residue amyloid beta-protein in both transfected cells and transgenic mice. Nature medicine 3:67-72.

Clinton J, Ambler MW, Roberts GW (1991) Post-traumatic Alzheimer's disease: preponderance of a single plaque type. Neuropathology and applied neurobiology 17:69-74.
Cohen TJ, Guo JL, Hurtado DE, Kwong LK, Mills IP, Trojanowski JQ, Lee VM (2011) The acetylation of tau inhibits its function and promotes pathological tau aggregation. Nature communications 2:252.
Colombo A, Repici M, Pesaresi M, Santambrogio S, Forloni G, Borsello T (2007) The TAT-JNK inhibitor peptide interferes with beta amyloid protein stability. Cell Death Differ 14:1845-1848.
Corder EH, Saunders AM, Strittmatter WJ, Schmechel DE, Gaskell PC, Small GW, Roses AD, Haines JL, Pericak-Vance MA (1993) Gene dose of apolipoprotein E type 4 allele and the risk of Alzheimer's disease in late onset families. Science (New York, NY 261:921-923.
Coronado VG, Xu L, Basavaraju SV, McGuire LC, Wald MM, Faul MD, Guzman BR, Hemphill JD (2011) Surveillance for traumatic brain injury-related deaths--United States, 1997-2007. MMWR Surveill Summ 60:1-32.
Corsellis JA (1989) Boxing and the brain. BMJ (Clinical research ed 298:105-109.
Corsellis JA, Brierley JB (1959) Observations on the pathology of insidious dementia following head injury. The Journal of mental science 105:714-720.
Crawford F, Hardy J, Mullan M, Goate A, Hughes D, Fidani L, Roques P, Rossor M, Chartier-Harlin MC (1991) Sequencing of exons 16 and 17 of the beta-amyloid precursor protein gene in 14 families with early onset Alzheimer's disease fails to reveal mutations in the beta-amyloid sequence. Neuroscience letters 133:1-2.
Cross DA, Alessi DR, Cohen P, Andjelkovich M, Hemmings BA (1995) Inhibition of glycogen synthase kinase-3 by insulin mediated by protein kinase B. Nature 378:785-789.
Cruz JC, Tseng HC, Goldman JA, Shih H, Tsai LH (2003) Aberrant Cdk5 activation by p25 triggers pathological events leading to neurodegeneration and neurofibrillary tangles. Neuron 40:471-483.
Czirr E, Leuchtenberger S, Dorner-Ciossek C, Schneider A, Jucker M, Koo EH, Pietrzik CU, Baumann K, Weggen S (2007) Insensitivity to Abeta42-lowering nonsteroidal anti-inflammatory drugs and gamma-secretase inhibitors is common among aggressive presenilin-1 mutations. The Journal of biological chemistry 282:24504-24513.
Czlonkowska A, Kurkowska-Jastrzebska I (2011) Inflammation and gliosis in neurological diseases--clinical implications. J Neuroimmunol 231:78-85.
D'Andrea MR, Nagele RG, Wang HY, Peterson PA, Lee DH (2001) Evidence that neurones accumulating amyloid can undergo lysis to form amyloid plaques in Alzheimer's disease. Histopathology 38:120-134.
De Strooper B, Saftig P, Craessaerts K, Vanderstichele H, Guhde G, Annaert W, Von Figura K, Van Leuven F (1998) Deficiency of presenilin-1 inhibits the normal cleavage of amyloid precursor protein. Nature 391:387-390.
DeFord SM, Wilson MS, Rice AC, Clausen T, Rice LK, Barabnova A, Bullock R, Hamm RJ (2002) Repeated mild brain injuries result in cognitive impairment in B6C3F1 mice. Journal of neurotrauma 19:427-438.

Dewachter I, Ris L, Croes S, Borghgraef P, Devijver H, Voets T, Nilius B, Godaux E, Van Leuven F (2008) Modulation of synaptic plasticity and Tau phosphorylation by wild-type and mutant presenilin1. Neurobiology of aging 29:639-652.
Diaz-Arrastia R, Gong Y, Fair S, Scott KD, Garcia MC, Carlile MC, Agostini MA, Van Ness PC (2003) Increased risk of late posttraumatic seizures associated with inheritance of APOE epsilon4 allele. Arch Neurol 60:818-822.
Dickson DW (1997) Neuropathological diagnosis of Alzheimer's disease: a perspective from longitudinal clinicopathological studies. Neurobiology of aging 18:S21-26.
Dikranian K, Cohen R, Mac Donald C, Pan Y, Brakefield D, Bayly P, Parsadanian A (2008) Mild traumatic brain injury to the infant mouse causes robust white matter axonal degeneration which precedes apoptotic death of cortical and thalamic neurons. Experimental neurology 211:551-560.
Drechsel DN, Hyman AA, Cobb MH, Kirschner MW (1992) Modulation of the dynamic instability of tubulin assembly by the microtubule-associated protein tau. Molecular biology of the cell 3:1141-1154.
Drewes G, Lichtenberg-Kraag B, Doring F, Mandelkow EM, Biernat J, Goris J, Doree M, Mandelkow E (1992) Mitogen activated protein (MAP) kinase transforms tau protein into an Alzheimer-like state. The EMBO journal 11:2131-2138.
Dunn-Meynell AA, Levin BE (1997) Histological markers of neuronal, axonal and astrocytic changes after lateral rigid impact traumatic brain injury. Brain research 761:25-41.
Erb DE, Povlishock JT (1988) Axonal damage in severe traumatic brain injury: an experimental study in cat. Acta neuropathologica 76:347-358.
Finder VH, Glockshuber R (2007) Amyloid-beta aggregation. Neuro-degenerative diseases 4:13-27.
Fleminger S, Oliver DL, Lovestone S, Rabe-Hesketh S, Giora A (2003) Head injury as a risk factor for Alzheimer's disease: the evidence 10 years on; a partial replication. Journal of neurology, neurosurgery, and psychiatry 74:857-862.
Floyd CL, Lyeth BG (2007) Astroglia: important mediators of traumatic brain injury. Progress in brain research 161:61-79.
Foda MA, Marmarou A (1994) A new model of diffuse brain injury in rats. Part II: Morphological characterization. Journal of neurosurgery 80:301-313.
Franklin KB, Paxinos G (1997) The mouse brain in stereotaxic coordinates. London: Academic Press.
Friedman G, Froom P, Sazbon L, Grinblatt I, Shochina M, Tsenter J, Babaey S, Yehuda B, Groswasser Z (1999) Apolipoprotein E-epsilon4 genotype predicts a poor outcome in survivors of traumatic brain injury. Neurology 52:244-248.
Games D, Adams D, Alessandrini R, Barbour R, Berthelette P, Blackwell C, Carr T, Clemens J, Donaldson T, Gillespie F, et al. (1995) Alzheimer-type neuropathology in transgenic mice overexpressing V717F beta-amyloid precursor protein. Nature 373:523-527.
Garman RH, Jenkins LW, Switzer RC, Bauman RA, Tong LC, Swauger PV, Parks SA, Ritzel DV, Dixon CE, Clark RS, Bayir H, Kagan V, Jackson EK, Kochanek PM (2011) Blast exposure in rats with body shielding is characterized primarily by diffuse axonal injury. Journal of neurotrauma 28:947-959.

Geddes JF, Whitwell HL, Graham DI (2000) Traumatic axonal injury: practical issues for diagnosis in medicolegal cases. Neuropathology and applied neurobiology 26:105-116.
Geddes JF, Vowles GH, Robinson SF, Sutcliffe JC (1996) Neurofibrillary tangles, but not Alzheimer-type pathology, in a young boxer. Neuropathology and applied neurobiology 22:12-16.
Geddes JF, Vowles GH, Beer TW, Ellison DW (1997) The diagnosis of diffuse axonal injury: implications for forensic practice. Neuropathology and applied neurobiology 23:339-347.
Geddes JF, Vowles GH, Nicoll JA, Revesz T (1999) Neuronal cytoskeletal changes are an early consequence of repetitive head injury. Acta neuropathologica 98:171-178.
Gennarelli TA (1983) Head injury in man and experimental animals: clinical aspects. Acta Neurochir Suppl (Wien) 32:1-13.
Gennarelli TA (1993) Mechanisms of brain injury. The Journal of emergency medicine 11 Suppl 1:5-11.
Gennarelli TA, Thibault LE, Adams JH, Graham DI, Thompson CJ, Marcincin RP (1982) Diffuse axonal injury and traumatic coma in the primate. Annals of neurology 12:564-574.
Gentleman SM, Nash MJ, Sweeting CJ, Graham DI, Roberts GW (1993) Beta-amyloid precursor protein (beta APP) as a marker for axonal injury after head injury. Neuroscience letters 160:139-144.
Gentleman SM, Roberts GW, Gennarelli TA, Maxwell WL, Adams JH, Kerr S, Graham DI (1995) Axonal injury: a universal consequence of fatal closed head injury? Acta neuropathologica 89:537-543.
Gerdts J, Sasaki Y, Vohra B, Marasa J, Milbrandt J (2011) Image-based Screening Identifies Novel Roles for I{kappa}B Kinase and Glycogen Synthase Kinase 3 in Axonal Degeneration. The Journal of biological chemistry 286:28011-28018.
Ghatan S, Larner S, Kinoshita Y, Hetman M, Patel L, Xia Z, Youle RJ, Morrison RS (2000) p38 MAP kinase mediates bax translocation in nitric oxide-induced apoptosis in neurons. The Journal of cell biology 150:335-347.
Goate A, Chartier-Harlin MC, Mullan M, Brown J, Crawford F, Fidani L, Giuffra L, Haynes A, Irving N, James L, et al. (1991) Segregation of a missense mutation in the amyloid precursor protein gene with familial Alzheimer's disease. Nature 349:704-706.
Goedert M, Jakes R (2005) Mutations causing neurodegenerative tauopathies. Biochimica et biophysica acta 1739:240-250.
Goedert M, Cohen ES, Jakes R, Cohen P (1992) p42 MAP kinase phosphorylation sites in microtubule-associated protein tau are dephosphorylated by protein phosphatase 2A1. Implications for Alzheimer's disease [corrected]. FEBS letters 312:95-99.
Goedert M, Spillantini MG, Potier MC, Ulrich J, Crowther RA (1989a) Cloning and sequencing of the cDNA encoding an isoform of microtubule-associated protein tau containing four tandem repeats: differential expression of tau protein mRNAs in human brain. The EMBO journal 8:393-399.

Goedert M, Spillantini MG, Jakes R, Rutherford D, Crowther RA (1989b) Multiple isoforms of human microtubule-associated protein tau: sequences and localization in neurofibrillary tangles of Alzheimer's disease. Neuron 3:519-526.
Goedert M, Hasegawa M, Jakes R, Lawler S, Cuenda A, Cohen P (1997) Phosphorylation of microtubule-associated protein tau by stress-activated protein kinases. FEBS letters 409:57-62.
Gong CX, Singh TJ, Grundke-Iqbal I, Iqbal K (1993) Phosphoprotein phosphatase activities in Alzheimer disease brain. Journal of neurochemistry 61:921-927.
Gong CX, Shaikh S, Wang JZ, Zaidi T, Grundke-Iqbal I, Iqbal K (1995) Phosphatase activity toward abnormally phosphorylated tau: decrease in Alzheimer disease brain. Journal of neurochemistry 65:732-738.
Gong CX, Lidsky T, Wegiel J, Zuck L, Grundke-Iqbal I, Iqbal K (2000) Phosphorylation of microtubule-associated protein tau is regulated by protein phosphatase 2A in mammalian brain. Implications for neurofibrillary degeneration in Alzheimer's disease. The Journal of biological chemistry 275:5535-5544.
Gotz J, Chen F, van Dorpe J, Nitsch RM (2001) Formation of neurofibrillary tangles in P301l tau transgenic mice induced by Abeta 42 fibrils. Science (New York, NY 293:1491-1495.
Gouras GK, Tsai J, Naslund J, Vincent B, Edgar M, Checler F, Greenfield JP, Haroutunian V, Buxbaum JD, Xu H, Greengard P, Relkin NR (2000) Intraneuronal Abeta42 accumulation in human brain. The American journal of pathology 156:15-20.
Grady MS, McLaughlin MR, Christman CW, Valadka AB, Fligner CL, Povlishock JT (1993) The use of antibodies targeted against the neurofilament subunits for the detection of diffuse axonal injury in humans. Journal of neuropathology and experimental neurology 52:143-152.
Graham DI, Gentleman SM, Lynch A, Roberts GW (1995) Distribution of beta-amyloid protein in the brain following severe head injury. Neuropathology and applied neurobiology 21:27-34.
Grimmelt AC, Eitzen S, Balakhadze I, Fischer B, Wolfer J, Schiffbauer H, Gorji A, Greiner C (2011) Closed traumatic brain injury model in sheep mimicking high-velocity, closed head trauma in humans. Cen Eur Neurosurg 72:120-126.
Grimwood S, Hogg J, Jay MT, Lad AM, Lee V, Murray F, Peachey J, Townend T, Vithlani M, Beher D, Shearman MS, Hutson PH (2005) Determination of guinea-pig cortical gamma-secretase activity ex vivo following the systemic administration of a gamma-secretase inhibitor. Neuropharmacology 48:1002-1011.
Guo JL, Lee VM (2011) Seeding of normal Tau by pathological Tau conformers drives pathogenesis of Alzheimer-like tangles. The Journal of biological chemistry 286:15317-15331.
Guo Q, Fu W, Sopher BL, Miller MW, Ware CB, Martin GM, Mattson MP (1999) Increased vulnerability of hippocampal neurons to excitotoxic necrosis in presenilin-1 mutant knock-in mice. Nature medicine 5:101-106.

Gyure KA, Durham R, Stewart WF, Smialek JE, Troncoso JC (2001) Intraneuronal abeta-amyloid precedes development of amyloid plaques in Down syndrome. Archives of pathology & laboratory medicine 125:489-492.

Haass C, Hung AY, Selkoe DJ, Teplow DB (1994) Mutations associated with a locus for familial Alzheimer's disease result in alternative processing of amyloid beta-protein precursor. The Journal of biological chemistry 269:17741-17748.

Harting MT, Jimenez F, Adams SD, Mercer DW, Cox CS, Jr. (2008) Acute, regional inflammatory response after traumatic brain injury: Implications for cellular therapy. Surgery 144:803-813.

Hartman RE, Laurer H, Longhi L, Bales KR, Paul SM, McIntosh TK, Holtzman DM (2002) Apolipoprotein E4 influences amyloid deposition but not cell loss after traumatic brain injury in a mouse model of Alzheimer's disease. The Journal of neuroscience : the official journal of the Society for Neuroscience 22:10083-10087.

Hausmann R, Riess R, Fieguth A, Betz P (2000) Immunohistochemical investigations on the course of astroglial GFAP expression following human brain injury. Int J Legal Med 113:70-75.

Hernandez F, Borrell J, Guaza C, Avila J, Lucas JJ (2002) Spatial learning deficit in transgenic mice that conditionally over-express GSK-3beta in the brain but do not form tau filaments. Journal of neurochemistry 83:1529-1533.

Hibi M, Lin A, Smeal T, Minden A, Karin M (1993) Identification of an oncoprotein- and UV-responsive protein kinase that binds and potentiates the c-Jun activation domain. Genes Dev 7:2135-2148.

Hicks RR, Smith DH, Lowenstein DH, Saint Marie R, McIntosh TK (1993) Mild experimental brain injury in the rat induces cognitive deficits associated with regional neuronal loss in the hippocampus. Journal of neurotrauma 10:405-414.

Holcomb L, Gordon MN, McGowan E, Yu X, Benkovic S, Jantzen P, Wright K, Saad I, Mueller R, Morgan D, Sanders S, Zehr C, O'Campo K, Hardy J, Prada CM, Eckman C, Younkin S, Hsiao K, Duff K (1998) Accelerated Alzheimer-type phenotype in transgenic mice carrying both mutant amyloid precursor protein and presenilin 1 transgenes. Nature medicine 4:97-100.

Holmes A, Wrenn CC, Harris AP, Thayer KE, Crawley JN (2002) Behavioral profiles of inbred strains on novel olfactory, spatial and emotional tests for reference memory in mice. Genes, brain, and behavior 1:55-69.

Hong M, Zhukareva V, Vogelsberg-Ragaglia V, Wszolek Z, Reed L, Miller BI, Geschwind DH, Bird TD, McKeel D, Goate A, Morris JC, Wilhelmsen KC, Schellenberg GD, Trojanowski JQ, Lee VM (1998) Mutation-specific functional impairments in distinct tau isoforms of hereditary FTDP-17. Science (New York, NY 282:1914-1917.

Horsburgh K, McCarron MO, White F, Nicoll JA (2000) The role of apolipoprotein E in Alzheimer's disease, acute brain injury and cerebrovascular disease: evidence of common mechanisms and utility of animal models. Neurobiology of aging 21:245-255.

Hughes K, Nikolakaki E, Plyte SE, Totty NF, Woodgett JR (1993) Modulation of the glycogen synthase kinase-3 family by tyrosine phosphorylation. The EMBO journal 12:803-808.

Hurtado DE, Molina-Porcel L, Iba M, Aboagye AK, Paul SM, Trojanowski JQ, Lee VM (2010) A{beta} accelerates the spatiotemporal progression of tau pathology and augments tau amyloidosis in an Alzheimer mouse model. The American journal of pathology 177:1977-1988.

Ikonomovic MD, Uryu K, Abrahamson EE, Ciallella JR, Trojanowski JQ, Lee VM, Clark RS, Marion DW, Wisniewski SR, DeKosky ST (2004) Alzheimer's pathology in human temporal cortex surgically excised after severe brain injury. Experimental neurology 190:192-203.

Ittner LM, Ke YD, Delerue F, Bi M, Gladbach A, van Eersel J, Wolfing H, Chieng BC, Christie MJ, Napier IA, Eckert A, Staufenbiel M, Hardeman E, Gotz J (2010) Dendritic function of tau mediates amyloid-beta toxicity in Alzheimer's disease mouse models. Cell 142:387-397.

Iwata A, Chen XH, McIntosh TK, Browne KD, Smith DH (2002) Long-term accumulation of amyloid-beta in axons following brain trauma without persistent upregulation of amyloid precursor protein genes. Journal of neuropathology and experimental neurology 61:1056-1068.

Iwatsubo T, Mann DM, Odaka A, Suzuki N, Ihara Y (1995) Amyloid beta protein (A beta) deposition: A beta 42(43) precedes A beta 40 in Down syndrome. Annals of neurology 37:294-299.

Jankowsky JL, Fadale DJ, Anderson J, Xu GM, Gonzales V, Jenkins NA, Copeland NG, Lee MK, Younkin LH, Wagner SL, Younkin SG, Borchelt DR (2004) Mutant presenilins specifically elevate the levels of the 42 residue beta-amyloid peptide in vivo: evidence for augmentation of a 42-specific gamma secretase. Human molecular genetics 13:159-170.

Johnson-Wood K, Lee M, Motter R, Hu K, Gordon G, Barbour R, Khan K, Gordon M, Tan H, Games D, Lieberburg I, Schenk D, Seubert P, McConlogue L (1997) Amyloid precursor protein processing and A beta42 deposition in a transgenic mouse model of Alzheimer disease. Proceedings of the National Academy of Sciences of the United States of America 94:1550-1555.

Johnson VE, Stewart W, Smith DH (2010) Traumatic brain injury and amyloid-beta pathology: a link to Alzheimer's disease? Nat Rev Neurosci 11:1-10.

Johnson VE, Stewart W, Smith DH (2011) Widespread Tau and Amyloid-Beta Pathology Many Years After a Single Traumatic Brain Injury in Humans. Brain pathology.

Kanaan NM, Morfini GA, Lapointe NE, Pigino GF, Patterson KR, Song Y, Andreadis A, Fu Y, Brady ST, Binder LI (2011) Pathogenic Forms of Tau Inhibit Kinesin-Dependent Axonal Transport through a Mechanism Involving Activation of Axonal Phosphotransferases. The Journal of neuroscience : the official journal of the Society for Neuroscience 31:9858-9868.

Kang J, Lemaire HG, Unterbeck A, Salbaum JM, Masters CL, Grzeschik KH, Multhaup G, Beyreuther K, Muller-Hill B (1987) The precursor of Alzheimer's disease amyloid A4 protein resembles a cell-surface receptor. Nature 325:733-736.

Kang JE, Cirrito JR, Dong H, Csernansky JG, Holtzman DM (2007) Acute stress increases interstitial fluid amyloid-beta via corticotropin-releasing factor and neuronal activity. Proceedings of the National Academy of Sciences of the United States of America 104:10673-10678.

Katzman R, Galasko DR, Saitoh T, Chen X, Pay MM, Booth A, Thomas RG (1996) Apolipoprotein-epsilon4 and head trauma: Synergistic or additive risks? Neurology 46:889-891.
Kelley BJ, Lifshitz J, Povlishock JT (2007) Neuroinflammatory responses after experimental diffuse traumatic brain injury. Journal of neuropathology and experimental neurology 66:989-1001.
Kins S, Crameri A, Evans DR, Hemmings BA, Nitsch RM, Gotz J (2001) Reduced protein phosphatase 2A activity induces hyperphosphorylation and altered compartmentalization of tau in transgenic mice. The Journal of biological chemistry 276:38193-38200.
Klyubin I, Betts V, Welzel AT, Blennow K, Zetterberg H, Wallin A, Lemere CA, Cullen WK, Peng Y, Wisniewski T, Selkoe DJ, Anwyl R, Walsh DM, Rowan MJ (2008) Amyloid beta protein dimer-containing human CSF disrupts synaptic plasticity: prevention by systemic passive immunization. The Journal of neuroscience : the official journal of the Society for Neuroscience 28:4231-4237.
Koliatsos VE, Cernak I, Xu L, Song Y, Savonenko A, Crain BJ, Eberhart CG, Frangakis CE, Melnikova T, Kim H, Lee D (2011) A mouse model of blast injury to brain: initial pathological, neuropathological, and behavioral characterization. Journal of neuropathology and experimental neurology 70:399-416.
Koo EH, Kopan R (2004) Potential role of presenilin-regulated signaling pathways in sporadic neurodegeneration. Nature medicine 10 Suppl:S26-33.
Koo EH, Sisodia SS, Archer DR, Martin LJ, Weidemann A, Beyreuther K, Fischer P, Masters CL, Price DL (1990) Precursor of amyloid protein in Alzheimer disease undergoes fast anterograde axonal transport. Proceedings of the National Academy of Sciences of the United States of America 87:1561-1565.
Kyriakis JM, Avruch J (2001) Mammalian mitogen-activated protein kinase signal transduction pathways activated by stress and inflammation. Physiological reviews 81:807-869.
LaFerla FM (2002) Calcium dyshomeostasis and intracellular signalling in Alzheimer's disease. Nat Rev Neurosci 3:862-872.
Laurer HL, Bareyre FM, Lee VM, Trojanowski JQ, Longhi L, Hoover R, Saatman KE, Raghupathi R, Hoshino S, Grady MS, McIntosh TK (2001) Mild head injury increasing the brain's vulnerability to a second concussive impact. Journal of neurosurgery 95:859-870.
Lemere CA, Blusztajn JK, Yamaguchi H, Wisniewski T, Saido TC, Selkoe DJ (1996a) Sequence of deposition of heterogeneous amyloid beta-peptides and APO E in Down syndrome: implications for initial events in amyloid plaque formation. Neurobiology of disease 3:16-32.
Lemere CA, Lopera F, Kosik KS, Lendon CL, Ossa J, Saido TC, Yamaguchi H, Ruiz A, Martinez A, Madrigal L, Hincapie L, Arango JC, Anthony DC, Koo EH, Goate AM, Selkoe DJ (1996b) The E280A presenilin 1 Alzheimer mutation produces increased A beta 42 deposition and severe cerebellar pathology. Nature medicine 2:1146-1150.
Leroy K, Boutajangout A, Authelet M, Woodgett JR, Anderton BH, Brion JP (2002) The active form of glycogen synthase kinase-3beta is associated with

granulovacuolar degeneration in neurons in Alzheimer's disease. Acta neuropathologica 103:91-99.
Levy-Lahad E, Wijsman EM, Nemens E, Anderson L, Goddard KA, Weber JL, Bird TD, Schellenberg GD (1995) A familial Alzheimer's disease locus on chromosome 1. Science (New York, NY 269:970-973.
Lewis J, Dickson DW, Lin WL, Chisholm L, Corral A, Jones G, Yen SH, Sahara N, Skipper L, Yager D, Eckman C, Hardy J, Hutton M, McGowan E (2001) Enhanced neurofibrillary degeneration in transgenic mice expressing mutant tau and APP. Science (New York, NY 293:1487-1491.
Lewis SB, Finnie JW, Blumbergs PC, Scott G, Manavis J, Brown C, Reilly PL, Jones NR, McLean AJ (1996) A head impact model of early axonal injury in the sheep. Journal of neurotrauma 13:505-514.
Lichtman SW, Seliger G, Tycko B, Marder K (2000) Apolipoprotein E and functional recovery from brain injury following postacute rehabilitation. Neurology 55:1536-1539.
Lifshitz J, Kelley BJ, Povlishock JT (2007) Perisomatic thalamic axotomy after diffuse traumatic brain injury is associated with atrophy rather than cell death. Journal of neuropathology and experimental neurology 66:218-229.
Lisnock J, Griffin P, Calaycay J, Frantz B, Parsons J, O'Keefe SJ, LoGrasso P (2000) Activation of JNK3 alpha 1 requires both MKK4 and MKK7: kinetic characterization of in vitro phosphorylated JNK3 alpha 1. Biochemistry 39:3141-3148.
Litersky JM, Johnson GV (1992) Phosphorylation by cAMP-dependent protein kinase inhibits the degradation of tau by calpain. The Journal of biological chemistry 267:1563-1568.
Litersky JM, Johnson GV, Jakes R, Goedert M, Lee M, Seubert P (1996) Tau protein is phosphorylated by cyclic AMP-dependent protein kinase and calcium/calmodulin-dependent protein kinase II within its microtubule-binding domains at Ser-262 and Ser-356. The Biochemical journal 316 (Pt 2):655-660.
Loane DJ, Byrnes KR (2010) Role of microglia in neurotrauma. Neurotherapeutics 7:366-377.
Loane DJ, Pocivavsek A, Moussa CE, Thompson R, Matsuoka Y, Faden AI, Rebeck GW, Burns MP (2009) Amyloid precursor protein secretases as therapeutic targets for traumatic brain injury. Nature medicine.
Longhi L, Saatman KE, Fujimoto S, Raghupathi R, Meaney DF, Davis J, McMillan BSA, Conte V, Laurer HL, Stein S, Stocchetti N, McIntosh TK (2005) Temporal window of vulnerability to repetitive experimental concussive brain injury. Neurosurgery 56:364-374; discussion 364-374.
Lu J, Goh SJ, Tng PY, Deng YY, Ling EA, Moochhala S (2009) Systemic inflammatory response following acute traumatic brain injury. Front Biosci 14:3795-3813.
Lucas JJ, Hernandez F, Gomez-Ramos P, Moran MA, Hen R, Avila J (2001) Decreased nuclear beta-catenin, tau hyperphosphorylation and neurodegeneration in GSK-3beta conditional transgenic mice. The EMBO journal 20:27-39.
Lyeth BG, Jenkins LW, Hamm RJ, Dixon CE, Phillips LL, Clifton GL, Young HF, Hayes RL (1990) Prolonged memory impairment in the absence of hippocampal cell death following traumatic brain injury in the rat. Brain research 526:249-258.

Mac Donald CL, Dikranian K, Bayly P, Holtzman D, Brody D (2007a) Diffusion tensor imaging reliably detects experimental traumatic axonal injury and indicates approximate time of injury. J Neurosci 27:11869-11876.
Mac Donald CL, Dikranian K, Song SK, Bayly PV, Holtzman DM, Brody DL (2007b) Detection of traumatic axonal injury with diffusion tensor imaging in a mouse model of traumatic brain injury. Experimental neurology 205:116-131.
Mann DM, Esiri MM (1989) The pattern of acquisition of plaques and tangles in the brains of patients under 50 years of age with Down's syndrome. Journal of the neurological sciences 89:169-179.
Mann DM, Iwatsubo T, Cairns NJ, Lantos PL, Nochlin D, Sumi SM, Bird TD, Poorkaj P, Hardy J, Hutton M, Prihar G, Crook R, Rossor MN, Haltia M (1996) Amyloid beta protein (Abeta) deposition in chromosome 14-linked Alzheimer's disease: predominance of Abeta42(43). Annals of neurology 40:149-156.
Marmarou CR, Walker SA, Davis CL, Povlishock JT (2005) Quantitative analysis of the relationship between intra- axonal neurofilament compaction and impaired axonal transport following diffuse traumatic brain injury. Journal of neurotrauma 22:1066-1080.
Masters CL, Simms G, Weinman NA, Multhaup G, McDonald BL, Beyreuther K (1985) Amyloid plaque core protein in Alzheimer disease and Down syndrome. Proceedings of the National Academy of Sciences of the United States of America 82:4245-4249.
Mastrangelo MA, Bowers WJ (2008) Detailed immunohistochemical characterization of temporal and spatial progression of Alzheimer's disease-related pathologies in male triple-transgenic mice. BMC neuroscience 9:81.
Mattson MP (2010) ER calcium and Alzheimer's disease: in a state of flux. Science signaling 3:pe10.
Mattson MP, LaFerla FM, Chan SL, Leissring MA, Shepel PN, Geiger JD (2000) Calcium signaling in the ER: its role in neuronal plasticity and neurodegenerative disorders. Trends Neurosci 23:222-229.
Maxwell WL, Watt C, Graham DI, Gennarelli TA (1993) Ultrastructural evidence of axonal shearing as a result of lateral acceleration of the head in non-human primates. Acta neuropathologica 86:136-144.
Mayeux R, Ottman R, Maestre G, Ngai C, Tang MX, Ginsberg H, Chun M, Tycko B, Shelanski M (1995) Synergistic effects of traumatic head injury and apolipoprotein-epsilon 4 in patients with Alzheimer's disease. Neurology 45:555-557.
Mazanetz MP, Fischer PM (2007) Untangling tau hyperphosphorylation in drug design for neurodegenerative diseases. Nat Rev Drug Discov 6:464-479.
McKee AC, Cantu RC, Nowinski CJ, Hedley-Whyte ET, Gavett BE, Budson AE, Santini VE, Lee HS, Kubilus CA, Stern RA (2009) Chronic traumatic encephalopathy in athletes: progressive tauopathy after repetitive head injury. Journal of neuropathology and experimental neurology 68:709-735.
Mercken M, Vandermeeren M, Lubke U, Six J, Boons J, Van de Voorde A, Martin JJ, Gheuens J (1992) Monoclonal antibodies with selective specificity for Alzheimer Tau are directed against phosphatase-sensitive epitopes. Acta neuropathologica 84:265-272.

Merrick SE, Trojanowski JQ, Lee VM (1997) Selective destruction of stable microtubules and axons by inhibitors of protein serine/threonine phosphatases in cultured human neurons. The Journal of neuroscience : the official journal of the Society for Neuroscience 17:5726-5737.

Middlemas A, Delcroix JD, Sayers NM, Tomlinson DR, Fernyhough P (2003) Enhanced activation of axonally transported stress-activated protein kinases in peripheral nerve in diabetic neuropathy is prevented by neurotrophin-3. Brain : a journal of neurology 126:1671-1682.

Miller BR, Press C, Daniels RW, Sasaki Y, Milbrandt J, DiAntonio A (2009) A dual leucine kinase-dependent axon self-destruction program promotes Wallerian degeneration. Nature neuroscience 12:387-389.

Min SW, Cho SH, Zhou Y, Schroeder S, Haroutunian V, Seeley WW, Huang EJ, Shen Y, Masliah E, Mukherjee C, Meyers D, Cole PA, Ott M, Gan L (2010) Acetylation of tau inhibits its degradation and contributes to tauopathy. Neuron 67:953-966.

Morgan D (2011) Immunotherapy for Alzheimer's disease. J Intern Med 269:54-63.

Mori C, Spooner ET, Wisniewsk KE, Wisniewski TM, Yamaguch H, Saido TC, Tolan DR, Selkoe DJ, Lemere CA (2002a) Intraneuronal Abeta42 accumulation in Down syndrome brain. Amyloid 9:88-102.

Mori T, Wang X, Jung JC, Sumii T, Singhal AB, Fini ME, Dixon CE, Alessandrini A, Lo EH (2002b) Mitogen-activated protein kinase inhibition in traumatic brain injury: in vitro and in vivo effects. Journal of cerebral blood flow and metabolism : official journal of the International Society of Cerebral Blood Flow and Metabolism 22:444-452.

Mortimer JA, van Duijn CM, Chandra V, Fratiglioni L, Graves AB, Heyman A, Jorm AF, Kokmen E, Kondo K, Rocca WA, et al. (1991) Head trauma as a risk factor for Alzheimer's disease: a collaborative re-analysis of case-control studies. EURODEM Risk Factors Research Group. International journal of epidemiology 20 Suppl 2:S28-35.

Mouton PR, Gokhale AM, Ward NL, West MJ (2002) Stereological length estimation using spherical probes. Journal of microscopy 206:54-64.

Muller-Hill B, Beyreuther K (1989) Molecular biology of Alzheimer's disease. Annual review of biochemistry 58:287-307.

Nakagawa Y, Reed L, Nakamura M, McIntosh TK, Smith DH, Saatman KE, Raghupathi R, Clemens J, Saido TC, Lee VM, Trojanowski JQ (2000) Brain trauma in aged transgenic mice induces regression of established abeta deposits. Experimental neurology 163:244-252.

Nakagawa Y, Nakamura M, McIntosh TK, Rodriguez A, Berlin JA, Smith DH, Saatman KE, Raghupathi R, Clemens J, Saido TC, Schmidt ML, Lee VM, Trojanowski JQ (1999) Traumatic brain injury in young, amyloid-beta peptide overexpressing transgenic mice induces marked ipsilateral hippocampal atrophy and diminished Abeta deposition during aging. J Comp Neurol 411:390-398.

Nemetz PN, Leibson C, Naessens JM, Beard M, Kokmen E, Annegers JF, Kurland LT (1999) Traumatic brain injury and time to onset of Alzheimer's disease: a population-based study. American journal of epidemiology 149:32-40.

Nijboer CH, van der Kooij MA, van Bel F, Ohl F, Heijnen CJ, Kavelaars A (2010) Inhibition of the JNK/AP-1 pathway reduces neuronal death and improves behavioral outcome after neonatal hypoxic-ischemic brain injury. Brain, behavior, and immunity 24:812-821.

Nikolaev A, McLaughlin T, O'Leary DD, Tessier-Lavigne M (2009) APP binds DR6 to trigger axon pruning and neuron death via distinct caspases. Nature 457:981-989.

Nix P, Hisamoto N, Matsumoto K, Bastiani M (2011) Axon regeneration requires coordinate activation of p38 and JNK MAPK pathways. Proceedings of the National Academy of Sciences of the United States of America 108:10738-10743.

Noble W, Planel E, Zehr C, Olm V, Meyerson J, Suleman F, Gaynor K, Wang L, LaFrancois J, Feinstein B, Burns M, Krishnamurthy P, Wen Y, Bhat R, Lewis J, Dickson D, Duff K (2005) Inhibition of glycogen synthase kinase-3 by lithium correlates with reduced tauopathy and degeneration in vivo. Proceedings of the National Academy of Sciences of the United States of America 102:6990-6995.

Noble W, Olm V, Takata K, Casey E, Mary O, Meyerson J, Gaynor K, LaFrancois J, Wang L, Kondo T, Davies P, Burns M, Veeranna, Nixon R, Dickson D, Matsuoka Y, Ahlijanian M, Lau LF, Duff K (2003) Cdk5 is a key factor in tau aggregation and tangle formation in vivo. Neuron 38:555-565.

Oddo S, Caccamo A, Kitazawa M, Tseng BP, LaFerla FM (2003a) Amyloid deposition precedes tangle formation in a triple transgenic model of Alzheimer's disease. Neurobiology of aging 24:1063-1070.

Oddo S, Billings L, Kesslak JP, Cribbs DH, LaFerla FM (2004) Abeta immunotherapy leads to clearance of early, but not late, hyperphosphorylated tau aggregates via the proteasome. Neuron 43:321-332.

Oddo S, Caccamo A, Shepherd JD, Murphy MP, Golde TE, Kayed R, Metherate R, Mattson MP, Akbari Y, LaFerla FM (2003b) Triple-transgenic model of Alzheimer's disease with plaques and tangles: intracellular Abeta and synaptic dysfunction. Neuron 39:409-421.

Oehmichen M, Theuerkauf I, Meissner C (1999) Is traumatic axonal injury (AI) associated with an early microglial activation? Application of a double-labeling technique for simultaneous detection of microglia and AI. Acta neuropathologica 97:491-494.

Olson RE, Copeland RA, Seiffert D (2001) Progress towards testing the amyloid hypothesis: inhibitors of APP processing. Current opinion in drug discovery & development 4:390-401.

Oppenheimer DR (1968) Microscopic lesions in the brain following head injury. Journal of neurology, neurosurgery, and psychiatry 31:299-306.

Ortolano F, Colombo A, Zanier ER, Sclip A, Longhi L, Perego C, Stocchetti N, Borsello T, De Simoni MG (2009) c-Jun N-terminal kinase pathway activation in human and experimental cerebral contusion. Journal of neuropathology and experimental neurology 68:964-971.

Osawa S, Funamoto S, Nobuhara M, Wada-Kakuda S, Shimojo M, Yagishita S, Ihara Y (2008) Phosphoinositides suppress gamma-secretase in both the detergent-

soluble and -insoluble states. The Journal of biological chemistry 283:19283-19292.
Otani N, Nawashiro H, Fukui S, Nomura N, Shima K (2002a) Temporal and spatial profile of phosphorylated mitogen-activated protein kinase pathways after lateral fluid percussion injury in the cortex of the rat brain. Journal of neurotrauma 19:1587-1596.
Otani N, Nawashiro H, Fukui S, Nomura N, Yano A, Miyazawa T, Shima K (2002b) Differential activation of mitogen-activated protein kinase pathways after traumatic brain injury in the rat hippocampus. Journal of cerebral blood flow and metabolism : official journal of the International Society of Cerebral Blood Flow and Metabolism 22:327-334.
Owen EH, Logue SF, Rasmussen DL, Wehner JM (1997) Assessment of learning by the Morris water task and fear conditioning in inbred mouse strains and F1 hybrids: implications of genetic background for single gene mutations and quantitative trait loci analyses. Neuroscience 80:1087-1099.
Patrick GN, Zukerberg L, Nikolic M, de la Monte S, Dikkes P, Tsai LH (1999) Conversion of p35 to p25 deregulates Cdk5 activity and promotes neurodegeneration. Nature 402:615-622.
Perez M, Ribe E, Rubio A, Lim F, Moran MA, Ramos PG, Ferrer I, Isla MT, Avila J (2005) Characterization of a double (amyloid precursor protein-tau) transgenic: tau phosphorylation and aggregation. Neuroscience 130:339-347.
Pettus EH, Christman CW, Giebel ML, Povlishock JT (1994) Traumatically induced altered membrane permeability: its relationship to traumatically induced reactive axonal change. Journal of neurotrauma 11:507-522.
Pierce JE, Trojanowski JQ, Graham DI, Smith DH, McIntosh TK (1996) Immunohistochemical characterization of alterations in the distribution of amyloid precursor proteins and beta-amyloid peptide after experimental brain injury in the rat. J Neurosci 16:1083-1090.
Planel E, Miyasaka T, Launey T, Chui DH, Tanemura K, Sato S, Murayama O, Ishiguro K, Tatebayashi Y, Takashima A (2004) Alterations in glucose metabolism induce hypothermia leading to tau hyperphosphorylation through differential inhibition of kinase and phosphatase activities: implications for Alzheimer's disease. J Neurosci 24:2401-2411.
Plassman BL, Havlik RJ, Steffens DC, Helms MJ, Newman TN, Drosdick D, Phillips C, Gau BA, Welsh-Bohmer KA, Burke JR, Guralnik JM, Breitner JC (2000) Documented head injury in early adulthood and risk of Alzheimer's disease and other dementias. Neurology 55:1158-1166.
Polvikoski T, Sulkava R, Haltia M, Kainulainen K, Vuorio A, Verkkoniemi A, Niinisto L, Halonen P, Kontula K (1995) Apolipoprotein E, dementia, and cortical deposition of beta-amyloid protein. The New England journal of medicine 333:1242-1247.
Povlishock JT, Becker DP (1985) Fate of reactive axonal swellings induced by head injury. Laboratory investigation; a journal of technical methods and pathology 52:540-552.

Povlishock JT, Christman CW (1995) The pathobiology of traumatically induced axonal injury in animals and humans: a review of current thoughts. Journal of neurotrauma 12:555-564.
Povlishock JT, Katz DI (2005) Update of neuropathology and neurological recovery after traumatic brain injury. The Journal of head trauma rehabilitation 20:76-94.
Querfurth HW, LaFerla FM (2010) Alzheimer's disease. The New England journal of medicine 362:329-344.
Raghupathi R (2004) Cell death mechanisms following traumatic brain injury. Brain pathology 14:215-222.
Raghupathi R, Mehr MF, Helfaer MA, Margulies SS (2004) Traumatic axonal injury is exacerbated following repetitive closed head injury in the neonatal pig. Journal of neurotrauma 21:307-316.
Raghupathi R, Muir JK, Fulp CT, Pittman RN, McIntosh TK (2003) Acute activation of mitogen-activated protein kinases following traumatic brain injury in the rat: implications for posttraumatic cell death. Experimental neurology 183:438-448.
Rapoport M, Dawson HN, Binder LI, Vitek MP, Ferreira A (2002) Tau is essential to beta -amyloid-induced neurotoxicity. Proceedings of the National Academy of Sciences of the United States of America 99:6364-6369.
Reynolds AJ, Hendry IA, Bartlett SE (2001) Anterograde and retrograde transport of active extracellular signal-related kinase 1 (ERK1) in the ligated rat sciatic nerve. Neuroscience 105:761-771.
Reynolds CH, Utton MA, Gibb GM, Yates A, Anderton BH (1997) Stress-activated protein kinase/c-jun N-terminal kinase phosphorylates tau protein. Journal of neurochemistry 68:1736-1744.
Roberson ED, Scearce-Levie K, Palop JJ, Yan F, Cheng IH, Wu T, Gerstein H, Yu GQ, Mucke L (2007) Reducing endogenous tau ameliorates amyloid beta-induced deficits in an Alzheimer's disease mouse model. Science (New York, NY 316:750-754.
Roberts GW, Allsop D, Bruton C (1990) The occult aftermath of boxing. Journal of neurology, neurosurgery, and psychiatry 53:373-378.
Roberts GW, Gentleman SM, Lynch A, Graham DI (1991) beta A4 amyloid protein deposition in brain after head trauma. Lancet 338:1422-1423.
Roberts GW, Gentleman SM, Lynch A, Murray L, Landon M, Graham DI (1994) Beta amyloid protein deposition in the brain after severe head injury: implications for the pathogenesis of Alzheimer's disease. Journal of neurology, neurosurgery, and psychiatry 57:419-425.
Robertson J, Loviny TL, Goedert M, Jakes R, Murray KJ, Anderton BH, Hanger DP (1993) Phosphorylation of tau by cyclic-AMP-dependent protein kinase. Dementia 4:256-263.
Rogaev EI, Sherrington R, Rogaeva EA, Levesque G, Ikeda M, Liang Y, Chi H, Lin C, Holman K, Tsuda T, et al. (1995) Familial Alzheimer's disease in kindreds with missense mutations in a gene on chromosome 1 related to the Alzheimer's disease type 3 gene. Nature 376:775-778.
Roy S, Zhang B, Lee VM, Trojanowski JQ (2005) Axonal transport defects: a common theme in neurodegenerative diseases. Acta neuropathologica 109:5-13.

Sandhir R, Onyszchuk G, Berman NE (2008) Exacerbated glial response in the aged mouse hippocampus following controlled cortical impact injury. Experimental neurology 213:372-380.

Saunders AM, Strittmatter WJ, Schmechel D, George-Hyslop PH, Pericak-Vance MA, Joo SH, Rosi BL, Gusella JF, Crapper-MacLachlan DR, Alberts MJ, et al. (1993) Association of apolipoprotein E allele epsilon 4 with late-onset familial and sporadic Alzheimer's disease. Neurology 43:1467-1472.

Scheuner D et al. (1996) Secreted amyloid beta-protein similar to that in the senile plaques of Alzheimer's disease is increased in vivo by the presenilin 1 and 2 and APP mutations linked to familial Alzheimer's disease. Nature medicine 2:864-870.

Schmechel DE, Saunders AM, Strittmatter WJ, Crain BJ, Hulette CM, Joo SH, Pericak-Vance MA, Goldgaber D, Roses AD (1993) Increased amyloid beta-peptide deposition in cerebral cortex as a consequence of apolipoprotein E genotype in late-onset Alzheimer disease. Proceedings of the National Academy of Sciences of the United States of America 90:9649-9653.

Schmidt ML, Zhukareva V, Newell KL, Lee VM, Trojanowski JQ (2001) Tau isoform profile and phosphorylation state in dementia pugilistica recapitulate Alzheimer's disease. Acta neuropathologica 101:518-524.

Schwetye KE, Cirrito JR, Esparza TJ, Mac Donald CL, Holtzman DM, Brody DL (2010) Traumatic brain injury reduces soluble extracellular amyloid-beta in mice: a methodologically novel combined microdialysis-controlled cortical impact study. Neurobiology of disease 40:555-564.

Seiffert D, Mitchell T, Stern AM, Roach A, Zhan Y, Grzanna R (2000) Positive-negative epitope-tagging of beta amyloid precursor protein to identify inhibitors of A beta processing. Brain Res Mol Brain Res 84:115-126.

Selkoe DJ (2001) Alzheimer's disease: genes, proteins, and therapy. Physiological reviews 81:741-766.

Selkoe DJ (2004) Cell biology of protein misfolding: the examples of Alzheimer's and Parkinson's diseases. Nature cell biology 6:1054-1061.

Shankar GM, Bloodgood BL, Townsend M, Walsh DM, Selkoe DJ, Sabatini BL (2007) Natural oligomers of the Alzheimer amyloid-beta protein induce reversible synapse loss by modulating an NMDA-type glutamate receptor-dependent signaling pathway. The Journal of neuroscience : the official journal of the Society for Neuroscience 27:2866-2875.

Shankar GM, Li S, Mehta TH, Garcia-Munoz A, Shepardson NE, Smith I, Brett FM, Farrell MA, Rowan MJ, Lemere CA, Regan CM, Walsh DM, Sabatini BL, Selkoe DJ (2008) Amyloid-beta protein dimers isolated directly from Alzheimer's brains impair synaptic plasticity and memory. Nature medicine 14:837-842.

Sherriff FE, Bridges LR, Sivaloganathan S (1994a) Early detection of axonal injury after human head trauma using immunocytochemistry for beta-amyloid precursor protein. Acta neuropathologica 87:55-62.

Sherriff FE, Bridges LR, Gentleman SM, Sivaloganathan S, Wilson S (1994b) Markers of axonal injury in post mortem human brain. Acta neuropathologica 88:433-439.

Sherrington R et al. (1995) Cloning of a gene bearing missense mutations in early-onset familial Alzheimer's disease. Nature 375:754-760.
Shitaka Y, Tran HT, Bennett RE, Sanchez L, Levy MA, Dikranian K, Brody DL (2011) Repetitive closed-skull traumatic brain injury in mice causes persistent multifocal axonal injury and microglial reactivity. Journal of neuropathology and experimental neurology 70:551-567.
Silva RM, Kuan CY, Rakic P, Burke RE (2005) Mixed lineage kinase-c-jun N-terminal kinase signaling pathway: a new therapeutic target in Parkinson's disease. Mov Disord 20:653-664.
Singleton RH, Zhu J, Stone JR, Povlishock JT (2002) Traumatically induced axotomy adjacent to the soma does not result in acute neuronal death. J Neurosci 22:791-802.
Smith C, Graham DI, Murray LS, Nicoll JA (2003a) Tau immunohistochemistry in acute brain injury. Neuropathology and applied neurobiology 29:496-502.
Smith CM, Radzio-Andzelm E, Madhusudan, Akamine P, Taylor SS (1999a) The catalytic subunit of cAMP-dependent protein kinase: prototype for an extended network of communication. Prog Biophys Mol Biol 71:313-341.
Smith DH, Meaney DF, Shull WH (2003b) Diffuse axonal injury in head trauma. The Journal of head trauma rehabilitation 18:307-316.
Smith DH, Chen XH, Iwata A, Graham DI (2003c) Amyloid beta accumulation in axons after traumatic brain injury in humans. Journal of neurosurgery 98:1072-1077.
Smith DH, Okiyama K, Thomas MJ, Claussen B, McIntosh TK (1991) Evaluation of memory dysfunction following experimental brain injury using the Morris water maze. Journal of neurotrauma 8:259-269.
Smith DH, Uryu K, Saatman KE, Trojanowski JQ, McIntosh TK (2003d) Protein accumulation in traumatic brain injury. Neuromolecular medicine 4:59-72.
Smith DH, Chen XH, Xu BN, McIntosh TK, Gennarelli TA, Meaney DF (1997) Characterization of diffuse axonal pathology and selective hippocampal damage following inertial brain trauma in the pig. Journal of neuropathology and experimental neurology 56:822-834.
Smith DH, Soares HD, Pierce JS, Perlman KG, Saatman KE, Meaney DF, Dixon CE, McIntosh TK (1995) A model of parasagittal controlled cortical impact in the mouse: cognitive and histopathologic effects. Journal of neurotrauma 12:169-178.
Smith DH, Chen XH, Nonaka M, Trojanowski JQ, Lee VM, Saatman KE, Leoni MJ, Xu BN, Wolf JA, Meaney DF (1999b) Accumulation of amyloid beta and tau and the formation of neurofilament inclusions following diffuse brain injury in the pig. Journal of neuropathology and experimental neurology 58:982-992.
Smith DH, Nakamura M, McIntosh TK, Wang J, Rodriguez A, Chen XH, Raghupathi R, Saatman KE, Clemens J, Schmidt ML, Lee VM, Trojanowski JQ (1998) Brain trauma induces massive hippocampal neuron death linked to a surge in beta-amyloid levels in mice overexpressing mutant amyloid precursor protein. The American journal of pathology 153:1005-1010.
Soares HD, Hicks RR, Smith D, McIntosh TK (1995) Inflammatory leukocytic recruitment and diffuse neuronal degeneration are separate pathological

processes resulting from traumatic brain injury. The Journal of neuroscience : the official journal of the Society for Neuroscience 15:8223-8233.
Sorbi S, Nacmias B, Piacentini S, Repice A, Latorraca S, Forleo P, Amaducci L (1995) ApoE as a prognostic factor for post-traumatic coma. Nature medicine 1:852.
Sperber BR, Leight S, Goedert M, Lee VM (1995) Glycogen synthase kinase-3 beta phosphorylates tau protein at multiple sites in intact cells. Neuroscience letters 197:149-153.
Stone JR, Singleton RH, Povlishock JT (2000) Antibodies to the C-terminus of the beta-amyloid precursor protein (APP): a site specific marker for the detection of traumatic axonal injury. Brain research 871:288-302.
Stone JR, Singleton RH, Povlishock JT (2001) Intra-axonal neurofilament compaction does not evoke local axonal swelling in all traumatically injured axons. Experimental neurology 172:320-331.
Stone JR, Okonkwo DO, Singleton RH, Mutlu LK, Helm GA, Povlishock JT (2002) Caspase-3-mediated cleavage of amyloid precursor protein and formation of amyloid Beta peptide in traumatic axonal injury. Journal of neurotrauma 19:601-614.
Strich SJ (1956) Diffuse degeneration of the cerebral white matter in severe dementia following head injury. Journal of neurology, neurosurgery, and psychiatry 19:163-185.
Strich SJ (1970) Lesions in the cerebral hemispheres after blunt head injury. J Clin Pathol Suppl (R Coll Pathol) 4:166-171.
Strittmatter WJ, Saunders AM, Schmechel D, Pericak-Vance M, Enghild J, Salvesen GS, Roses AD (1993) Apolipoprotein E: high-avidity binding to beta-amyloid and increased frequency of type 4 allele in late-onset familial Alzheimer disease. Proceedings of the National Academy of Sciences of the United States of America 90:1977-1981.
Szydlowska K, Tymianski M (2010) Calcium, ischemia and excitotoxicity. Cell calcium 47:122-129.
Teasdale GM, Murray GD, Nicoll JA (2005) The association between APOE epsilon4, age and outcome after head injury: a prospective cohort study. Brain : a journal of neurology 128:2556-2561.
Teasdale GM, Nicoll JA, Murray G, Fiddes M (1997) Association of apolipoprotein E polymorphism with outcome after head injury. Lancet 350:1069-1071.
Thinakaran G, Parent AT (2004) Identification of the role of presenilins beyond Alzheimer's disease. Pharmacol Res 50:411-418.
Tiraboschi P, Hansen LA, Masliah E, Alford M, Thal LJ, Corey-Bloom J (2004) Impact of APOE genotype on neuropathologic and neurochemical markers of Alzheimer disease. Neurology 62:1977-1983.
Tokuda T, Ikeda S, Yanagisawa N, Ihara Y, Glenner GG (1991) Re-examination of ex-boxers' brains using immunohistochemistry with antibodies to amyloid beta-protein and tau protein. Acta neuropathologica 82:280-285.
Tran HT, LaFerla FM, Holtzman DM, Brody DL (2011) Controlled Cortical Impact Traumatic Brain Injury in 3xTg-AD Mice Causes Acute Intra-axonal Amyloid-beta Accumulation and Independently Accelerates the Development of Tau Abnormalities. J Neurosci 31:9513-0525.

Tseng HC, Zhou Y, Shen Y, Tsai LH (2002) A survey of Cdk5 activator p35 and p25 levels in Alzheimer's disease brains. FEBS letters 523:58-62.
Tymianski M, Tator CH (1996) Normal and abnormal calcium homeostasis in neurons: a basis for the pathophysiology of traumatic and ischemic central nervous system injury. Neurosurgery 38:1176-1195.
Uryu K, Laurer H, McIntosh T, Pratico D, Martinez D, Leight S, Lee VM, Trojanowski JQ (2002) Repetitive mild brain trauma accelerates Abeta deposition, lipid peroxidation, and cognitive impairment in a transgenic mouse model of Alzheimer amyloidosis. J Neurosci 22:446-454.
Uryu K, Chen XH, Martinez D, Browne KD, Johnson VE, Graham DI, Lee VM, Trojanowski JQ, Smith DH (2007) Multiple proteins implicated in neurodegenerative diseases accumulate in axons after brain trauma in humans. Experimental neurology 208:185-192.
Van Den Heuvel C, Blumbergs P, Finnie J, Manavis J, Lewis S, Jones N, Reilly P, Pereira R (2000) Upregulation of amyloid precursor protein and its mRNA in an experimental model of paediatric head injury. J Clin Neurosci 7:140-145.
Verghese PB, Castellano JM, Holtzman DM (2011) Apolipoprotein E in Alzheimer's disease and other neurological disorders. Lancet neurology 10:241-252.
Virdee K, Yoshida H, Peak-Chew S, Goedert M (2007) Phosphorylation of human microtubule-associated protein tau by protein kinases of the AGC subfamily. FEBS letters 581:2657-2662.
Vogel J, Anand VS, Ludwig B, Nawoschik S, Dunlop J, Braithwaite SP (2009) The JNK pathway amplifies and drives subcellular changes in tau phosphorylation. Neuropharmacology 57:539-550.
Vossel KA, Zhang K, Brodbeck J, Daub AC, Sharma P, Finkbeiner S, Cui B, Mucke L (2010) Tau reduction prevents Abeta-induced defects in axonal transport. Science (New York, NY 330:198.
Wada T, Nakagawa K, Watanabe T, Nishitai G, Seo J, Kishimoto H, Kitagawa D, Sasaki T, Penninger JM, Nishina H, Katada T (2001) Impaired synergistic activation of stress-activated protein kinase SAPK/JNK in mouse embryonic stem cells lacking SEK1/MKK4: different contribution of SEK2/MKK7 isoforms to the synergistic activation. The Journal of biological chemistry 276:30892-30897.
Wang JZ, Grundke-Iqbal I, Iqbal K (2007) Kinases and phosphatases and tau sites involved in Alzheimer neurofibrillary degeneration. The European journal of neuroscience 25:59-68.
Wang JZ, Gong CX, Zaidi T, Grundke-Iqbal I, Iqbal K (1995) Dephosphorylation of Alzheimer paired helical filaments by protein phosphatase-2A and -2B. The Journal of biological chemistry 270:4854-4860.
Winton MJ, Lee EB, Sun E, Wong MM, Leight S, Zhang B, Trojanowski JQ, Lee VM (2011) Intraneuronal APP, Not Free A{beta} Peptides in 3xTg-AD Mice: Implications for Tau versus A{beta}-Mediated Alzheimer Neurodegeneration. J Neurosci 31:7691-7699.
Wirths O, Weis J, Szczygielski J, Multhaup G, Bayer TA (2006) Axonopathy in an APP/PS1 transgenic mouse model of Alzheimer's disease. Acta neuropathologica 111:312-319.

Wirths O, Multhaup G, Czech C, Blanchard V, Moussaoui S, Tremp G, Pradier L, Beyreuther K, Bayer TA (2001) Intraneuronal Abeta accumulation precedes plaque formation in beta-amyloid precursor protein and presenilin-1 double-transgenic mice. Neuroscience letters 306:116-120.

Yaghmai A, Povlishock J (1992) Traumatically induced reactive change as visualized through the use of monoclonal antibodies targeted to neurofilament subunits. Journal of neuropathology and experimental neurology 51:158-176.

Yan P, Bero AW, Cirrito JR, Xiao Q, Hu X, Wang Y, Gonzales E, Holtzman DM, Lee JM (2009) Characterizing the appearance and growth of amyloid plaques in APP/PS1 mice. J Neurosci 29:10706-10714.

Yang DD, Kuan CY, Whitmarsh AJ, Rincon M, Zheng TS, Davis RJ, Rakic P, Flavell RA (1997) Absence of excitotoxicity-induced apoptosis in the hippocampus of mice lacking the Jnk3 gene. Nature 389:865-870.

Yang T, Arslanova D, Gu Y, Augelli-Szafran C, Xia W (2008) Quantification of gamma-secretase modulation differentiates inhibitor compound selectivity between two substrates Notch and amyloid precursor protein. Molecular brain 1:15.

Yoshida H, Hastie CJ, McLauchlan H, Cohen P, Goedert M (2004) Phosphorylation of microtubule-associated protein tau by isoforms of c-Jun N-terminal kinase (JNK). Journal of neurochemistry 90:352-358.

Yoshiyama Y, Uryu K, Higuchi M, Longhi L, Hoover R, Fujimoto S, McIntosh T, Lee VM, Trojanowski JQ (2005) Enhanced neurofibrillary tangle formation, cerebral atrophy, and cognitive deficits induced by repetitive mild brain injury in a transgenic tauopathy mouse model. Journal of neurotrauma 22:1134-1141.

Zhang B, Maiti A, Shively S, Lakhani F, McDonald-Jones G, Bruce J, Lee EB, Xie SX, Joyce S, Li C, Toleikis PM, Lee VM, Trojanowski JQ (2005) Microtubule-binding drugs offset tau sequestration by stabilizing microtubules and reversing fast axonal transport deficits in a tauopathy model. Proceedings of the National Academy of Sciences of the United States of America 102:227-231.

Zhang Y, McLaughlin R, Goodyer C, LeBlanc A (2002) Selective cytotoxicity of intracellular amyloid beta peptide1-42 through p53 and Bax in cultured primary human neurons. The Journal of cell biology 156:519-529.

Zhou W, Xu D, Peng X, Zhang Q, Jia J, Crutcher KA (2008) Meta-analysis of APOE4 allele and outcome after traumatic brain injury. Journal of neurotrauma 25:279-290.